Structural analysis of three pivotal SERK dependent PRR complexes of *Arabidopsis thaliana*

By

Raghib Ishraq Alvy
20376005

A thesis submitted to the Department of Mathematics and Natural Sciences in partial fulfillment of the requirements for the degree of
Masters of Science in Biotechnology

Mathematics and Natural Sciences
Brac University
January 2021

Declaration

It is hereby declared that

1. The thesis submitted is my own original work while completing degree at Brac University.

2. The thesis does not contain material previously published or written by a third party, except where this is appropriately cited through full and accurate referencing.

3. The thesis does not contain material which has been accepted, or submitted, for any other degree or diploma at a university or other institution.

4. I have acknowledged all main sources of help.

Student's Full Name & Signature:

Raghib Ishraq Alvy
20376005

Approval

The thesis titled Structural analysis of three pivotal SERK dependent PRR complexes of *Arabidopsis thaliana* submitted by

1. Raghib Ishraq Alvy (20376005)

of Fall, 2020 has been accepted as satisfactory in partial fulfillment of the requirement for the degree of Masters of Science in Biotechnology on 19 January, 2021.

Examining Committee:

Supervisor:
(Member)

_____

M H M Mubassir
Lecturer
Department of Mathematics and Natural Sciences
Brac University

Program Coordinator:
(Member)

_____

Iftekhar Bin Naser, PhD
Assistant Professor
Department of Mathematics and Natural Sciences
Brac University

External Expert Examiner:
(Member)

_____

Dr. Md. Rokibur Rahman
Professor (Poultry Science), School of Agriculture and Rural Development (SARD)
Bangladesh Open University (BOU)

Departmental Head:
(Chair)

_____

Prof. Dr. A F M Yusuf Haider
Professor and Chairperson
Department of Mathematics and Natural Sciences
Brac University

Ethics Statement

No animal or living things were used in this study.

Abstract

Pattern Triggered Immunity (PTI) is distinguished with the activities of pattern recognition receptors (PRRs), which play an essential role in plant defense mechanism. During aggression of microbes, PRRs immediately bind with the PAMPs and recruit co-receptors to initiate the defense signal. Several plant PRRs have been discovered, very few of their functional parameters have been studied. In this study, the crystallographic structures of FLS2-flg22-BAK1 (PDB ID: 4MN8), HAESA-IDA-SERK1 (PDB ID: 5IYX) and PSKR-Phytosulphokine-SERK1 (PDB ID: 4Z64) complexes were simulated for 30ns. Simulated trajectories were analyzed for getting an overview of the immune response of PRRs towards PAMPs with the help of co-receptors. Moreover, MM/PBSA calculation revealed that interaction between FLS2-BAK1 and HAESA-SERK1 show similarity whereas PSKR interacts differently with SERK1. As PRRs play a major role in plant defense mechanism, it can be hypothesized that binding mechanism with PAMPs and co-receptors will help to understand the interaction pattern of PTI.

Keywords: Pattern Triggered Immunity; Pattern Recognition Receptors; MM/PBSA; PAMP; Molecular Dynamics; Bioinformatics

Dedication

I want to dedicate this work to

My Father

the very first sports mate and torch bearer of mine.

Thank you for being beside me every time on every situation.

Acknowledgement

I proclaim my submissive gratitude to the Creator of the universe, by who's grace I adapted the strength, patience and understanding to complete this thesis work.

I am countlessly indebted to my family members for their unconditional support, prayer and faith on me since my childhood.

I convey my sincere gratitude to Professor A.F.M Yusuf Haider, the Chairperson of the Department of Mathematics and Natural Sciences, late Professor A. A. Ziauddin Ahmed, former Chairperson of the Department of Mathematics and Natural Sciences and Professor Naiyyum Choudhury, former coordinator of the Biotechnology and Microbiology Program, for giving me the opportunity to continue my research work in my desired subject and to grow up with outstanding guidance during my study life in Brac University.

I would like reveal my gratitude to my supervisor, M H M Mubassir, Lecturer, Biotechnology Program, Department of Mathematics and Natural Sciences for his gentle and humble guidance, supervision and cooperation. His intellectual vision and constant support lead me to complete my research work through hardship. I will always grateful to him for giving me the worthy opportunity.

I would like to thank specially my better half Tasfia Tawhid Supti for her constant psychological support during the research work and her belief on my abilities make me motivated to do work harder. Moreover, I want to thank my mother for her support.

Sincerely,

Raghib Ishraq Alvy

Department of Mathematics and Natural Sciences

Brac University, Dhaka

Table of Contents

List of Figures

List of Tables

List of Acronyms

AA - Amino Acid

ETI - Effector Triggered Immunity

GROMACS - Groningen Machine for Chemical Simulations

H-bonds - Hydrogen Bonds

LRR - Leucine Rich Repeat Domain

MD - Molecular Dynamics

PAMP - Pathogen Associated Molecular Pattern

PDB - Protein Data Bank

PRR - Pattern Recognition Receptor

PRR-RKs - Pattern Recognition Receptor like kinases

PTI - Pattern Triggered Immunity

Rg - Radius of Gyration

RMSD - Root Means Square Deviation

RMSF - Root Means Square Fluctuations

List of Symbols

Aº - Angstrom

K - Kelvin

nm - Nano meter

ns - Nano second

ps - Pico second

Chapter 1

Introduction:

1.1 Background Study

Plants are surrounded innumerable pathogenic microbes but they remain green. To detect and eliminate these perilous pathogens, plants use their innate immune system.[1-4]

Plant pathogens utilize assorted life techniques. Bacteria, virus, fungi these types of pathogens proliferate in the apoplast, also known as intercellular spaces subsequent to get access stomata and hydathodes, individually, alternatively get access by means of damages. Plants, in contrast to well-evolved creatures (like a human being), have no versatile protector cells and a physical versatile resistant framework. Rather, they depend on the natural resistance of each cell and on foundational signals exuding from contamination destinations.[5]

The staggeringly sensitive impression of pathogen or microbe-associated molecular patterns (PAMPs or MAMPs) through pattern recognition receptors (PRRs) at the plant's cell surface is the first one of this system. For an example, for detecting abscission, plants get help from a pattern recognition receptors (PRR) ‘HAESA’ a leucine-rich repeat receptor kinase (LRR-RK) situated in the plasma membrane. Here comes the term ‘PRR triggered immunity (PTI)’ which defines reactions to different MAMPs and PAMPs.[2]

Alongside PTI, Effector Triggered Immunity (ETI) is another immune response system for plants where Intracellular Immune receptors are utilized and most of them are nucleotide-binding site leucine-rich repeat (NBS-LRR) proteins, which are used to differentiate directly or indirectly discharged harmfulness effectors.[6]

Thus, the first one of the plant immune system is transmembrane pattern recognition receptors (PRRs) that react step by step creating microbial or pathogen-associated molecular patterns (MAMPS or PAMPs), like IDA or flg22, and another one works within the cell by considering all things, using the polymorphic NB-LRR protein things scrambled by most R genes.[5, 7]

1.2 Research aim and objectives

This study aims at investigating structural dynamics of different complexes of pattern triggered immunity (PTI) in *Arabidopsis thaliana*, using in silico approach. The following objectives were set to achieve the aim:

- Analyzing the interaction between following PRRs, PAMPs and co-receptors by using Molecular Dynamics (md) Simulation and MM/PBSA (free energy binding) calculation
    a) FLS2- flg22- BAK1
    b) HAESA- IDA- SERK1
    c) PSKR- Phytosulphokine- SERK1
- Contribution of co-receptors in the above mentioned PTI complexes
- Finding prominent residues of the above-mentioned proteins
- Determining the stability of the above-mentioned complexes

1.3 Literature review

In this section, simple and general overview of pattern triggered immunity, the targeted model plant and its' morphology, some terminologies according to pattern triggered immunity is discussed. Computational approaches and analyzing terminologies are also overviewed at the end of this section.

1.3.1 *Arabidopsis Thaliana*

Arabidopsis Thaliana, in recent times becomes an vital model system to analyze genes and their functional system which is also a flowering plant.[8] In-plant science, for doing broad scope studies, *A. Thaliana* is the most acceptable in these days.[9] Recent research of *Arabidopsis* shows that to do fundamental study of the structural and functional area of biology for most of the eukaryotes this angiosperm is the perfect selection. As most of the eukaryotic organisms have a conventional genetic ancestry and this was pronounced while genome project.[10]

Having a very small nuclear (sn) genome make *Arabidopsis* more desirable model for plant genomics.[11] For the small genome, this angiosperm becomes highly resistant to ionizing radiation, the relation between radiation sensitivity and DNA contents in plants was proved around sixty years ago.[12, 13]

From the above, it can be understood easily the reasons behind make *Arabidopsis Thaliana* a suitable model for genome study. Alongside short nuclear genome, it has a quick generation time, a huge number of offspring and undoubtedly small size.[8, 14-16]

1.3.2 Morphology of *Arabidopsis Thaliana*

It needs almost six weeks to complete the entire life cycle of *Arabidopsis* thaliana including seed germination, rosette formation, main stem bolting, flowering and first seed maturation. Most of the things are very tiny after coming to a size such as 2mm long flower, self-pollination system because of open bud, pollen can be applied to the stigma surface for crossing.[10]

At maturity seed length is 0.5mm, into the rosette plant seedlings are developed which ranges from 2 to 10 cm in diameter according to growth conditions. Trichomes, small unicellular hairs cover the leaves which are used for studying cellular differentiation and morphogenesis.[10]

This mustard family (Cruciferae or Brassicaceae) member takes three weeks for bolting after planting. Silique forming a central gynoecium, pollen-bearing six stamens, four white petals containing inner whorls and four green sepals containing outer whorl compose flowers of A. thaliana. Almost 5000 total seeds with several hundred siliques are produced when the plants become 15-20 cm in height, which is a mature plant also.[10]

There is no evidence of symbiotic relationship with nitrogen-fixing microbes of the roots and very structure to study in culture.[10]

1.3.3 Study on *Arabidopsis Thaliana*

In 1873, Alexander Braun described a mutant plant near Berlin in the literature of botany, which was the very first *Arabidopsis's* non-taxonomic appearance.[17] In the AGAMOUS gene, the mutation happened which is known as floral ABC regulators in these days.[17, 18]

By publishing chromosome number of various plants one of the students of Strasburger's laboratory (Friedrich Laibach) made *Arabidopsis* features clear in 1907. Though the chromosomes of this plant are very small.[17, 19]

During Russian expedition in 1935 appearance of *Arabidopsis* was found again to use in genetics and cytogenetics instead of Drosophila because of small chromosome number and flowering time

is so rapid than others but small size and tiny structure made problems to differentiate chromosome pairs at that time.[17, 20, 21]

In 1943 *Arabidopsis* again cropped up because Laibach showed that it has a short generation time, ease to crosses, mutagenesis possibility, fecundity and so on features which made it a genetic model organism.[17, 22]

Revolution during the 1980s in plant genetics, molecular genetics and physiology make extensive acceptance of *Arabidopsis* as a model plant. There were several suggestions at that time for model plant choosing like petunia for its' ease of transformation and haploid lines availability, tomato for the mutant availability but in 1975 George Re´dei proposed *Arabidopsis* as a model plant for auxotrophic mutation finding, an article of Annual Review of Genetics described it takes attention of molecular cloners and young geneticists. [17, 23]

During summer 2001 conference on *Arabidopsis* research was took place (11th International Conference) wherein the presence of around 1000 people extensive acceptance of this plant for laboratory model system was led. A fusion of molecular and classical genetics in plant biology has been brought by this model genetic system with development, physiology and pathology of plants. Information transfer and cellular process mechanisms in plant life became understandable for the first time.[17]

1.3.4 Pattern Triggered Immunity (PTI)

According to the sensation of the microbe-associated or pathogen-associated molecular pattern (MAMPs or PAMPs) by pattern recognition receptor (PRRs), the very first action of plant immune response is triggered, which is Pattern triggered immunity (PTI).[1, 2, 5, 24, 25] To inhibit PTI, effector proteins have been attained by adapted pathogens through evolution which is transferred into the plant cell.[24, 26-28]

At the period of infection MAMPs (Microbe-Associated Molecular Patterns), DAMPs (damage-associated Molecular Patterns) evolved from the host and so many types of pathogens are released which are sensed by cell surface-localized Pattern Recognition Receptors (PRRs) and these PRRs activate PTI for immune response.[29, 30]

Because of the reserved nature of PAMPs (e.g., bacterial flagellin, fungal chitin), multiple microbes are fended off by PTI. Thus, it contributes to basal immunity during infection.[6]

For most of the non-host pathogens, PTI is effective by providing a strong and abstinent immune response. As a contributor to basal resistance PTI works against adapted pathogens where effectors proteins are employed to knock out PTI for host metabolism manipulation is called Effector-Triggered Susceptibility (ETS).[30]

A recent study proved that beside restricting pathogenic growth PTI creates nutrient deprivation to control colonization of microbes.[30, 31]

1.3.5 Effector-triggered Immunity (ETI)

Another immunity system of the plant is specialized in effectors identification by additional receptors, known as effector-triggered immunity (ETI). These receptors are obtained during co-evolution.[5, 24, 32]

Pathogen's effector protein(s) of the pathogen are identified by a Resistance (R) gene product within the plant cell, in ETI.[5, 24] Maximum R genes carry nucleotide-binding leucine-rich repeat (NB-LRR) proteins.[24, 33] When these NB-LRR proteins identify an effector, ETI starts, Effector identification process of NB-LRR depends on the results of their actions.[5, 24]

Basically, these effectors are the result of adapted pathogens and their intention is to redesign host's physiology for making it contagious compatible, but NB-LRR protein's identification ability creates a war of nerves between plants and their pathogens.[6]

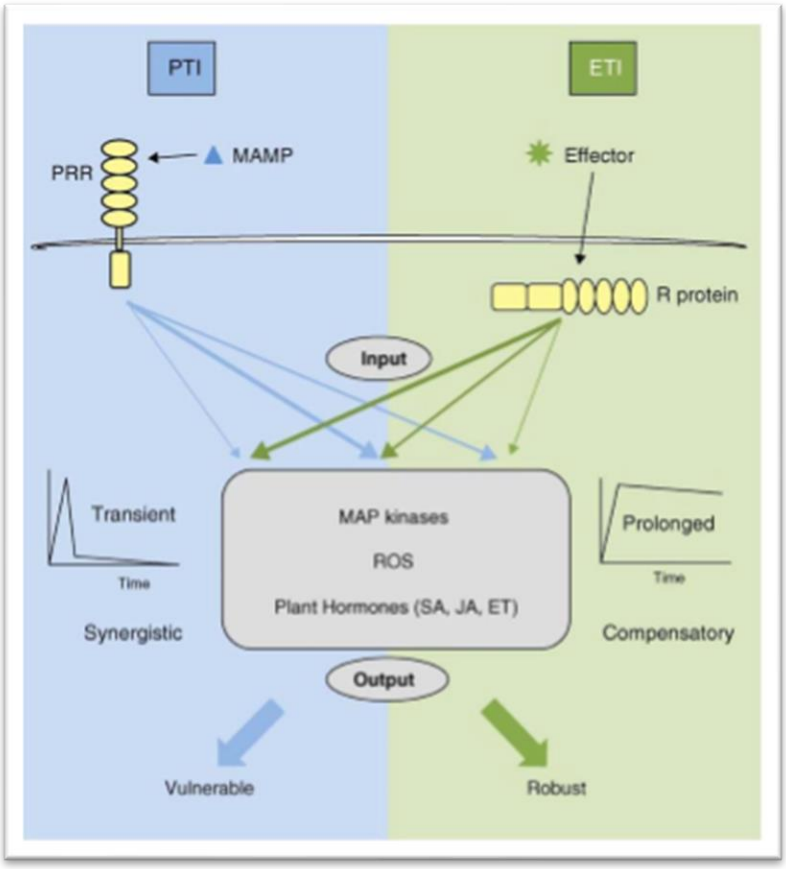

Fig 1.1: Differences in signaling between PTI and ETI.[25]

1.3.6 Pattern Recognition Receptor (PRR)

In *Arabidopsis thaliana*, above 200 genes encoding leucine-rich repeat receptor-like kinases and almost 1000 genes encoding putative secreted peptides have been determined, which shows that in plants for a cell to cell communication peptide ligand-receptor interactions are essential.[34-36]

LRR-RLK flagellin-sensitive 2 (FLS2) interacts with flg22, a gram-negative bacteria, has 22 residues epitope located at the N terminus.[37]

Flagellin sensing in *Arabidopsis* is identification of its highly protected N-terminal epitope (flg22) by the PRR- flagellin-sensitive 2 (FLS2). flg22 binding results FLS2 heteromerization with BRASSINOSTEROID INSENSITIVE 1–associated kinase 1 (BAK1) and their corresponding activation controlled by plant immunity.[38]

Inflorescence Deficient in Abscission (IDA)-HAESA / HAESA Like2 (HLS2) mainly control the floral organ abscission. At the bottom of organs to be shed the IDA mutant and the HAESA/HLS2

dual mutant hold their floral organs endlessly due to absence of collapse of the central lamella among cell layers of the abscission zone.[39]

Formerly named RLK5, *Arabidopsis* LRR-RLK HAESA is plasma membrane-associated containing serine/threonine-protein kinase activity. Beside abscission areas of the floral organs, HAESA is expressed at the bottom of the petioles and pedicels.[40]

Structure of HAESA with a PKGV-IDA peptide at 1.94 Å resolution has no extra electron density at the IDA N-terminus rather it identifies a dodecamer peptide comprising residues 58-69^{IDA}.[39]

IDL1, an IDA peptide family member can easily be sensed by HAESA, though it has low affinity.[39, 41] Though most of the PRRs are identified and illustrated clearly their mechanism of interaction with PAMPs is not specified yet. Interaction between PAMP IDA with PRR HAESA is studied here to identify PTI mechanism among them.

DcPSKR and PSKR1/2 (PSKRs) relate to the wide family of leucine-rich repeat receptor kinases (LRR-RKs) with an extracellular LRR domain and a cytoplasmic kinase domain (KD).[42, 43] The extracellular domains of the three LRR-RKs contain 21 LRRs with an island domain (ID) necessary for PSK perception.[43-45] PSK interaction stimulates signalling intervened by Ca21/CaM binding and the kinase activity of PSKR1, proposing that ligand binding triggers the PSKR1KD.[43]

PSK binding stimulated no oligomerization of PSKR1LRR or DcPSKRLRR, proposing that a co-receptor is essential for the activation on the basis of the dimerization model. PSKR1/2 and DcPSKR relate to the identical family of LRR-RKs as BRI1 that uses a SERK member as its co-receptor. In addition, PSK facilitates somatic embryogenesis, marker of DcSERK17.[43]

Phytosulfokine (PSK), a disulfated pentapeptide has a widespread function in plant development.[46, 47] PSKR senses PSK, a leucine-rich repeat receptor kinase (LRRRK).[44, 48] The fundamental system of identification of PSK, the activation of PSKR and the features of the elements downward of the primary binding still indefinable.[43]

1.3.7 Leucine-Rich Repeat Receptor-like Kinase

Specific receptors are working for conducting signals and sensing outside interaction in the cell surface of living organisms, but in the case of plants, this procedure is induced by receptor-like kinases (RLKs). Leucine-rich repeat RLK family is one of them and also the biggest family having two types of domains: Extracellular domain (ECD) and Kinase domain (KD). The differences between ECD and KD are: ECD contains a numerous number of LRR repeats which help to sense small molecules, entire protein or peptides but KD contains 12 subdomains which are basically conserved and fold into three-dimensional catalytic core consisting two-lobed structure and these subdomains are playing an important role in enzyme function.[49, 50]

1.3.8 Pathogen Associated Molecular Pattern (PAMP)

Pathogen Associated Molecular Patterns (PAMPs) are specific molecular pattern of microbes playing elicitor key function of innate immunity in the plant system.[51-54] Most probably specificities of recognizing immensely conserved molecules for different kingdoms gained independently by convergent evolution. [53, 55, 56] In the First stage, PAMPs sensing by the host leads activation of defense system rapidly by reinforcing cell wall by callose deposition, reactive oxygen species (ROS) production etc. These PAMP elicited fundamental defense system can be inhibited by virulence factors of successful pathogens just after the first stage. Finally, specialized resistance (R) proteins have been evolved to identify these virulence factors derived from pathogen and their effectiveness on the host.[53, 57-59]

Result of R protein-dependent perception, a hypersensitive response (HR) occurs that consists of localized cell death and capture of PAMPs expansion.[53, 60, 61]

1.3.9 Somatic Embryogenesis Receptor-Like kinase (SERK/BAK)

Somatic Embryogenesis Receptor-Like kinase (SERK), an LRR-RLK which works for marking the establishment of embryogenic cells within culture and it's expression within ovule primordia both in male and female gametophytes.[62] Inside vascular tissue of all organ, its' expression is highest but in sporophytic tissues, it expresses a complex pattern.[62-65]

In *Arabidopsis* plants, adventitious phrase of SERK1 has no outcome in an exact phenotype but in culture helps to increase somatic embryos. It is an element of a minor family of five related RLKs, all of which have typical Ser-Pro-rich juxta membrane region.[62, 64]

SERK1 engages with the KINASE-ASSOCIATED PROTEIN PHOSPHATASE (KAPP) which plays a role in receptor internalization.[62, 66]

Knockout alleles of SERK1 (SERK1-1 and SERK1-2) have no morphological phenotype on the other hand the combination with serk2 null mutant resulted in complete male-sterile plants.[62, 63, 67]

BAK1 is also known as SERK3, a part of the subfamily of SERK LRR-RKs.[68] BAK1 also creates heteromers with numerous other PRRs and is a significant element of plant immunity.[38, 69, 70] The flg22-stimulated FLS2-BAK1 heteromerization concludes in their trans-phosphorylation.[38, 71-73]

1.3.10 Computational approach for Molecular Dynamic (md) simulation

Simulating the motions of a system of specific particles scientifically known as Molecular dynamics. The system is generally tiny like an atom and a diatomic molecule undergoes a chemical reaction larger like a galaxy.[74, 75] For running a molecular dynamics simulation, knowledge of the interaction potentials for the particles is necessary.[75]

For getting conclusive details of specific particle motions as an act of time and answering about the properties of a model system simulations are used. Three different types of simulation method exist in the area of macromolecular research. The first one is working on a mean of sampling configuration space, which helps to define structures with the data obtaining from experiments on actual or real-life systems. The second method is used for describing the system at equilibrium with the help of structural and motional properties and the values of thermodynamic parameters. The actual dynamics are examined by the third method where the motion and development of specific particles with time are the main concern.[76]

For doing meaningful studies on biological macromolecules by using molecular dynamic (MD) simulation, programs availability and computational power must be required. The simulation was doing less than 10 ps in length in old days but the current scenario shows that 1000 times longer simulations of same sizes are often done within half of the time than previous. Besides time, another important fact in simulation is computational power by which multiple numbers of simulation can be performed. CHARMM20, AMBER21 and GROMOS22 are the most widely used programs.[76-79] Sometimes it becomes impossible to get the desired result in the laboratory

for not providing extreme and controlled temperature and pressure where computational simulations solve this problem.[80]

1.3.11 Protein Interaction Calculator (PIC)

For a better understanding of sequence-structure relationships, the stability of protein on the basis of structure and evolution of protein atomic interaction analysis in their tertiary structures is needed. Strategies for remote homology identification, recognition of protein folding, comparisons between protein structures and modelling a protein knowledge about sidechain interaction is used.[81-87] This knowledge also helps to understand the residue conservation in homologous proteins as well as site-directed mutagenesis research.[87-89] Moreover, interaction among subunits of multimeric proteins and also among interacting protein modules are the regions of acute knowledge.[87, 90-94] Characteristics of sidechain-sidechain interactions between protein modules give us an indication of developmental conservation of protein-protein interactions.[87, 95-97] Protein Interaction Calculator, a web-based server, working for analyzing different types of interactions in tertiary structures of proteins and protein-protein complexes. It has also solvent accessibility calculator to recognize of interacting motifs those are revealed. Basically, PIC server supports the atomic coordinate set of protein structure in the usual format which is PDB or Protein Data Bank format.[87]

1.3.12 MM/PBSA

Free energy calculation of the binding of tiny ligands to biological macromolecules is done by molecular mechanics energies together with the Poisson-Boltzmann and surface area solvation (MM/PBSA) method. This method is basically depending on molecular dynamics simulations of the receptor-ligand complex.[98] Calculation of free energy is used for drug design and determining protein structure.[99, 100] Specifically MM-PBSA unites molecular mechanics and continuum solvent models to compute affinities of ligand binding.[98] The MM-PBSA method has been designed and adjusted according to the type of uses. [98, 101-103] The method is used for protein designing, protein-protein interactions, conformer stability and re-scoring.[98, 102, 104-109] Here MM indicates for molecular mechanics, PB for Poisson-Boltzmann and SA for surface area. In this method, three different energy values as output are given according to their objectives.[110]

1.3.13 SASA, RMSD, RMSF, Rg

Solvent accessible surface area previously designed in a way that located out by the center of a probe sphere presenting a solvent molecule which capsized the surface of the molecule of concern. This invention used as a apparatus for striking the protein folding problem.[111, 112] Only quantifying area is not efficient for further studies so another method was developed. On that method without displacing van der Waals surface of the atoms which are available to the contact surface, make a connection by a network of concave and saddle-shaped surfaces.[111-113]

Latterly the method is developed again by which a minor problem is solved. The problem is if the probe sphere is rejected and lack experience van der Waals overlap then how to calculate SASA of that molecule? By improving algorithms for doing calculation of contact and reentrant surfaces and also for the solvent accessible area which helps to calculate SASA of any molecules.[111, 114-116]

Root mean square deviation (RMSD) is utilized to analyze the stability of protein during interaction for a several period of time which helps to understand the proteins stability character. Root mean square fluctuation (RMSF) is also analyzed like RMSD but in this case fluctuation of individual residues are studied. Low fluctuation indicates the possibility of more interaction. Radius of gyration (Rg) is used to determine the compactness of the protein. Coiling and uncoiling condition in the mean of the time is analyzed by Rg value.

1.3.14 Hydrogen Bond

The most important interatomic interaction in protein folding is the hydrogen bond.[117, 118] Comparing to covalent bond average intermolecular hydrogen bond energy is very low but their massive number of existences gives a major influence on protein folding in another sense it dominates the folding procedure but their role is mostly reserved for hydrophobic interaction. [117-120]

Most of the hydrogen bonds in proteins are main chains NH to CO bonds and bonds between main-chains and side-chains make a cluster around the caps of helices. Failure of main-chain NH or CO groups to form hydrogen bonds is very rare.[118]

Chapter 2

Materials and Methods

In this part procedures which were followed for analyzing the interaction between three different plant protein complexes are described. For analyzing different types of open-source computational tool and servers were used. Those are GROMACS 5.1, MM-PBSA, RCSB Protein Data Bank, Protein Interaction Calculator (PIC), XmGrace, UCSF Chimera and so on. All of the softwares are developed for the open-source platform and the analyzing procedures are performed on Linux based Ubuntu operating system.

2.1 Molecular dynamic simulation of PRR, PAMP and co-receptor

To begin with, complexes containing the receptor ectodomain FLS2, HAESA and PSKR incorporation with the PAMP flg22, IDA and Phytosulphokine and co-receptor SERK1 and BAK1 (PDB code: 4MN8, 5IYX and 4Z64) were collected from Protein Data Bank web server. The files were downloaded as '.pdb' format. The PDB files were opened in a text editor and those were edited by keeping all the residues of proteins inside. After saving the file, PIC data were collected in accordance with protein-protein interaction search category. Then the PDB files were submitted to molecular dynamic (md) simulation with GROMACS software individually.[121] Like a force field, GROMOS 54a7 united force field was selected for every simulations. The system was solvated, neutralized, energy minimized and equilibrated accordingly. During solvation, protein complex was inserted inside a cubic box with 1Å distance ranging from protein surface to the borders. Box newly created with the protein complex inside was solvated with SPC water model.[122] Before proceeding to energy minimization, the system was neutralized with genion tool of GROMACS. During equilibration, 1 ns NPT coordinates followed by 1 ns NVT coordinates were equilibrated while keeping persistent 1atm pressure and 300K temperature. Generated .gro files were converted to .pdb files using GROMACS tool. Again, solutions were removed apart from residues through text editor and updated the save file. These pdb files were used for PIC in case of protein-protein interaction data collection.

2.2 Analysis of binding mode of PRR, PAMP and co-receptor

Using UCSF Chimera, a molecular visualization system, the intermolecular interactions among PRR, PAMP and co-receptor were visualized in the complexes. H-bonds, hydrophobic interactions, ionic interactions, aromatic interactions and cation-Pi interactions were computed using the server - protein interaction calculator (PIC). All these analyses were done for the structural complex before and after the simulation. Calculation of binding free energy were done using the g_mmpbsa.

Table 2.2.1: Name of the complexes used in the study

Complexes	Sub-complexes	Proteins
Complex 1	Complex 1ai	FLS2 LRR+flg22 (BAK1 LRR presents inside complex)
	Complex 1aii	FLS2 LRR+BAK1 (flg22 presents inside complex)
	Complex 1aiii	flg22+BAK1 LRR (FLS2 LRR presents inside complex)
	Complex 1b	FLS2 LRR+flg22 (BAK1 LRR absents inside complex)
	Complex 1c	FLS2 LRR+BAK1 (flg22 absents inside complex)
Complex 2	Complex 2ai	HAESA LRR+IDA (SERK1 LRR presents inside complex)
	Complex 2aii	HAESA LRR+SERK1 (IDA presents inside complex)
	Complex 2aiii	IDA+SERK1 LRR (HAESA LRR presents inside complex)
	Complex 2b	HAESA LRR+IDA (SERK1 LRR absents inside complex)
	Complex 2c	HAESA LRR+SERK1 (IDA absents inside complex)
Complex 3	Complex 3ai	PSKR LRR+Phytosulphokine (SERK1 LRR presents inside complex)
	Complex 3aii	PSKR LRR+SERK1 (Phytosulphokine presents inside complex)
	Complex 3aiii	Phytosulphokine+SERK1 LRR (PSKR LRR presents inside complex)
	Complex 3b	PSKR LRR+Phytosulphokine (SERK1 LRR absents inside complex)
	Complex 3c	PSKR LRR+SERK1 (Phytosulphokine absents inside complex)

Every simulation is performed for 30 ns. Here Complex 1ai shows interaction between FLS2 and flg22 when BAK1 is present inside the complex, Complex 1aii shows interaction between FLS2 and BAK1 when flg22 is present and Complex 1aiii for interaction between flg22 and BAK1 when FLS2 is present. Complex 1b indicates the interaction of FLS2 and BAK1 in the absence of flg22 and Complex 1c shows interaction of FLS2 and flg22 in the absence of BAK1 inside. Complex 2ai shows interaction between HAESA and IDA when SERK1 is present inside the complex, Complex 2aii shows interaction between HAESA and SERK1 when IDA is present and Complex 2aiii for interaction between IDA and SERK1 when HAESA is present. Complex 2b indicates the interaction of HAESA and SERK1 in the absence of IDA and Complex 2c shows interaction of HAESA and IDA in the absence of SERK1 inside. Complex 3ai shows interaction between PSKR and Phytosulphokine when SERK1 is present inside the complex, Complex 3aii shows interaction between PSKR and SERK1 when Phytosulphokine is present and Complex 3aiii for interaction between Phytosulphokine and SERK1 when PSKR is present. Complex 3b indicates the interaction of PSKR and SERK1 in the absence of Phytosulphokine and Complex 3c shows interaction of PSKR and Phytosulphokine in the absence of SERK1 inside.

2.3 Comparative study between FLS2 LRR-flg22-BAK1, HAESA LRR-IDA-SERK1 and PSKR-Phytosulphokine-SERK1 complex

To compare the binding mechanism between HAESA LRR-IDA-SERK1 complex with FLS2 LRR-flg22-BAK1 crystal complex[123] and PSKR-Phytosulphokine-SERK1 complex[124], MM/PBSA calculation, RMSF, RMSD, Rg, SASA, H-Bond and PIC data were analyzed as well as visualization by using UCSF Chimera also used to determine the binding pattern and similarities and dissimilarities between these complexes.

Chapter 3

Result and Discussion

3.1 Analysis of binding mode of PRRs with PAMPs and co-receptors

A detailed analysis of the interaction between these proteins, the energy contribution of every residues was computed and interpreted in MM/PBSA plots.

3.1.1 Complex 1ai vs Complex 1c

From Table 3.1.1 and Table 3.1.3, Glu81, Asp102, Asp150, Asp176 and Asp222 from FLS2 and Gln65, Arg66, Arg72 and Lys77 from flg22 performed an essential function in the time of interaction, by building MM energy for both complex 1ai and complex 1c. Glu81, Asp102 and Asp176 of FLS2 shows utmost binding free energy for happening interaction with flg22 which are -69.2440 ± 0.4505 $kJmol^{-1}$, -59.6585 ± 0.3835 $kJmol^{-1}$ and -60.7058 ± 0.3107 $kJmol^{-1}$ (complex 1ai) and -37.4501 ± 0.5265 $kJmol^{-1}$, -46.6974 ± 0.3513 $kJmol^{-1}$ and -52.3653 ± 0.2984 $kJmol^{-1}$ (complex 1c). Glu81 from FLS2 interacts with flg22 more favorably in complex 1ai (-69.2440 ± 0.4505 $kJmol^{-1}$), but Asp102 and Asp176 show promising interaction in complex 1c (-46.6974 ± 0.3513 $kJmol^{-1}$ and -52.3653 ± 0.2984 $kJmol^{-1}$ respectively). For flg22, Arg72 and Lys77 are interacting more favorably with FLS2 in complex 1ai (-288.7622 ± 0.3931 $kJmol^{-1}$ and -279.0251 ± 0.6088 $kJmol^{-1}$) similarly show more favorable interaction in complex 1c (-283.8474 ± 0.4686 $kJmol^{-1}$ and -265.9476 ± 1.0339 $kJmol^{-1}$). (Fig 3.1.1 a)

3.1.2 Complex 2ai vs Complex 2c

From Table 3.6.1 and Table 3.6.3, Asp120, Glu123, Glu145, Glu191, Asp242, Glu263, Glu266, Glu310, Glu316, Glu335 and Glu382 from HAESA and Tyr56, Lys66 and Arg67 from IDA performed an essential function in the time of interaction, by building MM energy for both complex 2ai and complex 2c. Glu123, Asp242 and Glu335 of HAESA shows utmost binding free energy for happening interaction with IDA which are -52.9880 ± 0.2972 $kJmol^{-1}$, -46.0330 ± 0.2406 $kJmol^{-1}$ and 41.2149 ± 0.2578 $kJmol^{-1}$ (complex 2ai) and -39.0345 ± 0.5811 $kJmol^{-1}$, -37.4981 ± 0.3104 $kJmol^{-1}$ and -42.7000 ± 0.3930 $kJmol^{-1}$ (complex 2c). Glu123 from HAESA interacts with IDA more favorably in complex 2ai (-52.9880 ± 0.2972 $kJmol^{-1}$), but Asp120, Glu145 show promising interaction in complex 2c (-40.9692 ± 0.1698 $kJmol^{-1}$, -43.8408 ± 0.2207 $kJmol^{-1}$ respectively). For IDA, Tyr56 and Arg67 are interacting more favorably with HAESA in

complex 2ai (-127.4403 ± 0.6430 kJmol^{-1} and -129.4292 ± 0.3620 kJmol^{-1}) but shows more favorable interaction in complex 2c (-145.9164 ± 0.6184 kJmol^{-1} and -132.5575 ± 0.4306 kJmol^{-1}). (Fig 3.1.2 a)

3.1.3 Complex 3ai vs Complex 3c

From Table 3.11.1 and Table 3.11.3, Arg300, Arg327, Met507, Arg514, Glu529, Asp553, Glu574 from PSKR and Thr31, Gln32 from phytosulphokine performed an essential function in the time of interaction, by building MM energy for both complex 3ai and complex 3c. Arg300 of PSKR shows utmost binding free energy for happening interaction with phytosulphokine which is -6.9089 ± 0.1261 kJmol^{-1} (complex 3ai) and -7.1805 ± 0.1176 kJmol^{-1} (complex 3c). Asp529 from PSKR interacts with phytosulphokine more favorably in complex 3c (-9.3820 ± 0.3026 kJmol^{-1}), but Arg300, Met507 show promising interaction in complex 3ai (-6.9089 ± 0.1261 kJmol^{-1}, -3.0772 ± 0.0884 kJmol^{-1} respectively). For phytosulphokine, Thr31 and Gln32 are interacting more favorably with PSKR in complex 3ai (-3.8066 ± 0.1791 kJmol^{-1} and -2.1566 ± 0.7372 kJmol^{-1}) but Thr31 shows more favorable interaction in complex 3c (-14.8964 ± 0.2438 kJmol^{-1}). (Fig 3.1.3.a)

3.1.4 Complex 1aii vs Complex 1b

For FLS2 with BAK1 (Table 3.1.2 and Table 3.1.4), numerous residues contribute greatly to binding energy that are – Arg533, Lys551, Lys624, Lys647 and Lys673 for FLS2; and Asn26, Lys36, Lys44, Arg72, Arg138, Lys140, Lys141, Arg143, Arg146, Arg158 and Lys198 for BAK1. Asn26 of BAK1 shows utmost binding free energy when it collaborates with FLS2 which is -273.3219 ± 0.4366 kJmol^{-1} in complex 1aii and -249.5682 ± 0.5875 kJmol^{-1} in complex 1b. (Fig 3.1.1 b)

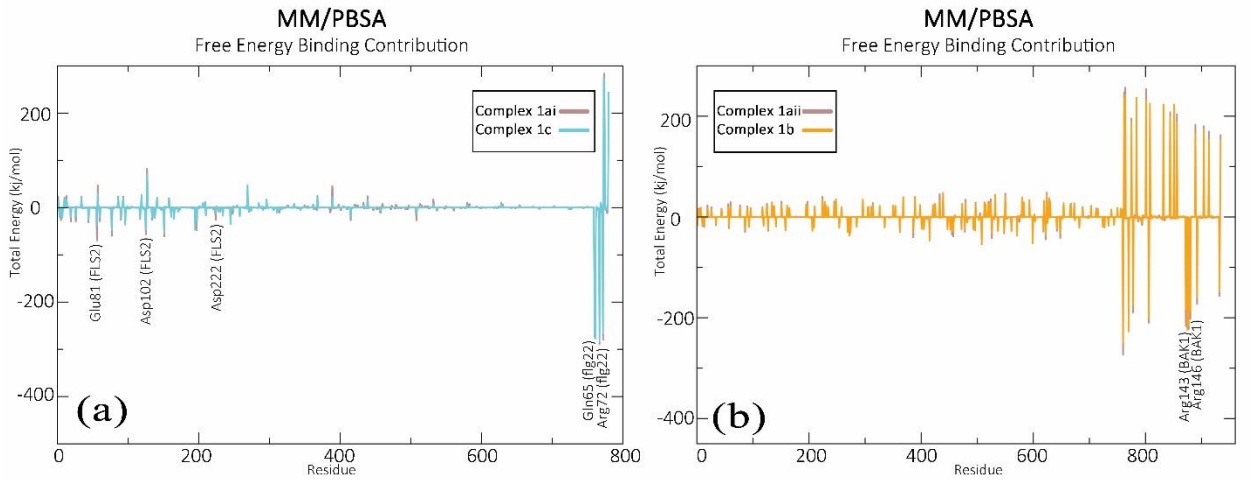

Fig 3.1.1: (a) MM/PBSA total energy value from 30ns MD trajectories. FLS2 and flg22 complex (brown) presence of co-receptor BAK1 inside the complex. FLS2 and flg22 complex (cyan) absence of co-receptor BAK1. (b) MM/PBSA total energy value from 30ns MD trajectories. FLS2 and BAK1 complex (brown) presence of PAMP flg22 inside the complex. FLS2 and BAK1 complex (orange) absence of PAMP flg22.

3.1.5 Complex 2aii vs Complex 2b

For HAESA with SERK1 (Table 3.6.2 and Table 3.6.4), numerous residues contribute greatly to binding energy that are – Lys337, Arg407, Arg503, Lys523 and Lys571 for HAESA; and Arg37, Lys142 and Arg144 for SERK1. Arg144 of SERK1 shows utmost binding free energy when it collaborates with HAESA which is -101.8198 ± 0.4057 kJmol^{-1} in complex 2aii and -102.9777 ± 0.3357 kJmol^{-1} in complex 2b. (Fig 3.1.2 b)

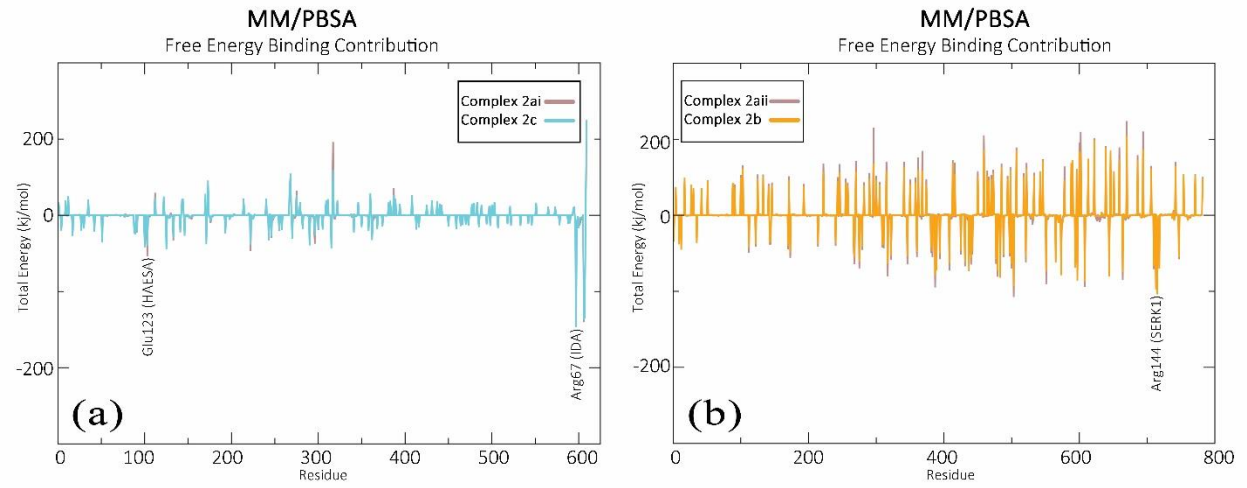

Fig 3.1.2: (a) MM/PBSA total energy value from 30ns MD trajectories. HAESA and IDA complex (brown) presence of co-receptor SERK1 inside the complex. HAESA and IDA complex (cyan) absence of co-receptor SERK1. (b) MM/PBSA total energy value from 30ns MD trajectories. HAESA and SERK1 complex (brown) presence of PAMP IDA inside the complex. HAESA and SERK1 complex (orange) absence of PAMP IDA.

3.1.6 Complex 3aii vs Complex 3c

For PSKR with SERK1 (Table 3.11.2 and Table 3.11.4), numerous residues contribute greatly to binding energy that are – Arg30, Lys87, Arg109, Lys113, Lys158, Arg492, Lys547, Lys548 and Lys599 for PSKR; and Glu29, Asp31, Asp42. Asp51, Glu68, Glu80 for SERK1. Asp42 of SERK1 shows utmost binding free energy when it collaborates with PSKR which is -38.6937 ± 0.249kJmol^{-1} in complex 3aii and -44.0446 ± 0.2704 kJmol^{-1} in complex 3b. (Fig 3.1.3 b)

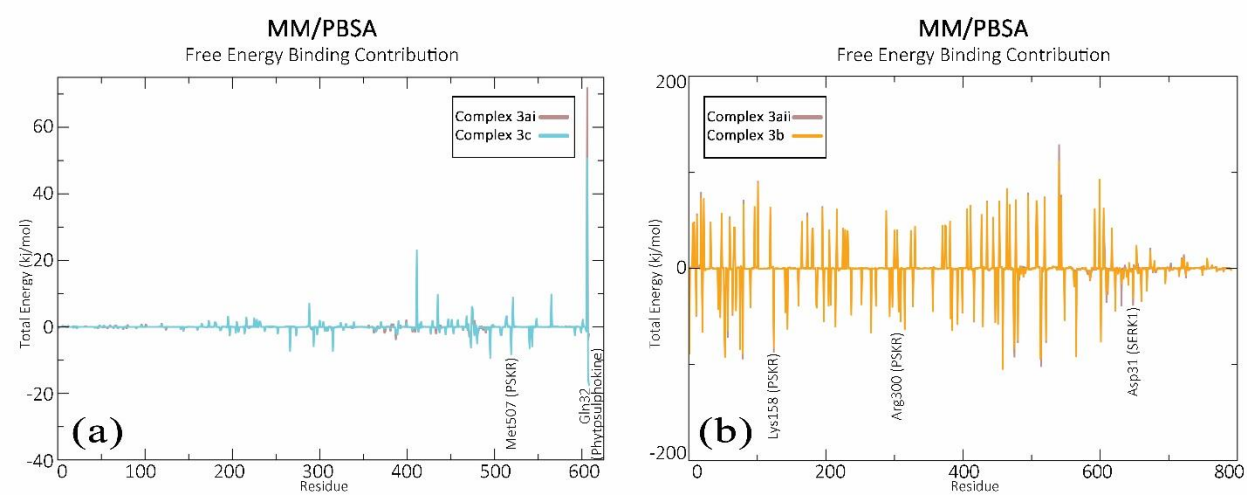

Fig 3.1.3: (a) MM/PBSA total energy value from 30ns MD trajectories. PSKR and Phytosulphokine complex (brown) presence of co-receptor SERK1 inside the complex. PSKR and Phytosulphokine complex (cyan) absence of co-receptor SERK1. (b) MM/PBSA total energy value from 30ns MD trajectories. PSKR and SERK1 complex (brown) presence of PAMP Phytosulphokine inside the complex. HAESA and SERK1 complex (orange) absence of PAMP Phytosulphokine.

3.1.7 Protein Interaction Calculator (PIC)

Protein Interaction Calculator (PIC), an online server was used to analyze the residues engaged in interactions both before and after the MD simulation.

During FLS2-flg22 collaboration, from the list of the residues which were discovered to be the most dynamic from the MM/PBSA calculation, only Arg72 and Lys77 from flg22 participated in various interactions both before and after the simulation. Arg72 form the protein-protein main chain – side chain hydrogen bond with FLS2 (Gln268) before simulation and protein-protein side chain – side chain hydrogen bond form with FLS2 (Gln268) after simulation and only Lys77 participates in ionic interaction with FLS2(Glu249) after simulation in complex 1c. Again, for the FLS2 and BAK1 interaction (complex 1aii an complex 1b), Lys673 of FLS2 participate in protein protein main chain – side chain hydrogen interaction with BAK1 residues (Arg143) after the simulation. From BAK1, Arg143 and Arg146 participate in protein protein side chain – side chain hydrogen interaction and ionic interaction with Asn674, Asp698, Met650 and Glu649 from FLS2 after the simulation in complex 1aii and complex 1b. (Table 3.2.1 – 3.4.4)

For the HAESA-IDA interaction, from the list of the residues which were discovered to be the most dynamic from the MM/PBSA calculation, only Tyr56 and Arg67 from IDA participated in various interactions both before and after the simulation. Arg67 form the protein-protein main chain – side chain hydrogen bond with HAESA (Lys337) before simulation and protein-protein side chain – side chain hydrogen bond form with HAESA (Met293) after simulation and only Tyr56 participates in hydrophobic interaction with HAESA(Tyr97) before simulation in complex 2c. Similarly, for HAESA, only Glu123 plays an essential function by participating in different interaction before and after simulation, basically for hydrogen bond with Val57 of IDA. Again, for the HAESA and SERK1 interaction (complex 2aii complex 2b), Lys571 of HAESA participate in in protein-protein cation-pi interaction and ionic interaction with SERK1 residues (Asp123, Tyr125) after the simulation. From SERK1 only Arg144 participates in an ionic interaction with Asp598 from HAESA after the simulation both complex 2aii and complex 2b. (Table 3.7.1 – 3.9.4)

In PSKR- Phytosulphokine interaction, from the list of the residues which were discovered to be the most dynamic from the MM/PBSA calculation, only Thr31 from phytosulphokine participated in various interactions both before and after the simulation. Thr31 of Phytosulphokine forms the protein-protein side chain – side chain hydrogen bond with PSKR (Ser370) in both complex 3ai and complex 3c and protein-protein main chain – side chain hydrogen bond with PSKR (Ser372, Phe506) only in complex 3c. Similarly, for PSKR, only Met507 plays an essential function by participating in hydrophobic interaction with Ile29 of Phytosulphokine after the simulation. Again, for the PSKR and SERK1 interaction (complex 3aii an complex 3b), Lys158 of PSKR participate in protein-protein ionic interaction with SERK1 residues (Asp31) after the simulation. From SERK1 only Asp31 participates in an ionic interaction with Lys158 from PSKR after the simulation both complex 3aii and complex 3b. (Table 3.12.1 – 3.14.4)

3.2 RMS Fluctuation (RMSF) of different complexes

RMS Fluctuations of the residues for all the simulated complexes were computed from the 30 ns MD trajectories.

3.2.1 Complex 1ai vs Complex 1c

Here, maximum residues fluctuated lower than 0.40 nm for FLS2, 0.35 nm for flg22 and 0.30 nm for BAK1. In addition, minimal fluctuation was shown by the residues of FLS2 (Glu81, Asp102, Asp150, Asp176, Asp222) that showed the most promising MM/PBSA values, in both complex 1ai and 1c. Glu81, Asp102 and Asp222 of FLS2 were denoted as the most prominent residue in the MM/PBSA, gave the lowest fluctuation (0.28 nm, 0.20 nm and 0.17 nm) in complex 1ai, as well as the second-lowest fluctuation (0.31 nm, 0.25 nm and 0.18 nm) in complex 1c. Again, the residues of FLS2 that fluctuated maximum are Ile54 (0.43 nm) and Asn770 (0.70 nm) for complex 1ai and Gln716 (0.49 nm) and His761 (0.82 nm) for complex 1c. In the case of flg22, Arg72 showed the lowest RMSF value of 0.34 nm in complex 1ai and a slightly decreased value of 0.30 nm in complex 1c. Another residue of flg22 is Gln65 with 0.27 nm in complex 1ai (considered as low fluctuating residue) but in complex 1c it gives 0.47 nm. (Fig 3.2.1 a)

3.2.2 Complex 2ai vs Complex 2c

Again, maximum residues fluctuated lower than 0.40 nm for HAESA, 0.11 nm for IDA and 0.30 nm for SERK1. In addition, minimal fluctuation was shown by the residues of HAESA (Asp120, Glu123, Glu145, Glu191, Asp242, Glu263, Glu266, Glu310, Glu316, Glu335 and Glu382) that showed the most promising MM/PBSA values, in both complex 2ai and 2c. Glu123 of HAESA was denoted as the most prominent residue in the MM/PBSA, gave the lowest fluctuation (0.24 nm) in complex 2ai, as well as the second-lowest fluctuation (0. 22 nm) in complex 2c. Again, the residues of HAESA that fluctuated maximum are Arg50 (0.76 nm) and Lys593 (0.42 nm) for both complex 2ai and complex 2c. In the case of IDA, Lys66 showed the lowest RMSF value of 0.13 nm in complex 2ai and a slightly raised value of 0.27 nm in complex 2c. Another residue of IDA is Arg67 with 0.16 nm in complex 2ai and 0.28 nm complex 2c, considered as low fluctuating residue. (Fig 3.2.2 a)

3.2.3 Complex 3ai vs Complex 3c

Moreover, maximum residues fluctuated lower than 0.40 nm for PSKR, 0.11 nm for Phytosulphokine and 0.30 nm for SERK1. In addition, minimal fluctuation was shown by the residues of PSKR (Arg300, Arg327, Met507, Arg514, Glu529, Asp553 and Glu574) that showed the most promising MM/PBSA values, in both complex 3ai and 3c. Arg300 of PSKR denoted as the most prominent residue in the MM/PBSA, gave the lowest fluctuation (0. 15 nm) in complex 3ai, as well as the second-lowest fluctuation (0. 13 nm) in complex 3c. Again, the residues of PSKR that fluctuated maximum are Asp51 (0.44 nm) and Ser57 (0.43 nm) for both complex 3ai and complex 3c. In the case of Phytosulphokine, Thr31 showed the lowest RMSF value of 0.08 nm in complex 3ai and a slightly went down value of 0.07 nm in complex 3c. Another low fluctuating residue of Phytosulphokine is Gln31 with 0.11 nm both in complex 3ai and complex 3c considered as low fluctuating residue. (Fig 3.2.3 a)

From this analysis it can be said that all of the complexes are fluctuated in almost same range and most fluctuated residues of PRR of all complexes are mostly from N-terminal and C-terminal. Moreover, PRRs and co-receptors of all of the complexes are fluctuated in a same range (less than 0.11 nm and 0.30 nm respectively). For PAMP, in every complex, two residues act as prominent by giving lower RMS fluctuation value than other residues. From PRR, N terminal residues show prominence for interacting with PAMP, though in complex 3, different view is found (Arg300 is the most prominent for PRR of complex 3).

3.2.4 Complex 1aii vs Complex 1b

When it comes to the FLS2 and BAK1 interaction, Arg533, Lys551, Lys624, Lys647, Lys673 of FLS2 gave significantly low fluctuations in both complex 1aii and complex 1b. The MM/PBSA values also disclosed that these particular residues provided more energy for interacting with BAK1. Additionally, Arg533 of FLS2 shows the lowest RMSF value both in complex 1aii (0.16nm) and complex 1b (0.15 nm) (Fig 3.2.1 b), which again addresses the results of the MM/PBSA calculation. Residues of FLS2 that fluctuated maximum in this situation were Asn770 in complex 1aii and Ile54 in complex 1b. Similarly, for BAK1, the residues (Asn26, Lys36, Lys44, Arg72, Arg138, Lys140, Lys141, Arg143, Arg146, Arg158 and Lys198) that had maximum energy contribution in the MM/PBSA also showed RMSF values that fluctuated minimum compared to the other residues of BAK1 (Fig 3.2.1 b). Among these residues, Lys44, Arg143 and

Arg146 showed the lowest fluctuation both in complex 1aii (0.26nm, 0.18nm and 0.18nm) and in complex 1b (0.19nm,0.15 nm and 0.18nm).

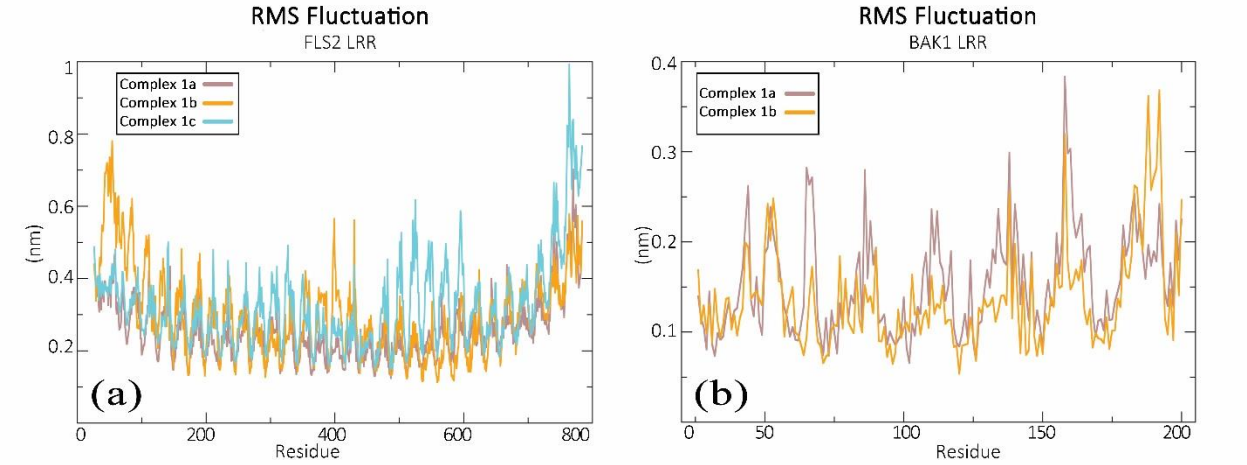

Fig 3.2.1: (a) RMSF value of FLS2 from 30ns MD trajectories. FLS2, flg22 complex (brown) presence of BAK1 in the complex, FLS2 and flg22 complex (cyan) absence of BAK1, FLS2 and BAK1 complex (orange) absence of flg22. (b) RMSF value of BAK1 from 30ns MD trajectories. FLS2, BAK1 complex (brown) in the presence of flg22, FLS2 and BAK1 complex (orange) absence of flg22.

3.2.5 Complex 2aii vs Complex 2b

In case of HAESA and SERK1 interaction, Lys337, Arg407, Arg503, Lys523 and Lys571 of HAESA gave significantly low fluctuations in both complex 2aii and complex 2b. The MM/PBSA values also disclosed that these particular residues provided more energy for interacting with SERK1. Additionally, Lys571 of HAESA shows the lowest RMSF value both in complex 2aii (0.27 nm) and complex 2b (0.27 nm) (Fig 3.2.2 b), which again addresses the results of the MM/PBSA calculation. Residues of HAESA that fluctuated maximum in this situation were Lys523. Similarly, for SERK1, the residues (Arg37, Lys142 and Arg144) that had maximum energy contribution in the MM/PBSA also showed RMSF values that fluctuated minimum compared to the other residues of SERK1 (Fig 3.2.2 b). Among these residues, Arg144 showed the lowest fluctuation both in complex 2aii (0.17 nm) and in complex 2c (0.14 nm).

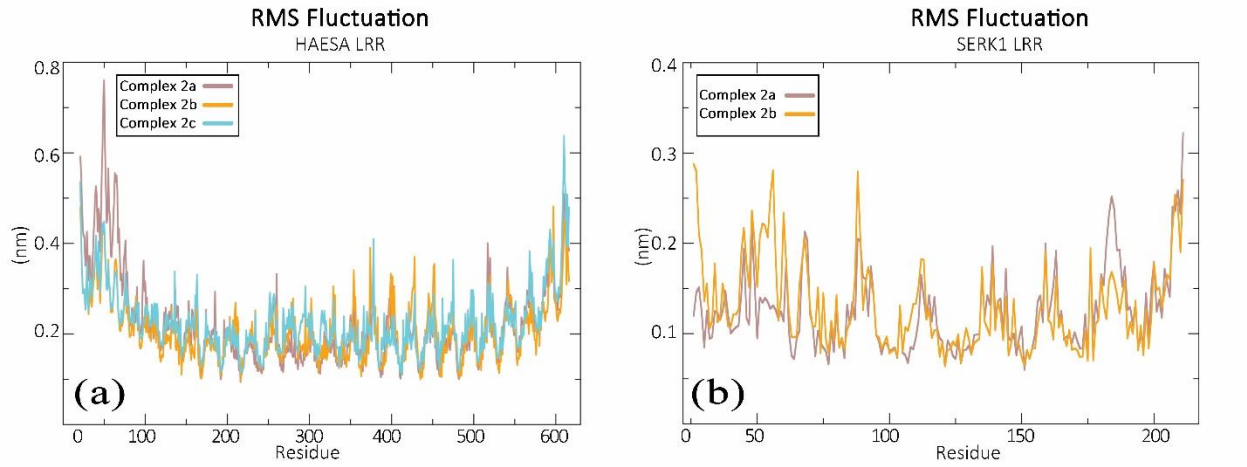

Fig 3.2.2: (a) RMSF value of HAESA from 30ns MD trajectories. HAESA, IDA complex (brown) presence of SERK1 in the complex, HAESA and IDA complex (cyan) absence of SERK1, HAESA and SERK1 complex (orange) absence of IDA. (b) RMSF value of SERK1 from 30ns MD trajectories. HAESA, SERK1 complex (brown) in the presence of IDA, HAESA and SERK1 complex (orange) absence of IDA.

3.2.6 Complex 3aii vs Complex 3b

In terms of PSKR and SERK1 interaction, Arg30, Lys87, Arg109, Lys113, Lys158, Arg492, Lys547, Lys548 and Lys599 of PSKR gave significantly low fluctuations in both complex 3aii and complex 3b. The MM/PBSA values also disclosed that these particular residues provided more energy for interacting with SERK1. Additionally, Lys158 of PSKR shows the lowest RMSF value both in complex 3aii and complex 3b (0.18 nm and 0.23 nm, respectively) (Fig 3.2.3 b), which again addresses the results of the MM/PBSA calculation. Residues of PSKR that fluctuated maximum in this situation were Asp51 and Ser57. Similarly, for SERK1, the residues (Glu29, Asp31, Asp42. Asp51, Glu68 and Glu80) that had maximum energy contribution in the MM/PBSA also showed RMSF values that fluctuated minimum compared to the other residues of SERK1 (Fig 3.2.3 b). Among these residues, Asp31 showed the lowest fluctuation both in complex 3aii (0.16 nm) and in complex 3c (0.14 nm).

From this, it is easily observed that C-terminal residues of PRRs are more responsible for interacting with co-receptors. Though for complex 3, N -terminal residue (Lys158) of PRR shows prominence for interacting with co-receptor. Overall, most of the characteristics of all of the complexes shows similarity.

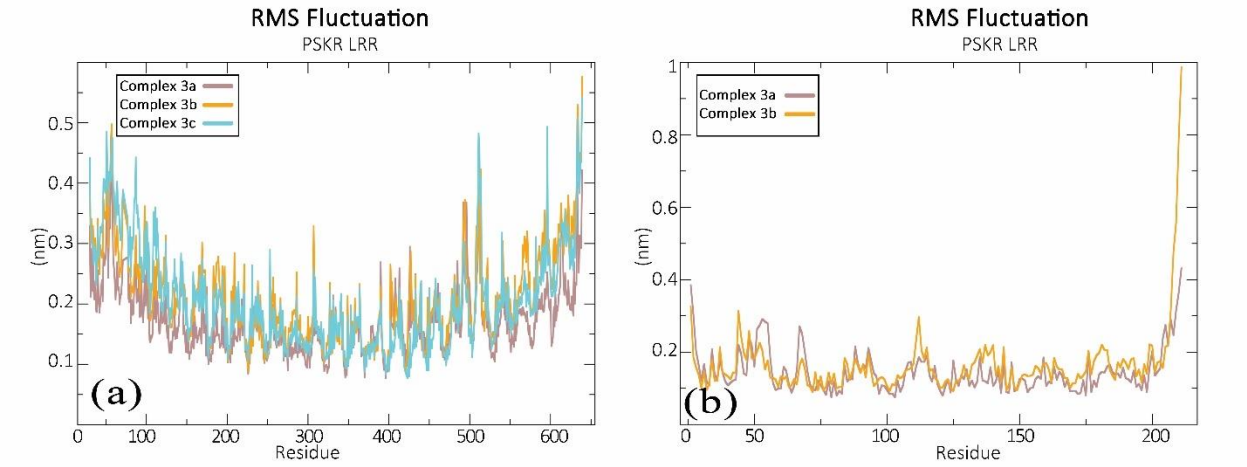

Fig 3.2.3: (a) RMSF value of PSKR from 30ns MD trajectories. PSKR, Phytosulphokine complex (brown) presence of SERK1 in the complex, PSKR and Phytosulphokine complex (cyan) absence of SERK1, PSKR and SERK1 complex (orange) absence of Phytosulphokine. (b) RMSF value of SERK1 from 30ns MD trajectories. PSKR, SERK1 complex (brown) in the presence of Phytosulphokine, PSKR and SERK1 complex (orange) absence of Phytosulphokine.

3.3 Determination of the prominent residues of PRR, PAMP and co-receptor

Synopsis of MM/PBSA calculations beside a detailed analysis of the energy contribution of every residue, PIC, and RMSF data, number of residues can be determined as the key role player in the interactions to happen between PRRs, PAMPs and co-receptors.

3.3.1 Complex 1

For the interaction between FLS2 and flg22, Glu81, Asp102 and Asp222 of FLS2 and seem to be these residues as showed by the maximum MM energy contribution (-90.0458 kJmol^{-1} , -100.3252 kJmol^{-1} and -76.1088 kJmol^{-1} for complex 1ai and -38.5397 kJmol^{-1} , -73.8161 kJmol^{-1} and -99.8434 kJmol^{-1} for complex 1c, respectively), minimum RMS fluctuation, the minimum non-polar energy, contribution in hydrogen bond formation and giving electrostatic energy for increasing binding affinity with flg22. At the time, similar analysis of the interactions between FLS2 and BAK1 is performed, Arg533 of FLS2 is discovered to be the most striking in every point (MM/PBSA, PIC and RMSF calculation). In complex 1aii, this residue gives -62.0426 kJmol^{-1} MM energy (which basically rises from electrostatic energy and little bit contributions from Van Der Waals energy) and in complex 1b, it gives -78.8675 kJmol^{-1} MM energy which is maximum in contrast to the other residues of FLS2. For flg22, as Gln65 and Arg72 provided greater MM

energy for interacting with FLS2 also engages in more interactions (protein-protein main chain-side chain hydrogen bond, protein protein side chain-side chain hydrogen bond and ionic interaction) with FLS2. Therefore, it can be pronounced as being prominent residue for the interaction with FLS2. For BAK1, Arg143 and Arg146 indicated supremacy when interacting with FLS2 with -239.1713 $kJmol^{-1}$ and -208.7224 $kJmol^{-1}$ MM energy which is maximum than rest of the residues of BAK1 in complex 1aii. In complex 1b, the MM energy of Arg143 and Arg146 are -293.1195 $kJmol^{-1}$ and 214.3675 $kJmol^{-1}$, which is also higher in contrast of the other residues of BAK1. While plotting a low RMS fluctuation, Arg143 also contributes in an ionic interaction beside hydrogen bond with FLS2 which causes this residue a perfect nominee for being a prominent residue. Therefore, from FLS2 Glu81, Asp102 and Asp222 from flg22 Gln65 and Arg72 and Arg143 and Arg146 of BAK1 are the most important residues when making interactions between these three proteins.

3.3.2 Complex 2

During the interaction of HAESA and IDA, Glu123 of HAESA seem to be these residues as showed by the maximum MM energy contribution (-61.3487 $kJmol^{-1}$ for complex 2ai and 104.9555 $kJmol^{-1}$ for complex 2c, respectively), minimum RMS fluctuation, the minimum non-polar energy, contribution in hydrogen bond formation and giving electrostatic energy for increasing binding affinity with IDA. At the time, similar analysis of the interactions between HAESA and SERK1 is performed, Lys571 of HAESA is is discovered to be the most striking in every point (MM/PBSA, PIC and RMSF calculation). In complex 2aii, it gives -141.1142 $kJmol^{-1}$ MM energy (which basically rises from electrostatic energy and little bit contributions from Van Der Waals energy) and in complex 2b, it gives -180.0614 $kJmol^{-1}$ MM energy which is maximum in contrast of the other residues of HAESA. Moreover, Lys158 of HAESA also participates in hydrogen bond with low RMS fluctuation. For IDA, though Arg67 provided greater MM energy for interacting with HAESA also engages in more interactions (protein-protein main chain-side chain hydrogen bond, protein protein side chain-side chain hydrogen bond and ionic interaction) with HAESA. Therefore, it can be pronounced as being prominent residues for the interaction with HAESA. For SERK1, Arg144 indicated supremacy when interacting with HAESA with -158.9823 $kJmol^{-1}$ MM energy which is maximum than rest of the residues of SERK1 in complex 2aii. In complex 2b, the MM energy of Arg144 is -161.4613 $kJmol^{-1}$, which is also higher in contrast of the other residues of SERK1. While plotting a low RMS fluctuation, Arg144 also contributes in

an ionic interaction beside hydrogen bond with HAESA which causes this residue a perfect nominee for being a prominent residue. Therefore, from HAESA Glu123 from IDA Arg67 and Arg144 of SERK1 are the most important residues when making interactions between these three proteins.

3.3.3 Complex 3

In case of PSKR and Phytosulphokine interaction, Arg300 and Met507 of PSKR seem to be these residues as showed by the maximum MM energy contribution (-13.9191 $kJmol^{-1}$ and -5.8067 $kJmol^{-1}$ for complex 3ai and -11.6455 $kJmol^{-1}$ and -12.7059 $kJmol^{-1}$ complex 3c, respectively), minimum RMS fluctuation, the minimum non-polar energy, contribution in hydrogen bond formation and giving electrostatic energy for increasing binding affinity with Phytosulphokine. At the time, similar analysis of the interactions between PSKR and SERK1 is performed, Lys158 of PSKR is discovered to be the most striking in every point (MM/PBSA, PIC and RMSF calculation). In complex 3aii, it gives -87.6139 $kJmol^{-1}$ MM energy (which basically rises from electrostatic energy and little bit contributions from Van Der Waals energy) and in complex 3b, it gives -87.0473 $kJmol^{-1}$ MM energy which is maximum in contrast of the other residues of PSKR. Moreover, Lys158 of PSKR also participates in ionic interaction with low RMS fluctuation. For Phytosulphokine, though Gln32 provided greater MM energy for interacting with PSKR, Thr31 engages in more interactions (protein-protein main chain-side chain hydrogen bond, protein-protein side chain-side chain hydrogen bond) with PSKR. Therefore, both of these residues can be pronounced as being prominent residues for the interaction with PSKR. For SERK1, Asp31 indicated supremacy when interacting with PSKR with -28.7104 $kJmol^{-1}$ MM energy which is maximum than rest of the residues of SERK1 in complex 3aii. In complex 3b, the MM energy of Asp31 is -26.2942 $kJmol^{-1}$, which is higher in contrast of the other residues of SERK1. While plotting a low RMS fluctuation, Asp31 also contributes in an ionic interaction with Lys158 of PSKR which causes this residue a perfect nominee for being a prominent residue. Therefore, from PSKR Lys158, Arg300 and Met507 from Phytosulphokine Thr31 and Gln32 and Asp31 of SERK1 are the most important residues when making interactions between these three proteins.

Though there are many important residues but in from of Van Der Waals energy contribution, electrostatic energy contribution, hydrogen bond creation, hydrophobic interactions along with

cation-pi interaction these residues perform the most essential role in PRR mediated pattern triggered immune complex formation.

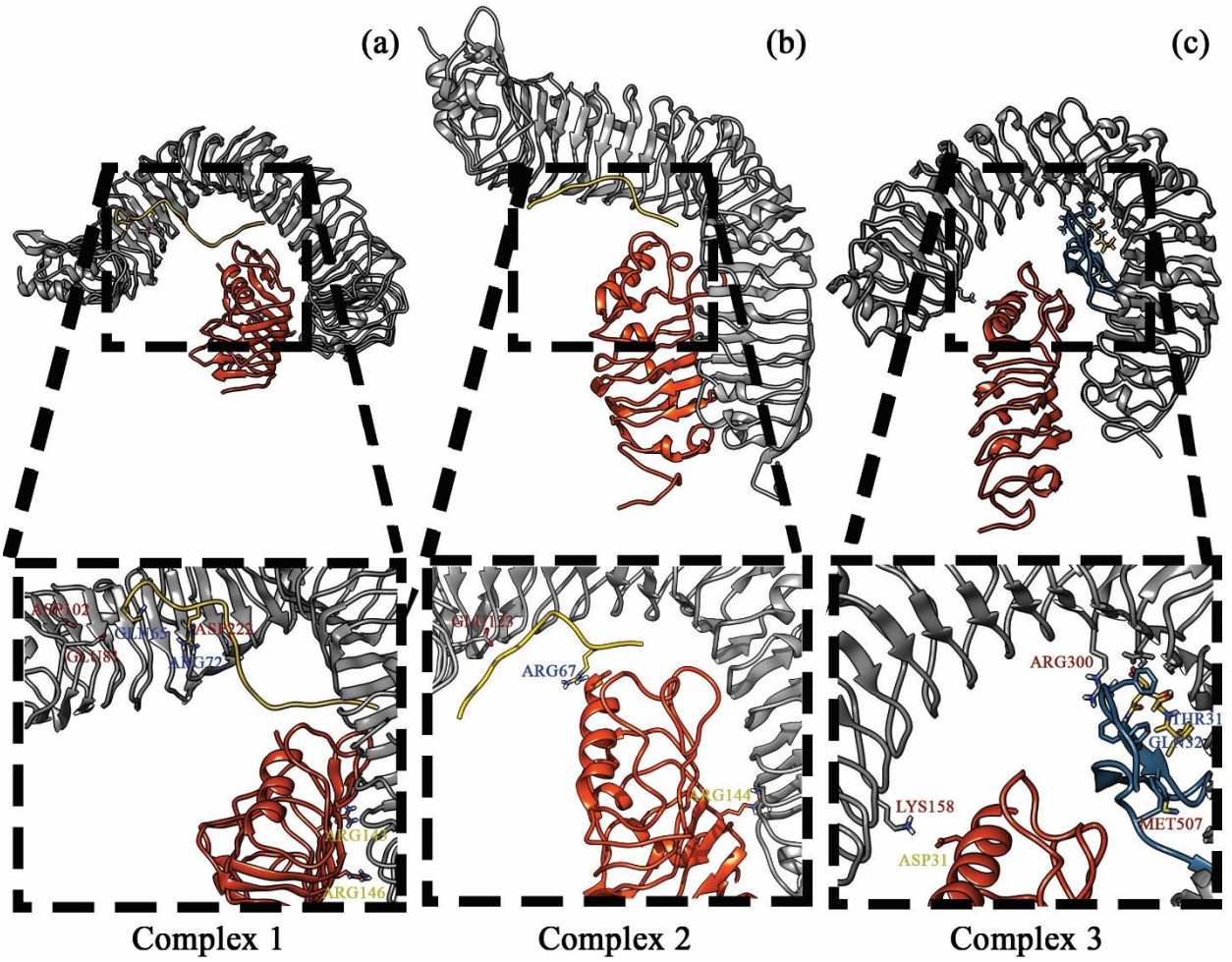

Fig 3.3.1: Visualization of binding pattern of prominent residues. (a) Prominent residues of complex 1 (FLS2-flg22-BAK1); (b) Prominent residues of complex 2 (HAESA-IDA-SERK1); (c) Prominent residues of complex 3 (PSKR-Phytosulphokine-SERK1).

Table 3.1.1: Binding free energy contribution of the key binding-site residues calculated from the binding energy decomposition for FLS2 (kJmol-1) 1ai and complex 1c.

Residue	MM Energy	Polar Energy	APolar Energy	Total Energy
GLU-28	-19.4845 ± 0.0382	0.3311 ± 0.0043	0.0000 ± 0.0000	-19.1528 ± 0.0359
GLU-28	-18.0550 ± 0.0662	0.2769 ± 0.0046	0.0000 ± 0.0000	-17.7792 ± 0.0610
GLU-30	-28.6200 ± 0.1151	2.0768 ± 0.0298	0.0000 ± 0.0000	-26.5405 ± 0.0976
GLU-30	-19.7693 ± 0.1191	0.5626 ± 0.0135	0.0000 ± 0.0000	-19.2042 ± 0.1068
GLU-32	-20.8500 ± 0.0431	0.5188 ± 0.0066	0.0000 ± 0.0000	-20.3319 ± 0.0389
GLU-32	-22.5424 ± 0.0884	1.0410 ± 0.0175	0.0000 ± 0.0000	-21.5013 ± 0.0751
ASP-44	-31.4971 ± 0.0644	2.0355 ± 0.0232	0.0000 ± 0.0000	-29.4620 ± 0.0571
ASP-44	-21.1642 ± 0.1732	0.8423 ± 0.0192	0.0000 ± 0.0000	-20.3154 ± 0.1502
ASP-51	-29.6718 ± 0.0882	0.7059 ± 0.0116	0.0000 ± 0.0000	-28.9633 ± 0.0814
ASP-51	-20.6295 ± 0.1591	0.3017 ± 0.0077	0.0000 ± 0.0000	-20.3275 ± 0.1562
ASP-69	-31.5962 ± 0.1236	0.7920 ± 0.0113	0.0000 ± 0.0000	-30.8003 ± 0.1175
ASP-69	-26.8477 ± 0.1138	0.7482 ± 0.0149	0.0000 ± 0.0000	-26.1025 ± 0.1017
GLU-81	-90.0458 ± 0.6579	20.9048 ± 0.9775	-0.1250 ± 0.0105	-69.2440 ± 0.4505
GLU-81	-38.5397 ± 0.5955	1.0855 ± 0.0789	-0.0006 ± 0.000	-37.4501 ± 0.5265
GLU-85	-29.8446 ± 0.0783	1.3567 ± 0.0133	0.0000 ± 0.0000	-28.4879 ± 0.0705
GLU-85	-20.0436 ± 0.1685	0.5948 ± 0.0127	0.0000 ± 0.0000	-19.4384 ± 0.1541
ASP-102	-100.3252 ± 0.5398	40.8126 ± 0.8133	-0.1204 ± 0.0055	-59.6585 ± 0.3835
ASP-102	-73.8161 ± 1.1619	27.2252 ± 1.0214	-0.1144 ± 0.00	-46.6974 ± 0.3513
GLU-115	-28.3988 ± 0.0710	2.6162 ± 0.0286	0.0000 ± 0.0000	-25.7802 ± 0.0480
GLU-115	-22.9813 ± 0.0887	1.2188 ± 0.0271	0.0000 ± 0.0000	-21.7644 ± 0.0665
GLU-121	-34.7442 ± 0.1183	2.7372 ± 0.0374	0.0000 ± 0.0000	-32.0110 ± 0.0970
GLU-121	-38.5382 ± 0.1799	2.5087 ± 0.0434	0.0000 ± 0.0000	-36.0315 ± 0.1439
GLU-142	-24.5895 ± 0.0539	1.0375 ± 0.0194	0.0000 ± 0.0000	-23.5512 ± 0.0417
GLU-142	-22.6567 ± 0.0669	0.8541 ± 0.0124	0.0000 ± 0.0000	-21.8071 ± 0.0571
ASP-150	-96.6032 ± 0.3161	40.3577 ± 0.3450	-0.1016 ± 0.0040	-56.3387 ± 0.2799
ASP-150	-75.8885 ± 0.5030	29.7044 ± 0.5237	-0.1536 ± 0.00	-46.3433 ± 0.3625
ASP-159	-26.8487 ± 0.1035	1.8199 ± 0.0314	0.0000 ± 0.0000	-25.0262 ± 0.0832
ASP-159	-22.0777 ± 0.0879	1.8251 ± 0.0302	0.0000 ± 0.0000	-20.2476 ± 0.0856
GLU-162	-19.7677 ± 0.0592	0.4699 ± 0.0091	0.0000 ± 0.0000	-19.2975 ± 0.0525
GLU-162	-22.4746 ± 0.0893	1.6320 ± 0.0322	0.0000 ± 0.0000	-20.8466 ± 0.0688
GLU-163	-22.3777 ± 0.0674	0.8109 ± 0.0137	0.0000 ± 0.0000	-21.5679 ± 0.0570
GLU-163	-23.8901 ± 0.0703	1.7851 ± 0.0318	0.0000 ± 0.0000	-22.1069 ± 0.0528
ASP-176	-76.2167 ± 0.4546	15.5832 ± 0.5680	-0.0547 ± 0.0052	-60.7058 ± 0.3107
ASP-176	-67.5414 ± 0.3154	15.1742 ± 0.3589	-0.0082 ± 0.00	-52.3653 ± 0.2984
GLU-186	-16.2290 ± 0.0435	0.1707 ± 0.0053	0.0000 ± 0.0000	-16.0572 ± 0.0401
GLU-186	-21.1386 ± 0.1218	1.5706 ± 0.0430	0.0000 ± 0.0000	-19.5647 ± 0.0849
ASP-190	-20.3069 ± 0.0661	0.3490 ± 0.0067	0.0000 ± 0.0000	-19.9589 ± 0.0603
ASP-190	-26.0005 ± 0.1171	1.8109 ± 0.0409	0.0000 ± 0.0000	-24.1830 ± 0.0868
ASP-220	-102.7353 ± 0.9134	71.0623 ± 1.0337	-1.0737 ± 0.0106	-32.7612 ± 0.3109
ASP-220	-101.9139 ± 0.8422	55.7213 ± 1.0748	-0.3726 ± 0.0	-46.6020 ± 0.4648
ASP-222	-76.1088 ± 0.8202	28.6178 ± 1.3963	-0.4044 ± 0.0152	-47.8386 ± 0.6863

ASP-222	-99.8434 ± 1.1204	73.3728 ± 1.9277	-0.6222 ± 0.01	-27.0650 ± 0.9259
ASP-235	-16.8366 ± 0.0492	0.1961 ± 0.0082	0.0000 ± 0.0000	-16.6412 ± 0.0440
ASP-235	-17.3424 ± 0.0996	0.7887 ± 0.0368	0.0000 ± 0.0000	-16.5553 ± 0.0818
GLU-249	-42.4935 ± 0.6814	16.7908 ± 0.9077	-0.1254 ± 0.0077	-25.8392 ± 0.3562
GLU-249	-54.0632 ± 0.9351	44.0061 ± 1.4235	-0.3888 ± 0.01	-10.4966 ± 0.6944
GLU-259	-15.8402 ± 0.0730	-0.0676 ± 0.0150	0.0000 ± 0.0000	-15.9080 ± 0.0647
GLU-259	-17.5980 ± 0.1538	0.5402 ± 0.0370	0.0000 ± 0.0000	-17.0578 ± 0.1195
GLU-283	-11.5215 ± 0.1147	-1.0685 ± 0.0232	0.0000 ± 0.0000	-12.5905 ± 0.0978
GLU-283	-19.6635 ± 0.3067	1.2231 ± 0.1024	0.0000 ± 0.0000	-18.4345 ± 0.2150
LYS-411	-13.4173 ± 0.2721	3.4140 ± 0.0840	-0.0010 ± 0.0005	-10.0068 ± 0.2467
LYS-411	-2.6458 ± 0.2152	2.4582 ± 0.0403	0.0000 ± 0.0000	-0.1933 ± 0.2205
ARG-440	-37.7830 ± 0.5015	11.4237 ± 0.4639	-0.0843 ± 0.0083	-26.4514 ± 0.2262
ARG-440	-25.3337 ± 0.6116	5.9638 ± 0.4419	-0.0184 ± 0.003	-19.3850 ± 0.3145
ARG-482	-14.1700 ± 0.1772	3.3370 ± 0.0297	0.0000 ± 0.0000	-10.8369 ± 0.1662
ARG-482	-8.2884 ± 0.3165	1.9342 ± 0.1462	-0.0108 ± 0.0026	-6.3597 ± 0.2234
ARG-533	-30.4169 ± 0.1918	3.7812 ± 0.0661	0.0000 ± 0.0000	-26.6458 ± 0.1614
ARG-533	-13.0712 ± 0.3080	0.9952 ± 0.0652	0.0000 ± 0.0000	-12.0820 ± 0.2572

Table 3.1.2: Binding free energy contribution of the key binding-site residues calculated from the binding energy decomposition for FLS2 (kJmol-1) from complex 1aii and complex 1b

Residue	MM Energy	Polar Energy	APolar Energy	Total Energy
SER-26	-15.9915 ± 0.0750	-0.0006 ± 0.0001	0.0000 ± 0.0000	-15.9878 ± 0.0742
SER-26	-14.6535 ± 0.0349	0.0001 ± 0.0000	0.0000 ± 0.0000	-14.6554 ± 0.0348
LYS-35	-17.7742 ± 0.0843	-0.0014 ± 0.0001	0.0000 ± 0.0000	-17.7717 ± 0.0834
LYS-35	-15.8445 ± 0.0429	-0.0001 ± 0.0000	0.0000 ± 0.0000	-15.8456 ± 0.0415
LYS-38	-19.6544 ± 0.0811	-0.0033 ± 0.0001	0.0000 ± 0.0000	-19.6613 ± 0.0819
LYS-38	-16.3515 ± 0.0583	-0.0004 ± 0.0000	0.0000 ± 0.0000	-16.3487 ± 0.0594
ARG-59	-16.1091 ± 0.0643	-0.0003 ± 0.0000	0.0000 ± 0.0000	-16.1106 ± 0.0627
ARG-59	-14.1435 ± 0.0422	0.0000 ± 0.0000	0.0000 ± 0.0000	-14.1450 ± 0.0421
LYS-82	-21.7761 ± 0.0927	-0.0085 ± 0.0003	0.0000 ± 0.0000	-21.7847 ± 0.0903
LYS-82	-17.4314 ± 0.0683	-0.0012 ± 0.0001	0.0000 ± 0.0000	-17.4345 ± 0.0687
LYS-111	-29.7465 ± 0.3323	-0.0607 ± 0.0035	0.0000 ± 0.0000	-29.8105 ± 0.3311
LYS-111	-24.4953 ± 0.0942	-0.0133 ± 0.0003	0.0000 ± 0.0000	-24.5051 ± 0.0955
LYS-118	-19.3987 ± 0.1302	-0.0056 ± 0.0003	0.0000 ± 0.0000	-19.4054 ± 0.1273
LYS-118	-17.6371 ± 0.0387	-0.0006 ± 0.0000	0.0000 ± 0.0000	-17.6363 ± 0.0402
LYS-144	-17.1785 ± 0.0999	-0.0030 ± 0.0004	0.0000 ± 0.0000	-17.1850 ± 0.1010
LYS-144	-16.7485 ± 0.0439	0.0000 ± 0.0000	0.0000 ± 0.0000	-16.7497 ± 0.0445
ARG-152	-26.9197 ± 0.1372	-0.0586 ± 0.0024	0.0000 ± 0.0000	-26.9759 ± 0.1430
ARG-152	-23.1382 ± 0.0704	-0.0171 ± 0.0006	0.0000 ± 0.0000	-23.1562 ± 0.0711
LYS-166	-18.2077 ± 0.1110	-0.0062 ± 0.0007	0.0000 ± 0.0000	-18.2162 ± 0.1120
LYS-166	-18.7222 ± 0.0468	-0.0015 ± 0.0001	0.0000 ± 0.0000	-18.7259 ± 0.0469
LYS-183	-26.0588 ± 0.2582	-0.0567 ± 0.0056	0.0000 ± 0.0000	-26.1072 ± 0.2671
LYS-183	-25.3940 ± 0.0972	-0.0165 ± 0.0005	0.0000 ± 0.0000	-25.4146 ± 0.0978
LYS-231	-16.0171 ± 0.1706	-0.0057 ± 0.0040	0.0000 ± 0.0000	-16.0220 ± 0.1658

LYS-231	-27.3464 ± 0.1518	-0.0350 ± 0.0013	0.0000 ± 0.0000	-27.3824 ± 0.1509
ARG-234	-16.1870 ± 0.1036	-0.0064 ± 0.0021	0.0000 ± 0.0000	-16.1865 ± 0.1021
ARG-234	-20.9224 ± 0.0651	0.0042 ± 0.0004	0.0000 ± 0.0000	-20.9221 ± 0.0663
LYS-279	-17.7744 ± 0.0682	-0.0290 ± 0.0017	0.0000 ± 0.0000	-17.8024 ± 0.0658
LYS-279	-21.4911 ± 0.0634	0.0062 ± 0.0005	0.0000 ± 0.0000	-21.4860 ± 0.0624
ARG-294	-29.0031 ± 0.1433	-0.2425 ± 0.0088	0.0000 ± 0.0000	-29.2410 ± 0.1468
ARG-294	-27.8489 ± 0.0822	0.1200 ± 0.0046	0.0000 ± 0.0000	-27.7267 ± 0.0860
LYS-297	-30.7376 ± 0.5138	-6.3434 ± 0.5023	-0.0968 ± 0.0077	-37.1470 ± 0.3420
LYS-297	-36.4048 ± 0.2390	-0.5302 ± 0.0880	-0.0038 ± 0.0013	-36.9472 ± 0.2461
LYS-299	-22.4588 ± 0.2617	-0.3817 ± 0.0327	0.0000 ± 0.0000	-22.8434 ± 0.2598
LYS-299	-31.1889 ± 0.1310	-0.0864 ± 0.0127	0.0000 ± 0.0000	-31.2811 ± 0.1371
ARG-310	-19.1432 ± 0.0524	-0.0189 ± 0.0021	0.0000 ± 0.0000	-19.1627 ± 0.0521
ARG-310	-19.8395 ± 0.0371	0.0677 ± 0.0013	0.0000 ± 0.0000	-19.7729 ± 0.0374
ARG-360	-20.4248 ± 0.0567	0.0166 ± 0.0013	0.0000 ± 0.0000	-20.4098 ± 0.0574
ARG-360	-20.6660 ± 0.0425	0.1048 ± 0.0021	0.0000 ± 0.0000	-20.5610 ± 0.0413
ARG-387	-29.9253 ± 0.1397	0.1145 ± 0.0073	0.0000 ± 0.0000	-29.8154 ± 0.1357
ARG-387	-28.5670 ± 0.1305	0.3379 ± 0.0111	0.0000 ± 0.0000	-28.2230 ± 0.1251
LYS-411	-40.6331 ± 0.2510	0.8054 ± 0.0656	-0.0072 ± 0.0018	-39.8483 ± 0.2344
LYS-411	-31.7625 ± 0.1290	1.2891 ± 0.0271	0.0000 ± 0.0000	-30.4747 ± 0.1261
ARG-426	-23.0395 ± 0.0564	0.1957 ± 0.0053	0.0000 ± 0.0000	-22.8447 ± 0.0558
ARG-426	-24.0706 ± 0.0524	0.6006 ± 0.0089	0.0000 ± 0.0000	-23.4680 ± 0.0481
ARG-430	-24.3269 ± 0.1008	0.1320 ± 0.0088	0.0000 ± 0.0000	-24.1939 ± 0.0961
ARG-430	-23.7841 ± 0.0648	0.5204 ± 0.0126	0.0000 ± 0.0000	-23.2602 ± 0.0612
ARG-440	-41.6006 ± 0.2327	-0.0764 ± 0.0179	-0.0001 ± 0.0001	-41.6839 ± 0.2284
ARG-440	-48.9536 ± 0.2416	2.4446 ± 0.1685	-0.0482 ± 0.0073	-46.5661 ± 0.2258
LYS-472	-24.2086 ± 0.0559	0.2848 ± 0.0068	0.0000 ± 0.0000	-23.9277 ± 0.0503
LYS-472	-24.8371 ± 0.0498	0.5332 ± 0.0086	0.0000 ± 0.0000	-24.3007 ± 0.0465
LYS-477	-25.2419 ± 0.0651	0.3401 ± 0.0102	0.0000 ± 0.0000	-24.9003 ± 0.0579
LYS-477	-24.6035 ± 0.0678	0.5847 ± 0.0144	0.0000 ± 0.0000	-24.0190 ± 0.0613
LYS-480	-36.0861 ± 0.2253	0.8720 ± 0.0464	0.0000 ± 0.0000	-35.2230 ± 0.2014
LYS-480	-30.0784 ± 0.1766	1.7437 ± 0.0471	0.0000 ± 0.0000	-28.3394 ± 0.1521
ARG-482	-61.1845 ± 0.8006	23.8251 ± 0.9073	-0.8044 ± 0.0231	-38.1284 ± 0.3214
ARG-482	-57.9774 ± 0.7019	30.0664 ± 0.8126	-0.9307 ± 0.0189	-28.8812 ± 0.3135
ARG-497	-24.3894 ± 0.0621	0.2053 ± 0.0072	0.0000 ± 0.0000	-24.1830 ± 0.0543
ARG-497	-25.3001 ± 0.0557	0.6430 ± 0.0150	0.0000 ± 0.0000	-24.6570 ± 0.0481
LYS-503	-29.5365 ± 0.1581	0.4078 ± 0.0500	-0.0002 ± 0.0002	-29.1285 ± 0.1255
LYS-503	-24.2899 ± 0.1732	0.5294 ± 0.0721	-0.0012 ± 0.0008	-23.7603 ± 0.1463
ARG-518	-23.9290 ± 0.0457	0.2349 ± 0.0050	0.0000 ± 0.0000	-23.6935 ± 0.0423
ARG-518	-24.3917 ± 0.0524	0.3851 ± 0.0068	0.0000 ± 0.0000	-24.0053 ± 0.0487
ARG-521	-26.5364 ± 0.0543	0.4596 ± 0.0106	0.0000 ± 0.0000	-26.0775 ± 0.0500
ARG-521	-25.9306 ± 0.0701	0.7965 ± 0.0142	0.0000 ± 0.0000	-25.1317 ± 0.0621
ARG-533	-62.0426 ± 0.3288	8.5470 ± 0.3010	-0.1276 ± 0.0088	-53.6145 ± 0.2184
ARG-533	-78.8675 ± 0.4160	28.1996 ± 0.4720	-0.5919 ± 0.0138	-51.2693 ± 0.2450
LYS-551	-44.3274 ± 0.3484	2.4381 ± 0.2656	-0.1216 ± 0.0094	-42.0190 ± 0.2499
LYS-551	-32.5932 ± 0.3062	0.9043 ± 0.0707	-0.0016 ± 0.0008	-31.6929 ± 0.2595

LYS-562	-25.3360 ± 0.0707	0.3379 ± 0.0069	0.0000 ± 0.0000	-25.0000 ± 0.0667
LYS-562	-28.1197 ± 0.0719	0.6421 ± 0.0102	0.0000 ± 0.0000	-27.4793 ± 0.0654
LYS-573	-33.1938 ± 0.0745	1.0915 ± 0.0144	0.0000 ± 0.0000	-32.1028 ± 0.0749
LYS-573	-30.4115 ± 0.1096	1.5232 ± 0.0266	0.0000 ± 0.0000	-28.8902 ± 0.0952
LYS-586	-26.1313 ± 0.0684	0.3906 ± 0.0076	0.0000 ± 0.0000	-25.7433 ± 0.0639
LYS-586	-28.6679 ± 0.0955	0.8401 ± 0.0175	0.0000 ± 0.0000	-27.8273 ± 0.0790
LYS-596	-38.0097 ± 0.1450	0.8778 ± 0.0168	0.0000 ± 0.0000	-37.1309 ± 0.1374
LYS-596	-38.8103 ± 0.2529	1.7600 ± 0.0693	0.0000 ± 0.0000	-37.0478 ± 0.1922
LYS-624	-49.3347 ± 0.4335	3.8054 ± 0.1948	-0.0170 ± 0.0036	-45.5503 ± 0.3586
LYS-624	-56.3894 ± 0.6138	4.2688 ± 0.3556	-0.0706 ± 0.0072	-52.2058 ± 0.4715
LYS-647	-44.9052 ± 0.3264	0.7773 ± 0.0722	0.0000 ± 0.0000	-44.1252 ± 0.2904
LYS-647	-36.9997 ± 0.1565	0.6268 ± 0.0295	0.0000 ± 0.0000	-36.3840 ± 0.1513
ARG-667	-27.4680 ± 0.2199	0.2550 ± 0.0208	0.0000 ± 0.0000	-27.2206 ± 0.2029
ARG-667	-21.8053 ± 0.0781	-0.2361 ± 0.0106	0.0000 ± 0.0000	-22.0423 ± 0.0791
LYS-673	-42.0043 ± 0.8395	0.9922 ± 0.5936	-0.2809 ± 0.0192	-41.2869 ± 0.5448
LYS-673	-36.5017 ± 0.4717	4.5245 ± 0.4412	-1.0662 ± 0.0246	-33.0448 ± 0.3746
ARG-707	-21.1159 ± 0.0834	0.0567 ± 0.0069	0.0000 ± 0.0000	-21.0559 ± 0.0768
ARG-707	-20.4886 ± 0.0715	-0.2203 ± 0.0077	0.0000 ± 0.0000	-20.7083 ± 0.0669
LYS-749	-14.4843 ± 0.2363	-0.5573 ± 0.0482	0.0000 ± 0.0000	-15.0416 ± 0.2154
LYS-749	-18.3430 ± 0.2309	-0.7190 ± 0.0153	0.0000 ± 0.0000	-19.0537 ± 0.2348
LYS-752	-20.4690 ± 0.1070	-0.1954 ± 0.0231	0.0000 ± 0.0000	-20.6692 ± 0.0924
LYS-752	-19.9743 ± 0.0810	-0.6370 ± 0.0199	0.0000 ± 0.0000	-20.6102 ± 0.0837
LYS-759	-16.7020 ± 0.0806	-0.0079 ± 0.0022	0.0000 ± 0.0000	-16.7128 ± 0.0782
LYS-759	-15.3085 ± 0.0409	-0.0774 ± 0.0023	0.0000 ± 0.0000	-15.3847 ± 0.0424
LYS-769	-15.4106 ± 0.1098	-0.0148 ± 0.0026	0.0000 ± 0.0000	-15.4272 ± 0.1093
LYS-769	-14.9445 ± 0.0768	-0.1020 ± 0.0037	0.0000 ± 0.0000	-15.0412 ± 0.0766

Table 3.1.3: Binding free energy contribution of the key binding-site residues calculated from the binding energy decomposition for flg22 (kJmol-1) from complex 1ai and complex 1c.

Residue	MM Energy	Polar Energy	APolar Energy	Total Energy
GLN-65	-326.5020 ± 0.8622	55.1584 ± 1.4229	-1.5357 ± 0.0315	-272.8677 ± 0.7470
GLN-65	-337.8266 ± 0.8555	82.3429 ± 1.6889	-2.6138 ± 0.0308	-258.1119 ± 0.9952
ARG-66	-333.4063 ± 0.7458	71.8469 ± 0.9609	-1.9591 ± 0.0285	-263.5505 ± 0.3729
ARG-66	-358.8691 ± 1.4175	83.2513 ± 1.5578	-1.9910 ± 0.0401	-277.5711 ± 0.3568
LEU-67	-31.9214 ± 0.1744	12.3520 ± 0.0966	-3.4453 ± 0.0176	-23.0183 ± 0.1525
LEU-67	-28.8683 ± 0.1647	9.7942 ± 0.1038	-3.1175 ± 0.0167	-22.1913 ± 0.1539
ARG-72	-338.0485 ± 1.5027	49.8907 ± 1.4798	-0.5764 ± 0.0280	-288.7622 ± 0.3931
ARG-72	-390.2580 ± 2.1173	108.5459 ± 2.3609	-2.0187 ± 0.0497	-283.8474 ± 0.4686
ILE-73	-6.5589 ± 0.2838	3.5472 ± 0.2213	-0.6261 ± 0.0228	-3.6335 ± 0.1506
ILE-73	-21.7116 ± 0.2073	6.8455 ± 0.1147	-1.8541 ± 0.0244	-16.7096 ± 0.1521
LYS-77	-330.4891 ± 1.0590	52.9911 ± 1.2206	-1.5168 ± 0.0160	-279.0251 ± 0.6088
LYS-77	-364.3560 ± 2.0130	100.3715 ± 2.5346	-1.9688 ± 0.0351	-265.9476 ± 1.0339

Table 3.1.4: Binding free energy contribution of the key binding-site residues calculated from the binding energy decomposition for BAK1 (kJmol-1) from complex 1aii and complex 1b

Residue	MM Energy	Polar Energy	APolar Energy	Total Energy
ASN-26	-271.1032 ± 0.6363	-2.1194 ± 0.5090	-0.0920 ± 0.0136	-273.3219 ± 0.4366
ASN-26	-249.9684 ± 0.5951	0.4179 ± 0.1304	0.0049 ± 0.0068	-249.5682 ± 0.5875
LYS-36	-208.6361 ± 0.4429	-2.0590 ± 0.2305	-0.0150 ± 0.0092	-210.6907 ± 0.3629
LYS-36	-230.4696 ± 0.4715	3.5627 ± 0.2024	-0.0159 ± 0.0127	-226.9060 ± 0.3933
LYS-44	-196.4738 ± 0.3773	8.2791 ± 0.4019	-0.9312 ± 0.0167	-189.1030 ± 0.4457
LYS-44	-191.7232 ± 0.5497	17.8566 ± 0.5178	-1.0941 ± 0.019	-174.9774 ± 0.5778
ARG-72	-245.9573 ± 0.5205	37.4464 ± 0.5944	-1.2260 ± 0.0146	-209.7216 ± 0.4135
ARG-72	-245.6591 ± 0.8093	44.9235 ± 0.9954	-1.4286 ± 0.015	-202.2167 ± 0.5128
ARG-138	-216.7042 ± 1.0756	0.7596 ± 0.3052	-0.0302 ± 0.0142	-215.9639 ± 0.9397
ARG-138	-183.5361 ± 0.3812	1.1629 ± 0.0452	0.0002 ± 0.0086	-182.3776 ± 0.3818
LYS-140	-218.6705 ± 0.7267	-0.5688 ± 0.0863	0.0022 ± 0.0086	-219.2223 ± 0.7547
LYS-140	-203.1248 ± 0.4117	1.3208 ± 0.0997	-0.0208 ± 0.0103	-201.8295 ± 0.4074
LYS-141	-215.4609 ± 0.4781	-0.1483 ± 0.1109	0.0010 ± 0.0097	-215.6251 ± 0.4615
LYS-141	-227.9880 ± 0.5145	3.8004 ± 0.3482	-0.0439 ± 0.0117	-224.2100 ± 0.3993
ARG-143	-239.1713 ± 1.0817	17.8697 ± 1.2220	-0.4860 ± 0.0293	-221.7985 ± 0.4340
ARG-143	-293.1195 ± 0.9733	80.7313 ± 1.0513	-1.4258 ± 0.023	-213.8224 ± 0.3995
ARG-146	-208.7224 ± 0.7817	7.0070 ± 0.5105	-0.2669 ± 0.0155	-201.9481 ± 0.6355
ARG-146	-214.3675 ± 0.9996	29.4604 ± 0.7430	-0.5882 ± 0.018	-185.4880 ± 0.5520
ARG-158	-172.1582 ± 0.4920	-0.1997 ± 0.0417	0.0023 ± 0.0077	-172.3882 ± 0.4925
ARG-158	-159.5594 ± 0.3788	0.4363 ± 0.0457	0.0211 ± 0.0091	-159.1043 ± 0.3664
LYS-198	-156.1475 ± 0.2710	-0.0778 ± 0.0786	-0.0140 ± 0.0095	-156.2310 ± 0.2798
LYS-198	-147.9814 ± 0.2251	0.4439 ± 0.0808	0.0028 ± 0.0085	-147.5408 ± 0.2387

Table 3.2.1: Protein-Protein Hydrophobic Interactions of complex 1a

Before Simulation					
Position	**Residue**	**Chain**	**Position**	**Residue**	**Chain**
53	LEU	B	83	LEU	C
53	LEU	B	85	ILE	C
148	TYR	A	67	LEU	C
172	LEU	A	67	LEU	C
196	MET	A	67	LEU	C
198	VAL	A	67	LEU	C
272	TYR	A	76	ALA	C
292	ALA	A	73	ILE	C
369	PHE	A	54	VAL	B
412	LEU	A	83	LEU	C
435	PHE	A	83	LEU	C
483	ILE	A	85	ILE	C

507	ILE	A	60	PHE	B
509	TYR	A	60	PHE	B
555	VAL	A	60	PHE	B
650	MET	A	144	PHE	B
650	MET	A	96	TYR	B
After Simulation					
Position	**Residue**	**Chain**	**Position**	**Residue**	**Chain**
53	LEU	B	83	LEU	C
53	LEU	B	85	ILE	C
148	TYR	A	67	LEU	C
172	LEU	A	67	LEU	C
198	VAL	A	67	LEU	C
246	VAL	A	76	ALA	C
267	VAL	A	73	ILE	C
272	TYR	A	76	ALA	C
292	ALA	A	73	ILE	C
369	PHE	A	54	VAL	B
412	LEU	A	83	LEU	C
435	PHE	A	83	LEU	C
483	ILE	A	85	ILE	C
507	ILE	A	60	PHE	B
555	VAL	A	60	PHE	B
600	LEU	A	100	TYR	B
650	MET	A	144	PHE	B
650	MET	A	96	TYR	B

Table 3.2.2: Protein-Protein Main Chain-Main Chain Hydrogen Bonds of complex 1a

Before Simulation								
DONOR				**ACCEPTOR**				
POS	**CHAIN**	**RES**	**ATOM**	**POS**	**CHAIN**	**RES**	**ATOM**	**Dd-a**
54	B	VAL	N	83	C	LEU	O	2.98
83	C	LEU	N	52	B	THR	O	2.93
After Simulation								
DONOR				**ACCEPTOR**				
POS	**CHAIN**	**RES**	**ATOM**	**POS**	**CHAIN**	**RES**	**ATOM**	**Dd-a**
54	B	VAL	N	83	C	LEU	O	3.1
83	C	LEU	N	52	B	THR	O	2.77

Table 3.2.3: Protein-Protein Main Chain-Side Chain Hydrogen Bonds of complex 1a

Before Simulation								
DONOR				ACCEPTOR				
POS	CHAIN	RES	ATOM	POS	CHAIN	RES	ATOM	Dd-a
152	A	ARG	NH2	65	C	GLN	O	2.73
152	A	ARG	NH2	65	C	GLN	O	2.73
268	A	GLN	OE1	72	C	ARG	O	3.5
268	A	GLN	OE1	72	C	ARG	O	3.5
294	A	ARG	NE	77	C	LYS	O	2.96
296	A	TYR	OH	77	C	LYS	O	3.39
437	A	SER	OG	84	C	GLN	O	2.95
530	A	GLN	NE2	44	B	LYS	O	2.74
530	A	GLN	NE2	44	B	LYS	O	2.74
67	C	LEU	N	148	A	TYR	OH	3.19
71	C	SER	N	220	A	ASP	OD2	3.13
77	C	LYS	N	272	A	TYR	OH	3.26
84	C	GLN	N	414	A	ASP	OD2	2.97
After Simulation								
DONOR				ACCEPTOR				
POS	CHAIN	RES	ATOM	POS	CHAIN	RES	ATOM	Dd-a
128	A	TYR	OH	65	C	GLN	O	3.47
152	A	ARG	NH2	65	C	GLN	O	2.88
152	A	ARG	NH2	65	C	GLN	O	2.88
268	A	GLN	OE1	72	C	ARG	O	2.99
268	A	GLN	OE1	72	C	ARG	O	2.99
268	A	GLN	NE2	73	C	ILE	O	3.45
268	A	GLN	NE2	73	C	ILE	O	3.45
294	A	ARG	NH1	73	C	ILE	O	3.05
294	A	ARG	NH1	73	C	ILE	O	3.05
294	A	ARG	NH1	76	C	ALA	O	3.4
294	A	ARG	NH1	76	C	ALA	O	3.4
296	A	TYR	OH	77	C	LYS	O	2.64
392	A	HIS	NE2	82	C	GLY	O	2.91
437	A	SER	OG	84	C	GLN	O	2.97
530	A	GLN	NE2	44	B	LYS	O	2.75
530	A	GLN	NE2	44	B	LYS	O	2.75
48	B	SER	N	506	A	ASN	OD1	2.89
143	B	ARG	NH1	673	A	LYS	O	3.45
143	B	ARG	NH1	673	A	LYS	O	3.45
65	C	GLN	N	128	A	TYR	OH	3.02

71	C	SER	N	220	A	ASP	OD1	2.85
71	C	SER	N	220	A	ASP	OD2	3.1
76	C	ALA	N	270	A	GLU	OE2	3.42
77	C	LYS	N	272	A	TYR	OH	3.23
84	C	GLN	N	414	A	ASP	OD2	2.71

Table 3.2.4: Protein-Protein Side Chain-Side Chain Hydrogen Bonds of complex 1a

Before Simulation								
DONOR				**ACCEPTOR**				
POS	**CHAIN**	**RES**	**ATOM**	**POS**	**CHAIN**	**RES**	**ATOM**	**Dd-a**
294	A	ARG	NE	78	C	ASP	OD1	2.98
294	A	ARG	NH2	78	C	ASP	OD1	3.42
294	A	ARG	NH2	78	C	ASP	OD1	3.42
316	A	HIS	ND1	78	C	ASP	OD1	3.24
316	A	HIS	ND1	78	C	ASP	OD2	2.86
320	A	SER	OG	79	C	ASP	OD2	2.42
344	A	HIS	NE2	79	C	ASP	OD2	3.38
393	A	ASP	OD1	84	C	GLN	NE2	2.87
393	A	ASP	OD1	84	C	GLN	NE2	2.87
417	A	HIS	NE2	84	C	GLN	NE2	3.46
625	A	ASN	ND2	100	B	TYR	OH	3.01
625	A	ASN	ND2	100	B	TYR	OH	3.01
625	A	ASN	ND2	124	B	TYR	OH	3.34
625	A	ASN	ND2	124	B	TYR	OH	3.34
674	A	ASN	OD1	96	B	TYR	OH	3.26
674	A	ASN	OD1	96	B	TYR	OH	3.26
698	A	ASP	OD2	167	B	GLN	OE1	2.42
698	A	ASP	OD2	167	B	GLN	OE1	2.42
698	A	ASP	OD2	167	B	GLN	NE2	2.43
698	A	ASP	OD2	167	B	GLN	NE2	2.43
96	B	TYR	OH	674	A	ASN	OD1	3.26
100	B	TYR	OH	625	A	ASN	ND2	3.01
124	B	TYR	OH	625	A	ASN	ND2	3.34
143	B	ARG	NH2	674	A	ASN	OD1	2.97
143	B	ARG	NH2	674	A	ASN	OD1	2.97
143	B	ARG	NH1	699	A	MET	SD	3.84
143	B	ARG	NH1	699	A	MET	SD	3.84
146	B	ARG	NH1	650	A	MET	SD	4
146	B	ARG	NH1	650	A	MET	SD	4
146	B	ARG	NH2	650	A	MET	SD	3.3

146	B	ARG	NH2	650	A	MET	SD	3.3
167	B	GLN	OE1	698	A	ASP	OD2	2.42
167	B	GLN	OE1	698	A	ASP	OD2	2.42
167	B	GLN	NE2	698	A	ASP	OD2	2.43
167	B	GLN	NE2	698	A	ASP	OD2	2.43
78	C	ASP	OD1	316	A	HIS	ND1	3.24
78	C	ASP	OD1	316	A	HIS	ND1	3.24
78	C	ASP	OD2	316	A	HIS	ND1	2.86
78	C	ASP	OD2	316	A	HIS	ND1	2.86
79	C	ASP	OD2	344	A	HIS	NE2	3.38
79	C	ASP	OD2	344	A	HIS	NE2	3.38
84	C	GLN	NE2	393	A	ASP	OD1	2.87
84	C	GLN	NE2	393	A	ASP	OD1	2.87
84	C	GLN	NE2	417	A	HIS	NE2	3.46
84	C	GLN	NE2	417	A	HIS	NE2	3.46

After Simulation

DONOR				**ACCEPTOR**				
POS	**CHAIN**	**RES**	**ATOM**	**POS**	**CHAIN**	**RES**	**ATOM**	**Dd-a**
268	A	GLN	NE2	75	C	SER	OG	3.04
268	A	GLN	NE2	75	C	SER	OG	3.04
294	A	ARG	NH2	74	C	ASN	OD1	2.97
294	A	ARG	NH2	74	C	ASN	OD1	2.97
294	A	ARG	NH2	74	C	ASN	ND2	3.46
294	A	ARG	NH2	74	C	ASN	ND2	3.46
294	A	ARG	NE	78	C	ASP	OD1	3.05
294	A	ARG	NE	78	C	ASP	OD2	3.44
294	A	ARG	NH2	78	C	ASP	OD1	3.48
294	A	ARG	NH2	78	C	ASP	OD1	3.48
294	A	ARG	NH2	78	C	ASP	OD2	3.25
294	A	ARG	NH2	78	C	ASP	OD2	3.25
297	A	LYS	NZ	79	C	ASP	OD2	3.2
316	A	HIS	NE2	74	C	ASN	OD1	3
320	A	SER	OG	79	C	ASP	OD2	2.82
392	A	HIS	ND1	84	C	GLN	NE2	3.12
393	A	ASP	OD1	84	C	GLN	OE1	3.38
393	A	ASP	OD1	84	C	GLN	OE1	3.38
393	A	ASP	OD1	84	C	GLN	NE2	3.04
393	A	ASP	OD1	84	C	GLN	NE2	3.04
627	A	GLN	NE2	98	B	GLU	OE1	3.31
627	A	GLN	NE2	98	B	GLU	OE1	3.31
674	A	ASN	ND2	96	B	TYR	OH	2.81

674	A	ASN	ND2	96	B	TYR	OH	2.81
698	A	ASP	OD2	167	B	GLN	NE2	2.71
698	A	ASP	OD2	167	B	GLN	NE2	2.71
96	B	TYR	OH	674	A	ASN	ND2	2.81
98	B	GLU	OE1	627	A	GLN	NE2	3.31
98	B	GLU	OE1	627	A	GLN	NE2	3.31
143	B	ARG	NH1	674	A	ASN	OD1	3.2
143	B	ARG	NH1	674	A	ASN	OD1	3.2
143	B	ARG	NH2	674	A	ASN	OD1	2.89
143	B	ARG	NH2	674	A	ASN	OD1	2.89
146	B	ARG	NH2	650	A	MET	SD	3
146	B	ARG	NH2	650	A	MET	SD	3
167	B	GLN	NE2	698	A	ASP	OD2	2.71
167	B	GLN	NE2	698	A	ASP	OD2	2.71
71	C	SER	OG	220	A	ASP	OD2	2.66
74	C	ASN	OD1	316	A	HIS	NE2	3
74	C	ASN	OD1	316	A	HIS	NE2	3
75	C	SER	OG	268	A	GLN	NE2	3.04
84	C	GLN	NE2	392	A	HIS	ND1	3.12
84	C	GLN	NE2	392	A	HIS	ND1	3.12
84	C	GLN	OE1	393	A	ASP	OD1	3.38
84	C	GLN	OE1	393	A	ASP	OD1	3.38
84	C	GLN	NE2	393	A	ASP	OD1	3.04
84	C	GLN	NE2	393	A	ASP	OD1	3.04

Table 3.2.5: Protein-Protein Ionic Interactions of complex 1a

Before Simulation					
Position	**Residue**	**Chain**	**Position**	**Residue**	**Chain**
249	GLU	A	77	LYS	C
294	ARG	A	78	ASP	C
297	LYS	A	79	ASP	C
316	HIS	A	78	ASP	C
344	HIS	A	79	ASP	C
649	GLU	A	146	ARG	B
After Simulation					
Position	**Residue**	**Chain**	**Position**	**Residue**	**Chain**
294	ARG	A	78	ASP	C
297	LYS	A	79	ASP	C
344	HIS	A	79	ASP	C
649	GLU	A	146	ARG	B

698	ASP	A	143	ARG	B

Table 3.2.6: Protein-Protein Aromatic-Aromatic Interactions of complex 1a

Before Simulation						
Position	**Residue**	**Chain**	**Position**	**Residue**	**Chain**	**D(centroid-centroid)**
509	TYR	A	60	PHE	B	6.91
After Simulation						
NO PROTEIN-PROTEIN AROMATIC-AROMATIC INTERACTIONS FOUND						

Table 3.2.7: Protein-Protein Aromatic-Sulphur Interactions of complex 1a

Before Simulation						
Position	**Residue**	**Chain**	**Position**	**Residue**	**Chain**	**D(Centroid-Sulphur)**
144	PHE	B	650	MET	A	3.38
After Simulation						
Position	**Residue**	**Chain**	**Position**	**Residue**	**Chain**	**D(Centroid-Sulphur)**
144	PHE	B	650	MET	A	3.87

Table 3.2.8: Protein-Protein Cation-Pi Interactions of complex 1a

Before Simulation						
Position	**Residue**	**Chain**	**Position**	**Residue**	**Chain**	**D(cation-Pi)**
676	PHE	A	143	ARG	B	5.71
After Simulation						
NO PROTEIN-PROTEIN CATION-PI INTERACTIONS FOUND						

Table 3.3.1: Protein-Protein Hydrophobic Interactions of complex 1b

Before Simulation					
Position	**Residue**	**Chain**	**Position**	**Residue**	**Chain**
369	PHE	A	54	VAL	B
507	ILE	A	60	PHE	B
509	TYR	A	60	PHE	B

555	VAL	A	60	PHE	B
650	MET	A	144	PHE	B
650	MET	A	96	TYR	B
After Simulation					
Position	**Residue**	**Chain**	**Position**	**Residue**	**Chain**
369	PHE	A	54	VAL	B
507	ILE	A	60	PHE	B
509	TYR	A	60	PHE	B
555	VAL	A	60	PHE	B
650	MET	A	144	PHE	B
650	MET	A	96	TYR	B
676	PHE	A	96	TYR	B

Table 3.3.2: Protein-Protein Main Chain-Side Chain Hydrogen Bonds of complex 1b

Before Simulation								
DONOR				**ACCEPTOR**				
POS	**CHAIN**	**RES**	**ATOM**	**POS**	**CHAIN**	**RES**	**ATOM**	**Dd-a**
530	A	GLN	NE2	44	B	LYS	O	2.74
530	A	GLN	NE2	44	B	LYS	O	2.74
After Simulation								
DONOR				**ACCEPTOR**				
POS	**CHAIN**	**RES**	**ATOM**	**POS**	**CHAIN**	**RES**	**ATOM**	**Dd-a**
530	A	GLN	NE2	44	B	LYS	O	2.89
530	A	GLN	NE2	44	B	LYS	O	2.89
143	B	ARG	NH1	673	A	LYS	O	3.07
143	B	ARG	NH1	673	A	LYS	O	3.07

Table 3.3.3: Protein-Protein Side Chain-Side Chain Hydrogen Bonds of complex 1b

Before Simulation								
DONOR				**ACCEPTOR**				
POS	**CHAIN**	**RES**	**ATOM**	**POS**	**CHAIN**	**RES**	**ATOM**	**Dd-a**
625	A	ASN	ND2	100	B	TYR	OH	3.01
625	A	ASN	ND2	100	B	TYR	OH	3.01
625	A	ASN	ND2	124	B	TYR	OH	3.34
625	A	ASN	ND2	124	B	TYR	OH	3.34
674	A	ASN	OD1	96	B	TYR	OH	3.26
674	A	ASN	OD1	96	B	TYR	OH	3.26
698	A	ASP	OD2	167	B	GLN	OE1	2.42
698	A	ASP	OD2	167	B	GLN	OE1	2.42

698	A	ASP	OD2	167	B	GLN	NE2	2.43
698	A	ASP	OD2	167	B	GLN	NE2	2.43
96	B	TYR	OH	674	A	ASN	OD1	3.26
100	B	TYR	OH	625	A	ASN	ND2	3.01
124	B	TYR	OH	625	A	ASN	ND2	3.34
143	B	ARG	NH2	674	A	ASN	OD1	2.97
143	B	ARG	NH2	674	A	ASN	OD1	2.97
143	B	ARG	NH1	699	A	MET	SD	3.84
143	B	ARG	NH1	699	A	MET	SD	3.84
146	B	ARG	NH1	650	A	MET	SD	4
146	B	ARG	NH1	650	A	MET	SD	4
146	B	ARG	NH2	650	A	MET	SD	3.3
146	B	ARG	NH2	650	A	MET	SD	3.3
167	B	GLN	OE1	698	A	ASP	OD2	2.42
167	B	GLN	OE1	698	A	ASP	OD2	2.42
167	B	GLN	NE2	698	A	ASP	OD2	2.43
167	B	GLN	NE2	698	A	ASP	OD2	2.43

After Simulation

DONOR				**ACCEPTOR**				
POS	**CHAIN**	**RES**	**ATOM**	**POS**	**CHAIN**	**RES**	**ATOM**	**Dd-a**
627	A	GLN	NE2	98	B	GLU	OE1	3
627	A	GLN	NE2	98	B	GLU	OE1	3
627	A	GLN	NE2	98	B	GLU	OE2	3.47
627	A	GLN	NE2	98	B	GLU	OE2	3.47
627	A	GLN	OE1	100	B	TYR	OH	2.66
627	A	GLN	OE1	100	B	TYR	OH	2.66
674	A	ASN	ND2	96	B	TYR	OH	3.25
674	A	ASN	ND2	96	B	TYR	OH	3.25
698	A	ASP	OD1	167	B	GLN	NE2	2.76
698	A	ASP	OD1	167	B	GLN	NE2	2.76
72	B	ARG	NH1	652	A	GLN	OE1	3.2
72	B	ARG	NH1	652	A	GLN	OE1	3.2
96	B	TYR	OH	674	A	ASN	ND2	3.25
98	B	GLU	OE1	627	A	GLN	NE2	3
98	B	GLU	OE1	627	A	GLN	NE2	3
98	B	GLU	OE2	627	A	GLN	NE2	3.47
98	B	GLU	OE2	627	A	GLN	NE2	3.47
100	B	TYR	OH	627	A	GLN	OE1	2.66
120	B	SER	OG	650	A	MET	SD	3.97
143	B	ARG	NH2	674	A	ASN	OD1	2.82
143	B	ARG	NH2	674	A	ASN	OD1	2.82

143	B	ARG	NE	699	A	MET	SD	3.63
143	B	ARG	NH1	699	A	MET	SD	3.75
143	B	ARG	NH1	699	A	MET	SD	3.75
146	B	ARG	NH2	650	A	MET	SD	3.09
146	B	ARG	NH2	650	A	MET	SD	3.09
167	B	GLN	NE2	698	A	ASP	OD1	2.76
167	B	GLN	NE2	698	A	ASP	OD1	2.76

Table 3.3.4: Protein-Protein Ionic Interactions of complex 1b

Before Simulation					
Position	**Residue**	**Chain**	**Position**	**Residue**	**Chain**
649	GLU	A	146	ARG	B
After Simulation					
Position	**Residue**	**Chain**	**Position**	**Residue**	**Chain**
649	GLU	A	146	ARG	B
698	ASP	A	143	ARG	B

Table 3.3.5: Protein-Protein Aromatic-Aromatic Interactions of complex 1b

Before Simulation						
Position	**Residue**	**Chain**	**Position**	**Residue**	**Chain**	**D (centroid-centroid**
509	TYR	A	60	PHE	B	6.91
After Simulation						
Position	**Residue**	**Chain**	**Position**	**Residue**	**Chain**	**D (centroid-centroid**
509	TYR	A	60	PHE	B	6.79

Table 3.3.6: Protein-Protein Aromatic-Sulphur Interactions of complex 1b

Before Simulation						
Position	**Residue**	**Chain**	**Position**	**Residue**	**Chain**	**D(Centroid-Sulphur)**
144	PHE	B	650	MET	A	3.38
After Simulation						
Position	**Residue**	**Chain**	**Position**	**Residue**	**Chain**	**D(Centroid-Sulphur)**
144	PHE	B	650	MET	A	4.12

Table 3.3.7: Protein-Protein Cation-Pi Interactions of complex 1b

Before Simulation						
Position	**Residue**	**Chain**	**Position**	**Residue**	**Chain**	**D(cation-Pi)**
676	PHE	A	143	ARG	B	5.71
After Simulation						
NO PROTEIN-PROTEIN CATION-PI INTERACTIONS FOUND						

Table 3.4.1: Protein-Protein Hydrophobic Interactions of complex 1c

Before Simulation					
Position	**Residue**	**Chain**	**Position**	**Residue**	**Chain**
148	TYR	A	67	LEU	C
172	LEU	A	67	LEU	C
196	MET	A	67	LEU	C
198	VAL	A	67	LEU	C
272	TYR	A	76	ALA	C
292	ALA	A	73	ILE	C
412	LEU	A	83	LEU	C
435	PHE	A	83	LEU	C
483	ILE	A	85	ILE	C
After Simulation					
Position	**Residue**	**Chain**	**Position**	**Residue**	**Chain**
148	TYR	A	67	LEU	C
172	LEU	A	67	LEU	C
196	MET	A	67	LEU	C
198	VAL	A	67	LEU	C
267	VAL	A	73	ILE	C
272	TYR	A	76	ALA	C
292	ALA	A	73	ILE	C
435	PHE	A	83	LEU	C
463	ALA	A	85	ILE	C

Table 3.4.2: Protein-Protein Main Chain-Side Chain Hydrogen Bonds of complex 1c

Before Simulation								
DONOR				**ACCEPTOR**				
POS	**CHAIN**	**RES**	**ATOM**	**POS**	**CHAIN**	**RES**	**ATOM**	**Dd-a**
152	A	ARG	NH2	65	C	GLN	O	2.73
152	A	ARG	NH2	65	C	GLN	O	2.73
268	A	GLN	OE1	72	C	ARG	O	3.5
268	A	GLN	OE1	72	C	ARG	O	3.5

294	A	ARG	NE	77	C	LYS	O	2.96
296	A	TYR	OH	77	C	LYS	O	3.39
437	A	SER	OG	84	C	GLN	O	2.95
67	C	LEU	N	148	A	TYR	OH	3.19
71	C	SER	N	220	A	ASP	OD2	3.13
77	C	LYS	N	272	A	TYR	OH	3.26
84	C	GLN	N	414	A	ASP	OD2	2.97
After Simulation								
DONOR				**ACCEPTOR**				
POS	**CHAIN**	**RES**	**ATOM**	**POS**	**CHAIN**	**RES**	**ATOM**	**Dd-a**
128	A	TYR	OH	65	C	GLN	O	3.01
152	A	ARG	NH1	65	C	GLN	O	3.17
152	A	ARG	NH1	65	C	GLN	O	3.17
152	A	ARG	NH2	65	C	GLN	O	3.16
152	A	ARG	NH2	65	C	GLN	O	3.16
294	A	ARG	NH1	73	C	ILE	O	2.71
294	A	ARG	NH1	73	C	ILE	O	2.71
294	A	ARG	NH2	73	C	ILE	O	3.42
294	A	ARG	NH2	73	C	ILE	O	3.42
296	A	TYR	OH	77	C	LYS	O	2.76
392	A	HIS	NE2	82	C	GLY	O	2.7
416	A	SER	OG	84	C	GLN	O	3.23
65	C	GLN	N	128	A	TYR	OH	3.22
68	C	SER	N	148	A	TYR	OH	3
71	C	SER	N	220	A	ASP	OD1	2.88
77	C	LYS	N	272	A	TYR	OH	3.23

Table 3.4.3: Protein-Protein Side Chain-Side Chain Hydrogen Bonds of complex 1c

Before Simulation								
DONOR				**ACCEPTOR**				
POS	**CHAIN**	**RES**	**ATOM**	**POS**	**CHAIN**	**RES**	**ATOM**	**Dd-a**
294	A	ARG	NE	78	C	ASP	OD1	2.98
294	A	ARG	NH2	78	C	ASP	OD1	3.42
294	A	ARG	NH2	78	C	ASP	OD1	3.42
316	A	HIS	ND1	78	C	ASP	OD1	3.24
316	A	HIS	ND1	78	C	ASP	OD2	2.86
320	A	SER	OG	79	C	ASP	OD2	2.42
344	A	HIS	NE2	79	C	ASP	OD2	3.38
393	A	ASP	OD1	84	C	GLN	NE2	2.87
393	A	ASP	OD1	84	C	GLN	NE2	2.87

417	A	HIS	NE2	84	C	GLN	NE2	3.46
78	C	ASP	OD1	316	A	HIS	ND1	3.24
78	C	ASP	OD1	316	A	HIS	ND1	3.24
78	C	ASP	OD2	316	A	HIS	ND1	2.86
78	C	ASP	OD2	316	A	HIS	ND1	2.86
79	C	ASP	OD2	344	A	HIS	NE2	3.38
79	C	ASP	OD2	344	A	HIS	NE2	3.38
84	C	GLN	NE2	393	A	ASP	OD1	2.87
84	C	GLN	NE2	393	A	ASP	OD1	2.87
84	C	GLN	NE2	417	A	HIS	NE2	3.46
84	C	GLN	NE2	417	A	HIS	NE2	3.46
After Simulation								
DONOR				**ACCEPTOR**				
POS	**CHAIN**	**RES**	**ATOM**	**POS**	**CHAIN**	**RES**	**ATOM**	**Dd-a**
294	A	ARG	NE	78	C	ASP	OD1	3.08
294	A	ARG	NE	78	C	ASP	OD2	3.31
294	A	ARG	NH2	78	C	ASP	OD2	3.12
294	A	ARG	NH2	78	C	ASP	OD2	3.12
297	A	LYS	NZ	79	C	ASP	OD1	3.12
297	A	LYS	NZ	79	C	ASP	OD2	2.88

Table 3.4.4: Protein-Protein Ionic Interactions of complex 1c

Before Simulation					
Position	**Residue**	**Chain**	**Position**	**Residue**	**Chain**
249	GLU	A	77	LYS	C
294	ARG	A	78	ASP	C
297	LYS	A	79	ASP	C
316	HIS	A	78	ASP	C
344	HIS	A	79	ASP	C
After Simulation					
Position	**Residue**	**Chain**	**Position**	**Residue**	**Chain**
249	GLU	A	77	LYS	C
294	ARG	A	78	ASP	C
297	LYS	A	79	ASP	C
316	HIS	A	78	ASP	C
344	HIS	A	79	ASP	C

Table 3.5: Summary of interactions among FLS2, flg22 and BAK1 before and after simulation

Complex	Inter. Bet.	H-Bond		Hydrophobic Interaction		Ionic Interaction		Cation - Pi Interaction		Aromatic - Aromatic Interaction		Aromatic - Sulphur Interaction	
		B. MD	*A. MD*	*B. MD*	*A. MD*	*B. MD*	*A. MD*	*B. MD*	*A. MD*	*B. MD*	*A. MD*	*B. MD*	*A. MD*
FLS2+ flg22+ BAK1	*FLS2 + flg22*	31	50	9	10	5	3	0	0	0	0	0	0
	FLS2 + BAK1	27	22	6	6	1	2	1	0	1	0	1	1
	flg22 + BAK1	2	2	2	2	0	0	0	0	0	0	0	0
FLS2+ BAK1	*FLS2 + BAK1*	27	32	6	6	1	2	1	0	1	1	1	1
FLS2+ flg22	*FLS2 + flg22*	31	22	9	9	5	5	0	0	0	0	0	0

Table 3.6.1: Binding free energy contribution of the key binding-site residues calculated from the binding energy decomposition for HAESA (kJmol-1) 2ai and complex 2c.

Residue	MM Energy	Polar Energy	APolar Energy	Total Energy
ASP-24	-17.9692 ± 0.0335	0.0775 ± 0.0028	0.0000 ± 0.0000	-17.8916 ± 0.0334
ASP-24	-19.3906 ± 0.0540	0.1828 ± 0.0042	0.0000 ± 0.0000	-19.2068 ± 0.0517
ASP-37	-25.1087 ± 0.0994	0.1795 ± 0.0089	0.0000 ± 0.0000	-24.9305 ± 0.0930
ASP-37	-27.2807 ± 0.1288	0.5395 ± 0.0158	0.0000 ± 0.0000	-26.7371 ± 0.1161
ASP-47	-17.2825 ±0.0455	0.0202 ± 0.0009	0.0000 ± 0.0000	-17.2621 ± 0.0447
ASP-47	-19.0895 ± 0.0615	0.0711 ± 0.0019	0.0000 ± 0.0000	-19.0174 ± 0.0611
ASP-50	-14.8495 ± 0.0328	0.0050 ± 0.0002	0.0000 ± 0.0000	-14.8441 ± 0.0335
ASP-50	-16.5176 ± 0.0432	0.0171 ± 0.0004	0.0000 ± 0.0000	-16.5014 ± 0.0452
ASP-62	-17.0342 ± 0.0424	0.0207 ± 0.0008	0.0000 ± 0.0000	-17.0144 ± 0.0426
ASP-62	-20.4319 ± 0.0525	0.0746 ± 0.0019	0.0000 ± 0.0000	-20.3566 ± 0.0523
ASP-71	-26.8943 ± 0.1078	0.2925 ± 0.0147	0.0000 ± 0.0000	-26.6010 ± 0.1015
ASP-71	-35.8261 ± 0.2205	1.3666 ± 0.0409	0.0000 ± 0.0000	-34.4596 ± 0.1946
ASP-108	-22.3548 ± 0.0506	0.1269 ± 0.0049	0.0000 ± 0.0000	-22.2258 ± 0.0474
ASP-108	-21.2392 ± 0.0470	0.2219 ± 0.0062	0.0000 ± 0.0000	-21.0194 ± 0.0434
ASP-109	-23.5868 ± 0.0731	0.2883 ± 0.0096	0.0000 ± 0.0000	-23.2961 ± 0.0696

ASP-109	-24.7654 ± 0.0573	0.6555 ± 0.0123	0.0000 ± 0.0000	-24.1089 ± 0.0513
ASP-111	-21.6114 ± 0.0375	0.1719 ± 0.0056	0.0000 ± 0.0000	-21.4385 ± 0.0333
ASP-111	-20.2837 ± 0.0365	0.2354 ± 0.0056	0.0000 ± 0.0000	-20.0466 ± 0.0344
ASP-120	-37.2338 ± 0.1383	1.0309 ± 0.0514	0.0000 ± 0.0000	-36.1994 ± 0.1190
ASP-120	-45.7181 ± 0.2447	4.7438 ± 0.1134	0.0000 ± 0.0000	-40.9692 ± 0.1698
GLU-123	-61.3487 ± 0.6952	8.8228 ± 0.8705	-0.4238 ± 0.0232	-52.9880 ± 0.2972
GLU-123	-104.9555 ± 1.3586	67.0034 ± 1.8274	-0.9944 ± 0.0147	-39.0345 ± 0.5811
GLU-145	-37.8312 ± 0.1350	0.3102 ± 0.0380	-0.0004 ± 0.0003	-37.5190 ± 0.1499
GLU-145	-45.4401 ± 0.2380	1.6028 ± 0.0752	-0.0057 ± 0.0014	-43.8408 ± 0.2207
ASP-153	-33.3191 ± 0.0826	1.1193 ± 0.0401	0.0000 ± 0.0000	-32.1972 ± 0.0565
ASP-153	-29.8094 ± 0.1318	1.1297 ± 0.0491	0.0000 ± 0.0000	-28.6837 ± 0.0905
GLU-161	-21.4253 ± 0.0287	0.1172 ± 0.0035	0.0000 ± 0.0000	-21.3079 ± 0.0265
GLU-161	-20.4663 ± 0.0420	0.1492 ± 0.0069	0.0000 ± 0.0000	-20.3170 ± 0.0374
GLU-166	-24.8056 ± 0.0607	0.1698 ± 0.0063	0.0000 ± 0.0000	-24.6363 ± 0.0612
GLU-166	-26.0848 ± 0.0727	0.1572 ± 0.0125	0.0000 ± 0.0000	-25.9264 ± 0.0728
GLU-191	-34.3330 ± 0.1026	0.2526 ± 0.0215	0.0000 ± 0.0000	-34.0838 ± 0.1004
GLU-191	-37.1960 ± 0.1338	0.0361 ± 0.0411	0.0000 ± 0.0000	-37.1579 ± 0.1470
GLU-213	-22.2129 ± 0.0367	0.2358 ± 0.0061	0.0000 ± 0.0000	-21.9765 ± 0.0354
GLU-213	-23.0147 ± 0.0515	0.0658 ± 0.0089	0.0000 ± 0.0000	-22.9491 ± 0.0497
ASP-242	-61.0453 ± 0.3040	15.1173 ± 0.4583	-0.1024 ± 0.0065	-46.0330 ± 0.2406
ASP-242	-61.7083 ± 0.5590	24.5231 ± 0.7521	-0.3178 ± 0.0098	-37.4981 ± 0.3104
GLU-263	-30.3975 ± 0.1550	1.1661 ± 0.0329	0.0000 ± 0.0000	-29.2381 ± 0.1574
GLU-263	-31.4822 ± 0.1435	-0.2151 ± 0.0357	-0.0001 ± 0.0001	-31.6889 ± 0.1500
GLU-266	-73.0030 ± 0.4374	44.7941 ± 0.8179	-0.3444 ± 0.0073	-28.5574 ± 0.4409
GLU-266	-64.9408 ± 0.8916	39.1842 ± 1.3704	-0.4313 ± 0.0139	-26.2106 ± 0.5717
GLU-275	-20.0095 ± 0.0412	0.4655 ± 0.0145	0.0000 ± 0.0000	-19.5448 ± 0.0311
GLU-275	-18.9691 ± 0.0681	0.1901 ± 0.0103	0.0000 ± 0.0000	-18.7789 ± 0.0607
GLU-278	-18.5402 ± 0.0390	0.3172 ± 0.0087	0.0000 ± 0.0000	-18.2229 ± 0.0318
GLU-278	-18.3850 ± 0.0604	0.1287 ± 0.0081	0.0000 ± 0.0000	-18.2591 ± 0.0551
ASP-290	-64.9301 ± 0.2564	45.9196 ± 0.5041	-0.2324 ± 0.0044	-19.2365 ± 0.3545
ASP-290	-51.9891 ± 0.4747	22.3831 ± 0.7551	-0.1905 ± 0.0088	-29.7785 ± 0.4869
ASP-302	-16.8561 ± 0.0316	0.1674 ± 0.0072	0.0000 ± 0.0000	-16.6898 ± 0.0252
ASP-302	-17.4771 ± 0.0447	0.0688 ± 0.0065	0.0000 ± 0.0000	-17.4073 ± 0.0414
GLU-310	-31.9370 ± 0.1221	0.5513 ± 0.0283	0.0000 ± 0.0000	-31.3915 ± 0.1064
GLU-310	-38.2052 ± 0.3084	-0.2394 ± 0.0880	-0.0006 ± 0.0006	-38.4621 ± 0.2750
GLU-316	-42.6124 ± 0.2372	6.3286 ± 0.2701	-0.0089 ± 0.0020	-36.2889 ± 0.1854
GLU-316	-24.1270 ± 0.3182	-0.8089 ± 0.1715	-0.0045 ± 0.0015	-24.9282 ± 0.2336
GLU-320	-18.3671 ± 0.0356	0.1680 ± 0.0148	0.0000 ± 0.0000	-18.2003 ± 0.0253
GLU-320	-17.6012 ± 0.0739	0.0561 ± 0.0111	0.0000 ± 0.0000	-17.5478 ± 0.0670
GLU-325	-15.2891 ± 0.0280	-0.0461 ± 0.0056	0.0000 ± 0.0000	-15.3351 ± 0.0265
GLU-325	-17.7381 ± 0.0601	-0.0532 ± 0.0149	0.0000 ± 0.0000	-17.7920 ± 0.0578
GLU-335	-45.0168 ± 0.2824	3.9103 ± 0.3658	-0.1023 ± 0.0045	-41.2149 ± 0.2578
GLU-335	-47.1187 ± 0.6230	4.5331 ± 0.7047	-0.1014 ± 0.0079	-42.7000 ± 0.3930
ASP-361	-35.0254 ± 0.3364	36.4123 ± 0.4153	-0.5349 ± 0.0062	0.8227 ± 0.2851
ASP-361	-26.5281 ± 0.3234	4.8100 ± 0.4258	-0.1085 ± 0.0074	-21.8103 ± 0.2848

GLU-370	-13.2515 ± 0.0256	-0.3475 ± 0.0058	0.0000 ± 0.0000	-13.5981 ± 0.0244
GLU-370	-14.4999 ± 0.0417	-0.0510 ± 0.0059	0.0000 ± 0.0000	-14.5490 ± 0.0410
GLU-378	-17.6538 ± 0.0646	-0.2281 ± 0.0044	0.0000 ± 0.0000	-17.8846 ± 0.0660
GLU-378	-19.3079 ± 0.0976	-0.0735 ± 0.0072	0.0000 ± 0.0000	-19.3806 ± 0.1011
GLU-382	-25.0410 ± 0.1976	-5.7343 ± 0.1126	-0.0068 ± 0.0013	-30.7854 ± 0.2044
GLU-382	-30.8744 ± 0.2122	-0.6916 ± 0.0762	0.0000 ± 0.0000	-31.5532 ± 0.2210
ASP-388	-9.6252 ± 0.0846	-3.7673 ± 0.0638	0.0000 ± 0.0000	-13.3922 ± 0.0479
ASP-388	-16.6724 ± 0.1418	-0.4870 ± 0.0438	0.0000 ± 0.0000	-17.1647 ± 0.1136
GLU-394	-11.9049 ± 0.0236	-0.3464 ± 0.0046	0.0000 ± 0.0000	-12.2520 ± 0.0223
GLU-394	-13.5788 ± 0.0370	-0.0677 ± 0.0059	0.0000 ± 0.0000	-13.6460 ± 0.0352
GLU-433	-6.7096 ± 0.0734	-6.2266 ± 0.0824	0.0000 ± 0.0000	-12.9379 ± 0.0521
GLU-433	-15.9984 ± 0.2007	-1.8101 ± 0.1613	0.0000 ± 0.0000	-17.8110 ± 0.1380
ASP-436	-10.5165 ± 0.0310	-1.3278 ± 0.0163	0.0000 ± 0.0000	-11.8442 ± 0.0254
ASP-436	-14.8204 ± 0.0998	-0.3470 ± 0.0301	0.0000 ± 0.0000	-15.1685 ± 0.0851
GLU-470	-12.2238 ± 0.0236	-0.3266 ± 0.0032	0.0000 ± 0.0000	-12.5505 ± 0.0229
GLU-470	-13.9218 ± 0.0342	-0.0468 ± 0.0035	0.0000 ± 0.0000	-13.9699 ± 0.0369
GLU-479	-11.7476 ± 0.0512	-1.0954 ± 0.0139	0.0000 ± 0.0000	-12.8417 ± 0.0474
GLU-479	-17.4554 ± 0.1156	-0.1427 ± 0.0153	0.0000 ± 0.0000	-17.5981 ± 0.1228
GLU-484	-10.8079 ± 0.0203	-0.2509 ± 0.0032	0.0000 ± 0.0000	-11.0598 ± 0.0194
GLU-484	-13.1785 ± 0.0557	-0.0489 ± 0.0044	0.0000 ± 0.0000	-13.2279 ± 0.0566
ASP-486	-10.3360 ± 0.0152	-0.2124 ± 0.0026	0.0000 ± 0.0000	-10.5489 ± 0.0150
ASP-486	-11.9363 ± 0.0285	-0.0330 ± 0.0026	0.0000 ± 0.0000	-11.9707 ± 0.0276
GLU-490	-10.3407 ± 0.0132	-0.0795 ± 0.0012	0.0000 ± 0.0000	-10.4201 ± 0.0126
GLU-490	-11.3754 ± 0.0264	-0.0108 ± 0.0009	0.0000 ± 0.0000	-11.3861 ± 0.0260
GLU-493	-11.4791 ± 0.0173	-0.0712 ± 0.0009	0.0000 ± 0.0000	-11.5501 ± 0.0171
GLU-493	-12.5942 ± 0.0266	-0.0107 ± 0.0008	0.0000 ± 0.0000	-12.6048 ± 0.0268
ASP-505	-11.4751 ± 0.0264	-0.4902 ± 0.0056	0.0000 ± 0.0000	-11.9666 ± 0.0242
ASP-505	-14.5518 ± 0.0653	-0.0654 ± 0.0061	0.0000 ± 0.0000	-14.6105 ± 0.0654
GLU-514	-9.8865 ± 0.0124	-0.0268 ± 0.0003	0.0000 ± 0.0000	-9.9135 ± 0.0126
GLU-514	-10.9626 ± 0.0223	-0.0052 ± 0.0004	0.0000 ± 0.0000	-10.9676 ± 0.0223
GLU-518	-11.5686 ± 0.0232	-0.0344 ± 0.0007	0.0000 ± 0.0000	-11.6018 ± 0.0226
GLU-518	-13.1496 ± 0.0347	-0.0074 ± 0.0006	0.0000 ± 0.0000	-13.1573 ± 0.0356
GLU-527	-12.7527 ± 0.0331	-0.2453 ± 0.0034	0.0000 ± 0.0000	-12.9992 ± 0.0332
GLU-527	-16.2011 ± 0.0844	-0.0196 ± 0.0030	0.0000 ± 0.0000	-16.2182 ± 0.0863
GLU-538	-9.8971 ± 0.0122	-0.0152 ± 0.0002	0.0000 ± 0.0000	-9.9120 ± 0.0125
GLU-538	-10.7557 ± 0.0223	-0.0020 ± 0.0002	0.0000 ± 0.0000	-10.7577 ± 0.0225
GLU-542	-11.6862 ± 0.0177	-0.0462 ± 0.0006	0.0000 ± 0.0000	-11.7326 ± 0.0178
GLU-542	-12.9370 ± 0.0341	-0.0096 ± 0.0007	0.0000 ± 0.0000	-12.9454 ± 0.0341
ASP-553	-11.4944 ± 0.0205	-0.0844 ± 0.0010	0.0000 ± 0.0000	-11.5782 ± 0.0204
ASP-553	-13.0337 ± 0.0423	-0.0107 ± 0.0011	0.0000 ± 0.0000	-13.0455 ± 0.0429
GLU-562	-9.8384 ± 0.0130	-0.0088 ± 0.0001	0.0000 ± 0.0000	-9.8472 ± 0.0130
GLU-562	-10.4863 ± 0.0218	-0.0009 ± 0.0001	0.0000 ± 0.0000	-10.4879 ± 0.0217
GLU-566	-11.5354 ± 0.0174	-0.0168 ± 0.0002	0.0000 ± 0.0000	-11.5513 ± 0.0179
GLU-566	-12.2555 ± 0.0324	-0.0028 ± 0.0002	0.0000 ± 0.0000	-12.2572 ± 0.0321
ASP-598	-11.5870 ± 0.0209	-0.0044 ± 0.0002	0.0000 ± 0.0000	-11.5929 ± 0.0207

ASP-598	-12.0709 ± 0.0402	0.0005 ± 0.0002	0.0000 ± 0.0000	-12.0708 ± 0.0412
ASP-608	-10.1033 ± 0.0159	-0.0041 ± 0.0001	0.0000 ± 0.0000	-10.1071 ± 0.0159
ASP-608	-10.4771 ± 0.0298	-0.0006 ± 0.0000	0.0000 ± 0.0000	-10.4784 ± 0.0292
ILE-616	-9.5987 ± 0.0156	-0.0018 ± 0.0000	0.0000 ± 0.0000	-9.6007 ± 0.0157
ILE-616	-10.1427 ± 0.0272	-0.0002 ± 0.0000	0.0000 ± 0.0000	-10.1444 ± 0.0283

Table 3.6.2: Binding free energy contribution of the key binding-site residues calculated from the binding energy decomposition for HAESA (kJmol-1) 2aii and complex 2b.

Residue	MM Energy	Polar Energy	APolar Energy	Total Energy
LEU-21	-33.1869 ± 0.0781	0.0544 ± 0.0673	0.0044 ± 0.0056	-33.1258 ± 0.1060
LEU-21	-32.8348 ± 0.0780	0.0789 ± 0.0680	-0.0070 ± 0.0042	-32.7634 ± 0.1068
ARG-29	-36.6814 ± 0.1016	-0.0032 ± 0.0263	0.0054 ± 0.0052	-36.6744 ± 0.1053
ARG-29	-37.3284 ± 0.1098	0.0227 ± 0.0219	-0.0013 ± 0.0051	-37.3074 ± 0.1157
LYS-32	-43.9291 ± 0.1613	0.1209 ± 0.0594	0.0001 ± 0.0064	-43.8045 ± 0.1709
LYS-32	-44.3154 ± 0.1547	0.0015 ± 0.0605	0.0061 ± 0.0049	-44.3061 ± 0.1673
LYS-55	-35.0204 ± 0.1170	-0.0444 ± 0.0688	-0.0067 ± 0.0050	-35.0611 ± 0.1332
LYS-55	-35.7468 ± 0.1243	-0.0155 ± 0.0710	-0.0092 ± 0.0045	-35.7696 ± 0.1336
LYS-132	-48.3948 ± 0.0879	0.0584 ± 0.0557	0.0000 ± 0.0057	-48.3322 ± 0.1008
LYS-132	-41.9798 ± 0.1063	0.0078 ± 0.0688	-0.0082 ± 0.0039	-41.9767 ± 0.1322
LYS-142	-40.0941 ± 0.0644	-0.0289 ± 0.0605	0.0006 ± 0.0055	-40.1250 ± 0.0912
LYS-142	-36.5012 ± 0.0845	0.0605 ± 0.0616	-0.0053 ± 0.0042	-36.4421 ± 0.1023
ARG-163	-37.6188 ± 0.0434	0.0329 ± 0.0339	0.0042 ± 0.0053	-37.5845 ± 0.0539
ARG-163	-35.3305 ± 0.0556	0.0504 ± 0.0308	-0.0029 ± 0.0041	-35.2843 ± 0.0605
LYS-164	-37.2666 ± 0.0458	-0.0250 ± 0.0631	-0.0028 ± 0.0058	-37.2918 ± 0.0754
LYS-164	-34.8580 ± 0.0619	0.0725 ± 0.0643	0.0082 ± 0.0050	-34.7760 ± 0.0933
LYS-190	-43.6209 ± 0.0989	-0.1959 ± 0.0618	-0.0055 ± 0.0053	-43.8200 ± 0.1214
LYS-190	-38.6437 ± 0.0897	0.0083 ± 0.0556	-0.0004 ± 0.0045	-38.6349 ± 0.1079
LYS-193	-54.6722 ± 0.1097	-0.1908 ± 0.0489	0.0118 ± 0.0061	-54.8448 ± 0.1207
LYS-193	-47.9450 ± 0.1417	0.0395 ± 0.0528	-0.0009 ± 0.0063	-47.9096 ± 0.1521
ARG-234	-39.9752 ± 0.0526	-0.0380 ± 0.0338	-0.0034 ± 0.0051	-40.0201 ± 0.0635
ARG-234	-36.2988 ± 0.0600	0.0379 ± 0.0310	0.0058 ± 0.0057	-36.2525 ± 0.0673
LYS-260	-39.2702 ± 0.0524	-0.1095 ± 0.0662	-0.0067 ± 0.0050	-39.3887 ± 0.0890
LYS-260	-35.8446 ± 0.0758	-0.0453 ± 0.0625	0.0007 ± 0.0043	-35.8898 ± 0.0989
LYS-287	-49.2767 ± 0.0888	-0.2061 ± 0.0675	-0.0029 ± 0.0048	-49.4823 ± 0.1088
LYS-287	-44.0960 ± 0.1445	0.0664 ± 0.0683	0.0054 ± 0.0052	-44.0332 ± 0.1589
ARG-288	-62.2832 ± 0.0918	-0.9215 ± 0.0286	-0.0007 ± 0.0061	-63.2065 ± 0.0921
ARG-288	-53.8585 ± 0.2107	-0.0686 ± 0.0248	-0.0013 ± 0.0062	-53.9396 ± 0.2169
LYS-295	-67.2177 ± 0.2624	-1.4354 ± 0.0713	-0.0092 ± 0.0046	-68.6684 ± 0.2900
LYS-295	-59.4986 ± 0.1857	-0.0192 ± 0.0582	-0.0082 ± 0.0040	-59.5214 ± 0.1942
LYS-299	-44.2690 ± 0.0887	-0.2407 ± 0.0657	0.0025 ± 0.0050	-44.5086 ± 0.1105
LYS-299	-39.9287 ± 0.0795	0.0232 ± 0.0655	0.0110 ± 0.0046	-39.8883 ± 0.1036
ARG-329	-41.1119 ± 0.0466	-0.0941 ± 0.0274	-0.0041 ± 0.0047	-41.2102 ± 0.0555
ARG-329	-37.6030 ± 0.0880	-0.0156 ± 0.0291	-0.0039 ± 0.0045	-37.6240 ± 0.0931
LYS-331	-42.1175 ± 0.0542	-0.1230 ± 0.0655	-0.0015 ± 0.0043	-42.2409 ± 0.0825

LYS-331	-38.4033 ± 0.1221	0.0568 ± 0.0648	0.0010 ± 0.0051	-38.3481 ± 0.1345
LYS-337	-76.9700 ± 0.1860	-2.0167 ± 0.0727	-0.0004 ± 0.0034	-78.9809 ± 0.1707
LYS-337	-62.7187 ± 0.3520	-0.1732 ± 0.0691	-0.0005 ± 0.0035	-62.9100 ± 0.3601
ARG-342	-55.5487 ± 0.1894	-1.8698 ± 0.0728	-0.0045 ± 0.0050	-57.4273 ± 0.1990
ARG-342	-52.0202 ± 0.1509	-0.0038 ± 0.0288	-0.0036 ± 0.0047	-52.0219 ± 0.1417
ARG-366	-65.9519 ± 0.3962	2.4549 ± 0.2250	-0.0169 ± 0.0042	-63.5220 ± 0.2544
ARG-366	-53.0042 ± 0.1489	0.0299 ± 0.0309	-0.0011 ± 0.0050	-52.9791 ± 0.1496
LYS-380	-54.2605 ± 0.1057	0.0853 ± 0.0578	-0.0008 ± 0.0060	-54.1715 ± 0.1203
LYS-380	-46.8817 ± 0.2726	-0.0620 ± 0.0569	-0.0026 ± 0.0057	-46.9559 ± 0.2728
LYS-401	-48.6801 ± 0.0914	0.2823 ± 0.0645	-0.0010 ± 0.0057	-48.3927 ± 0.1121
LYS-401	-41.0697 ± 0.1576	0.1437 ± 0.0609	-0.0027 ± 0.0044	-40.9251 ± 0.1650
LYS-403	-54.2529 ± 0.1277	0.1795 ± 0.0670	-0.0051 ± 0.0068	-54.0749 ± 0.1418
LYS-403	-46.5329 ± 0.1997	0.0135 ± 0.0620	-0.0077 ± 0.0058	-46.5291 ± 0.2124
ARG-407	-110.1744 ± 0.4762	17.3134 ± 0.4468	-1.0069 ± 0.0173	-93.8483 ± 0.2288
ARG-407	-77.8162 ± 0.5425	0.1460 ± 0.1509	-0.0335 ± 0.0081	-77.6915 ± 0.5539
ARG-409	-115.7889 ± 0.9025	54.3453 ± 1.1173	-1.6671 ± 0.0141	-63.0947 ± 0.3262
ARG-409	-71.0534 ± 0.4541	0.0029 ± 0.1321	-0.0651 ± 0.0101	-71.1184 ± 0.4132
LYS-414	-59.1874 ± 0.2384	2.4376 ± 0.1120	0.0004 ± 0.0046	-56.7642 ± 0.1769
LYS-414	-49.8189 ± 0.1668	-0.0565 ± 0.0496	0.0071 ± 0.0049	-49.8697 ± 0.1798
ARG-428	-72.3170 ± 0.2102	0.5465 ± 0.0382	-0.0002 ± 0.0063	-71.7624 ± 0.2126
ARG-428	-62.0767 ± 0.5148	-0.0944 ± 0.0359	0.0060 ± 0.0056	-62.1705 ± 0.5284
LYS-445	-51.2303 ± 0.0839	0.3888 ± 0.0660	0.0109 ± 0.0075	-50.8286 ± 0.1040
LYS-445	-45.3545 ± 0.1905	0.0566 ± 0.0606	-0.0017 ± 0.0057	-45.2966 ± 0.1935
LYS-451	-66.6023 ± 0.1721	0.5125 ± 0.0652	-0.0072 ± 0.0053	-66.0949 ± 0.1897
LYS-451	-60.1667 ± 0.3284	0.0024 ± 0.0615	0.0062 ± 0.0062	-60.1766 ± 0.3333
ARG-457	-128.1137 ± 0.4951	57.0362 ± 0.7508	-1.3597 ± 0.0162	-72.4483 ± 0.4142
ARG-457	-73.1780 ± 0.6678	2.1387 ± 0.3211	-0.0740 ± 0.0116	-71.1336 ± 0.5233
LYS-460	-68.4617 ± 0.3964	4.8053 ± 0.3630	-0.1178 ± 0.0090	-63.7722 ± 0.2640
LYS-460	-54.7896 ± 0.2825	-0.0355 ± 0.0576	-0.0116 ± 0.0049	-54.8254 ± 0.2841
ARG-462	-51.8617 ± 0.1221	1.0658 ± 0.0400	-0.0023 ± 0.0048	-50.7967 ± 0.1053
ARG-462	-44.6136 ± 0.1676	-0.0136 ± 0.0321	-0.0098 ± 0.0044	-44.6367 ± 0.1653
LYS-497	-63.5686 ± 0.1266	0.7294 ± 0.0611	-0.0013 ± 0.0054	-62.8358 ± 0.1331
LYS-497	-56.5447 ± 0.2746	0.0696 ± 0.0652	0.0015 ± 0.0051	-56.4771 ± 0.2669
ARG-503	-97.8501 ± 0.5944	19.2316 ± 0.5875	-0.5100 ± 0.0232	-79.1197 ± 0.2409
ARG-503	-99.8606 ± 1.5487	19.4445 ± 1.3480	-0.6856 ± 0.0325	-81.1087 ± 0.5668
LYS-508	-54.6750 ± 0.1495	0.2805 ± 0.0764	-0.0012 ± 0.0048	-54.3980 ± 0.1690
LYS-508	-50.5014 ± 0.2303	-0.2486 ± 0.0663	-0.0001 ± 0.0065	-50.7559 ± 0.2405
ARG-517	-53.0356 ± 0.1147	0.1951 ± 0.0383	-0.0006 ± 0.0057	-52.8450 ± 0.1207
ARG-517	-49.0365 ± 0.1623	-0.0976 ± 0.0337	0.0038 ± 0.0050	-49.1292 ± 0.1629
ARG-520	-69.6664 ± 0.2912	0.6475 ± 0.0369	-0.0019 ± 0.0064	-69.0207 ± 0.2836
ARG-520	-62.2441 ± 0.3349	-0.2563 ± 0.0311	-0.0013 ± 0.0066	-62.5076 ± 0.3457
LYS-523	-107.7222 ± 0.5511	1.3867 ± 0.0989	-0.0048 ± 0.0066	-106.3612 ± 0.5201
LYS-523	-92.3293 ± 0.8887	0.4139 ± 0.1782	-0.0058 ± 0.0071	-91.8755 ± 0.8115
LYS-541	-61.2099 ± 0.1577	0.1295 ± 0.0631	0.0084 ± 0.0061	-61.0694 ± 0.1708
LYS-541	-53.8068 ± 0.1124	-0.2494 ± 0.0689	0.0092 ± 0.0047	-54.0464 ± 0.1316

LYS-571	-141.1142 ± 0.7543	54.0109 ± 1.1925	-2.2692 ± 0.0245	-89.3525 ± 0.6560
LYS-571	-180.0614 ± 1.3705	109.1597 ± 2.4072	-1.8714 ± 0.0317	-72.8725 ± 1.085
LYS-585	-59.3955 ± 0.1163	-0.0843 ± 0.0583	0.0196 ± 0.0067	-59.4622 ± 0.1247
LYS-585	-60.5968 ± 0.1409	-0.3748 ± 0.0592	-0.0004 ± 0.0066	-60.9745 ± 0.1500
LYS-593	-83.8032 ± 0.8067	10.1608 ± 0.6778	-0.3921 ± 0.0171	-74.0297 ± 0.3772
LYS-593	-81.1101 ± 0.6187	3.5515 ± 0.3203	-0.1264 ± 0.0110	-77.6855 ± 0.4396
ARG-614	-62.2371 ± 0.2020	-0.0929 ± 0.0286	-0.0116 ± 0.0046	-62.3424 ± 0.2092
ARG-614	-67.7230 ± 0.4271	-0.0860 ± 0.0410	0.0024 ± 0.0048	-67.8118 ± 0.4211
LYS-615	-51.0670 ± 0.0848	-0.0823 ± 0.0687	-0.0021 ± 0.0055	-51.1438 ± 0.1086
LYS-615	-51.0031 ± 0.1513	-0.2028 ± 0.0682	-0.0042 ± 0.0037	-51.2091 ± 0.1647

Table 3.6.3: Binding free energy contribution of the key binding-site residues calculated from the binding energy decomposition for IDA (kJmol-1) 2ai and complex 2c.

Residue	MM Energy	Polar Energy	APolar Energy	Total Energy
TYR-56	-160.8983 ± 0.9717	34.5004 ± 1.0720	-1.0623 ± 0.0293	-127.4403 ± 0.6430
TYR-56	-233.8540 ± 1.1565	90.0173 ± 1.1658	-2.0357 ± 0.0359	-145.9164 ± 0.6184
ILE-59	-9.8737 ± 0.2234	3.5390 ± 0.1351	-0.6512 ± 0.0230	-6.9942 ± 0.1835
ILE-59	-16.8313 ± 0.1149	3.0874 ± 0.0611	-1.8605 ± 0.0173	-15.6089 ± 0.1089
LYS-66	-151.5967 ± 0.4313	12.4396 ± 0.2260	-0.0745 ± 0.0087	-139.2387 ± 0.3322
LYS-66	-150.6779 ± 0.7475	14.6202 ± 0.7580	-0.1969 ± 0.0158	-136.2600 ± 0.6964
ARG-67	-165.5938 ± 0.9192	38.0500 ± 1.1364	-1.9039 ± 0.0348	-129.4292 ± 0.3620
ARG-67	-161.4076 ± 0.9499	30.1827 ± 0.8641	-1.3616 ± 0.0300	-132.5575 ± 0.4306

Table 3.6.4: Binding free energy contribution of the key binding-site residues calculated from the binding energy decomposition for SERK1 (kJmol-1) 2aii and complex 2b.

Residue	MM Energy	Polar Energy	APolar Energy	Total Energy
ALA-26	-150.1375 ± 0.4964	67.9136 ± 0.9376	-0.9567 ± 0.0144	-83.2022 ± 0.7246
ALA-26	-84.8246 ± 0.3289	-0.6084 ± 0.0770	-0.0026 ± 0.0060	-85.4350 ± 0.3466
ARG-37	-92.8306 ± 0.2821	-0.5352 ± 0.0599	-0.0020 ± 0.0093	-93.3773 ± 0.2825
ARG-37	-85.1885 ± 0.3428	-1.0609 ± 0.0493	-0.0063 ± 0.0079	-86.2433 ± 0.3578
ARG-73	-150.5307 ± 0.7240	83.7562 ± 0.7649	-1.6157 ± 0.0161	-68.3922 ± 0.4363
ARG-73	-107.7962 ± 1.2959	29.6625 ± 1.4262	-0.9849 ± 0.0311	-79.1028 ± 0.4598
LYS-93	-85.6829 ± 0.3401	1.6509 ± 0.1159	-0.0000 ± 0.0085	-84.0495 ± 0.3458
LYS-93	-73.5555 ± 0.2099	-0.0132 ± 0.0768	-0.0077 ± 0.0097	-73.5755 ± 0.2293
LYS-139	-70.9703 ± 0.2346	1.2426 ± 0.0879	0.0063 ± 0.0076	-69.7238 ± 0.2397
LYS-139	-64.9767 ± 0.1882	-0.1889 ± 0.0933	-0.0110 ± 0.0086	-65.1621 ± 0.2057
LYS-142	-93.1152 ± 0.3569	2.1989 ± 0.0933	0.0100 ± 0.0087	-90.8911 ± 0.3619
LYS-142	-97.0787 ± 0.3451	0.2452 ± 0.0928	-0.0253 ± 0.0087	-96.8668 ± 0.3439
ARG-144	-158.9823 ± 0.8196	57.7221 ± 1.0149	-0.5393 ± 0.0184	-101.8198 ± 0.405
ARG-144	-161.4613 ± 0.5680	59.7313 ± 0.7349	-1.2634 ± 0.0175	-102.9777 ± 0.335
ARG-147	-130.9202 ± 0.5185	66.9371 ± 0.5971	-1.5659 ± 0.0143	-65.5524 ± 0.3911
ARG-147	-87.2802 ± 0.9540	19.0898 ± 0.8611	-1.0203 ± 0.0184	-69.2421 ± 0.4306

ARG-176	-56.6132 ± 0.1780	-0.2551 ± 0.0491	0.0054 ± 0.0106	-56.8609 ± 0.1800
ARG-176	-53.7475 ± 0.1834	-0.4873 ± 0.0520	0.0060 ± 0.0091	-54.2350 ± 0.1949

Table 3.7.1: Protein-Protein Hydrophobic Interactions of complex 2a

Before Simulation					
Position	**Residue**	**Chain**	**Position**	**Residue**	**Chain**
97	TYR	A	56	TYR	B
171	ALA	A	59	ILE	B
196	TYR	A	59	ILE	B
196	TYR	A	60	PRO	B
218	TRP	A	59	ILE	B
339	PHE	A	55	VAL	C
478	ILE	A	61	PHE	C
548	VAL	A	101	TYR	C
551	TYR	A	97	TYR	C
574	VAL	A	97	TYR	C
594	ILE	A	169	VAL	C
594	ILE	A	189	LEU	C
595	TYR	A	145	PHE	C
595	TYR	A	169	VAL	C
After Simulation					
Position	**Residue**	**Chain**	**Position**	**Residue**	**Chain**
171	ALA	A	59	ILE	B
195	ALA	A	59	ILE	B
196	TYR	A	59	ILE	B
196	TYR	A	60	PRO	B
218	TRP	A	59	ILE	B
478	ILE	A	61	PHE	C
548	VAL	A	101	TYR	C
551	TYR	A	97	TYR	C
574	VAL	A	97	TYR	C
594	ILE	A	169	VAL	C
594	ILE	A	189	LEU	C

Table 3.7.2: Protein-Protein Main Chain-Main Chain Hydrogen Bonds of complex 2a

Before Simulation								
DONOR				**ACCEPTOR**				
POS	**CHAIN**	**RES**	**ATOM**	**POS**	**CHAIN**	**RES**	**ATOM**	**Dd-a**
68	B	HIS	N	53	C	THR	O	3.19
55	C	VAL	N	68	B	HIS	O	3.14

After Simulation								
DONOR				ACCEPTOR				
POS	CHAIN	RES	ATOM	POS	CHAIN	RES	ATOM	Dd-a
68	B	HIS	N	53	C	THR	O	2.73
55	C	VAL	N	68	B	HIS	O	3.28

Table 3.7.3: Protein-Protein Main Chain-Side Chain Hydrogen Bonds of complex 2a

Before Simulation								
DONOR				ACCEPTOR				
POS	CHAIN	RES	ATOM	POS	CHAIN	RES	ATOM	Dd-a
123	A	GLU	OE1	57	B	VAL	O	3.45
123	A	GLU	OE1	57	B	VAL	O	3.45
123	A	GLU	OE2	57	B	VAL	O	2.65
123	A	GLU	OE2	57	B	VAL	O	2.65
264	A	GLN	NE2	62	B	SER	O	3.15
264	A	GLN	NE2	62	B	SER	O	3.15
266	A	GLU	OE1	63	B	ALA	O	3.34
266	A	GLU	OE1	63	B	ALA	O	3.34
313	A	ASN	ND2	65	B	SER	O	3.31
313	A	ASN	ND2	65	B	SER	O	3.31
337	A	LYS	NZ	65	B	SER	O	2.88
337	A	LYS	NZ	67	B	ARG	O	2.66
361	A	ASP	OD2	69	B	ASN	OXT	2.98
361	A	ASP	OD2	69	B	ASN	OXT	2.98
457	A	ARG	NH2	58	C	CYS	O	3.11
457	A	ARG	NH2	58	C	CYS	O	3.11
57	B	VAL	N	123	A	GLU	OE1	2.7
65	B	SER	N	290	A	ASP	OD2	2.97
67	B	ARG	NH2	55	C	VAL	O	3.39
67	B	ARG	NH2	55	C	VAL	O	3.39
69	B	ASN	N	361	A	ASP	OD2	2.48
101	C	TYR	OH	548	A	VAL	O	3.42
144	C	ARG	NH2	594	A	ILE	O	3.04
144	C	ARG	NH2	594	A	ILE	O	3.04
147	C	ARG	NH2	572	A	LEU	O	3.38
147	C	ARG	NH2	572	A	LEU	O	3.38
After Simulation								
DONOR				ACCEPTOR				
POS	CHAIN	RES	ATOM	POS	CHAIN	RES	ATOM	Dd-a
123	A	GLU	OE1	57	B	VAL	O	3.36

123	A	GLU	OE1	57	B	VAL	O	3.36
264	A	GLN	NE2	62	B	SER	O	2.87
264	A	GLN	NE2	62	B	SER	O	2.87
266	A	GLU	OE1	62	B	SER	O	3.23
266	A	GLU	OE1	62	B	SER	O	3.23
337	A	LYS	NZ	65	B	SER	O	2.85
337	A	LYS	NZ	67	B	ARG	O	2.93
457	A	ARG	NH2	58	C	CYS	O	2.75
457	A	ARG	NH2	58	C	CYS	O	2.75
57	B	VAL	N	123	A	GLU	OE1	2.83
69	B	ASN	N	361	A	ASP	OD2	2.96
147	C	ARG	NH1	572	A	LEU	O	3.36
147	C	ARG	NH1	572	A	LEU	O	3.36

Table 3.7.4: Protein-Protein Side Chain-Side Chain Hydrogen Bonds of complex 2a

Before Simulation								
DONOR				**ACCEPTOR**				
POS	**CHAIN**	**RES**	**ATOM**	**POS**	**CHAIN**	**RES**	**ATOM**	**Dd-a**
240	A	ASN	ND2	62	B	SER	OG	2.98
240	A	ASN	ND2	62	B	SER	OG	2.98
264	A	GLN	NE2	62	B	SER	OG	3.17
264	A	GLN	NE2	62	B	SER	OG	3.17
407	A	ARG	NE	69	B	ASN	OD1	3.19
407	A	ARG	NE	69	B	ASN	ND2	3.14
407	A	ARG	NH2	69	B	ASN	OD1	2.52
407	A	ARG	NH2	69	B	ASN	OD1	2.52
409	A	ARG	NH1	69	B	ASN	OD1	2.58
409	A	ARG	NH1	69	B	ASN	OD1	2.58
526	A	ASN	ND2	75	C	ASP	OD2	3.49
526	A	ASN	ND2	75	C	ASP	OD2	3.49
550	A	ASN	OD1	101	C	TYR	OH	2.7
550	A	ASN	OD1	101	C	TYR	OH	2.7
550	A	ASN	ND2	101	C	TYR	OH	3.38
550	A	ASN	ND2	101	C	TYR	OH	3.38
551	A	TYR	OH	75	C	ASP	OD1	2.73
573	A	ASN	ND2	99	C	GLU	OE2	2.85
573	A	ASN	ND2	99	C	GLU	OE2	2.85
573	A	ASN	OD1	121	C	SER	OG	2.72
573	A	ASN	OD1	121	C	SER	OG	2.72
573	A	ASN	OD1	123	C	ASP	OD2	3.45
573	A	ASN	OD1	123	C	ASP	OD2	3.45

62	B	SER	OG	240	A	ASN	ND2	2.98
62	B	SER	OG	242	A	ASP	OD2	2.72
62	B	SER	OG	264	A	GLN	NE2	3.17
67	B	ARG	NH1	293	A	MET	SD	3.99
67	B	ARG	NH1	293	A	MET	SD	3.99
67	B	ARG	NH1	316	A	GLU	OE1	2.68
67	B	ARG	NH1	316	A	GLU	OE1	2.68
67	B	ARG	NH1	316	A	GLU	OE2	3.24
67	B	ARG	NH1	316	A	GLU	OE2	3.24
73	C	ARG	NH1	526	A	ASN	ND2	3.34
73	C	ARG	NH1	526	A	ASN	ND2	3.34
73	C	ARG	NH2	527	A	GLU	OE1	2.56
73	C	ARG	NH2	527	A	GLU	OE1	2.56
75	C	ASP	OD2	526	A	ASN	ND2	3.49
75	C	ASP	OD2	526	A	ASN	ND2	3.49
99	C	GLU	OE2	573	A	ASN	ND2	2.85
99	C	GLU	OE2	573	A	ASN	ND2	2.85
101	C	TYR	OH	550	A	ASN	OD1	2.7
101	C	TYR	OH	550	A	ASN	ND2	3.38
121	C	SER	OG	573	A	ASN	OD1	2.72
123	C	ASP	OD2	573	A	ASN	OD1	3.45
123	C	ASP	OD2	573	A	ASN	OD1	3.45
147	C	ARG	NH2	573	A	ASN	OD1	3.07
147	C	ARG	NH2	573	A	ASN	OD1	3.07
After Simulation								
DONOR				**ACCEPTOR**				
POS	**CHAIN**	**RES**	**ATOM**	**POS**	**CHAIN**	**RES**	**ATOM**	**Dd-a**
361	A	ASP	OD2	69	B	ASN	ND2	3.09
361	A	ASP	OD2	69	B	ASN	ND2	3.09
407	A	ARG	NE	69	B	ASN	OD1	3
409	A	ARG	NH1	69	B	ASN	OD1	2.97
409	A	ARG	NH1	69	B	ASN	OD1	2.97
526	A	ASN	ND2	75	C	ASP	OD1	3.28
526	A	ASN	ND2	75	C	ASP	OD1	3.28
526	A	ASN	ND2	75	C	ASP	OD2	2.82
526	A	ASN	ND2	75	C	ASP	OD2	2.82
550	A	ASN	ND2	99	C	GLU	OE1	2.78
550	A	ASN	ND2	99	C	GLU	OE1	2.78
551	A	TYR	OH	75	C	ASP	OD1	3.09
573	A	ASN	OD1	99	C	GLU	OE2	3.47
573	A	ASN	OD1	99	C	GLU	OE2	3.47

573	A	ASN	ND2	99	C	GLU	OE1	3.18
573	A	ASN	ND2	99	C	GLU	OE1	3.18
573	A	ASN	ND2	99	C	GLU	OE2	2.84
573	A	ASN	ND2	99	C	GLU	OE2	2.84
573	A	ASN	OD1	121	C	SER	OG	2.78
573	A	ASN	OD1	121	C	SER	OG	2.78
62	B	SER	OG	242	A	ASP	OD2	2.66
67	B	ARG	NH1	293	A	MET	SD	2.94
67	B	ARG	NH1	293	A	MET	SD	2.94
67	B	ARG	NH1	316	A	GLU	OE1	3.17
67	B	ARG	NH1	316	A	GLU	OE1	3.17
67	B	ARG	NH1	316	A	GLU	OE2	3.34
67	B	ARG	NH1	316	A	GLU	OE2	3.34
67	B	ARG	NH2	27	C	ASN	OD1	3.08
67	B	ARG	NH2	27	C	ASN	OD1	3.08
69	B	ASN	ND2	361	A	ASP	OD2	3.09
69	B	ASN	ND2	361	A	ASP	OD2	3.09
73	C	ARG	NH1	527	A	GLU	OE1	3.12
73	C	ARG	NH1	527	A	GLU	OE1	3.12
75	C	ASP	OD1	526	A	ASN	ND2	3.28
75	C	ASP	OD1	526	A	ASN	ND2	3.28
75	C	ASP	OD2	526	A	ASN	ND2	2.82
75	C	ASP	OD2	526	A	ASN	ND2	2.82
99	C	GLU	OE1	550	A	ASN	ND2	2.78
99	C	GLU	OE1	550	A	ASN	ND2	2.78
99	C	GLU	OE1	573	A	ASN	ND2	3.18
99	C	GLU	OE1	573	A	ASN	ND2	3.18
99	C	GLU	OE2	573	A	ASN	OD1	3.47
99	C	GLU	OE2	573	A	ASN	OD1	3.47
99	C	GLU	OE2	573	A	ASN	ND2	2.84
99	C	GLU	OE2	573	A	ASN	ND2	2.84
121	C	SER	OG	573	A	ASN	OD1	2.78
147	C	ARG	NH1	573	A	ASN	OD1	3.18
147	C	ARG	NH1	573	A	ASN	OD1	3.18
147	C	ARG	NH2	573	A	ASN	OD1	2.83
147	C	ARG	NH2	573	A	ASN	OD1	2.83

Table 3.7.5: Protein-Protein Ionic Interactions of complex 2a

Before Simulation					
Position	**Residue**	**Chain**	**Position**	**Residue**	**Chain**
68	HIS	B	51	ASP	C
316	GLU	A	67	ARG	B
503	ARG	A	75	ASP	C
527	GLU	A	73	ARG	C
571	LYS	A	171	ASP	C
598	ASP	A	144	ARG	C
After Simulation					
Position	**Residue**	**Chain**	**Position**	**Residue**	**Chain**
316	GLU	A	67	ARG	B
503	ARG	A	75	ASP	C
527	GLU	A	73	ARG	C
598	ASP	A	144	ARG	C

Table 3.7.6: Protein-Protein Aromatic-Aromatic Interactions of complex 2a

Before Simulation						
Position	**Residue**	**Chain**	**Position**	**Residue**	**Chain**	**D(centroid-centroid)**
551	TYR	A	97	TYR	C	5.48
After Simulation						
Position	**Residue**	**Chain**	**Position**	**Residue**	**Chain**	**D(centroid-centroid)**
551	TYR	A	97	TYR	C	5.27

Table 3.7.7: Protein-Protein Cation-Pi Interactions of complex 2a

Before Simulation						
Position	**Residue**	**Chain**	**Position**	**Residue**	**Chain**	**D(cation-Pi)**
551	TYR	A	73	ARG	C	4.2
After Simulation						
Position	**Residue**	**Chain**	**Position**	**Residue**	**Chain**	**D(cation-Pi)**
551	TYR	A	73	ARG	C	4.06

Table 3.8.1: Protein-Protein Hydrophobic Interactions of complex 2b

Before Simulation					
Position	**Residue**	**Chain**	**Position**	**Residue**	**Chain**
339	PHE	A	55	VAL	C
478	ILE	A	61	PHE	C
548	VAL	A	101	TYR	C
551	TYR	A	97	TYR	C
574	VAL	A	97	TYR	C
594	ILE	A	169	VAL	C
594	ILE	A	189	LEU	C
595	TYR	A	145	PHE	C
595	TYR	A	169	VAL	C
After Simulation					
Position	**Residue**	**Chain**	**Position**	**Residue**	**Chain**
478	ILE	A	61	PHE	C
548	VAL	A	101	TYR	C
551	TYR	A	97	TYR	C
574	VAL	A	97	TYR	C
594	ILE	A	169	VAL	C
595	TYR	A	145	PHE	C
595	TYR	A	169	VAL	C

Table 3.8.2: Protein-Protein Main Chain-Side Chain Hydrogen Bonds of complex 2b

Before Simulation								
DONOR				**ACCEPTOR**				
POS	**CHAIN**	**RES**	**ATOM**	**POS**	**CHAIN**	**RES**	**ATOM**	**Dd-a**
457	A	ARG	NH2	58	C	CYS	O	3.11
457	A	ARG	NH2	58	C	CYS	O	3.11
101	C	TYR	OH	548	A	VAL	O	3.42
144	C	ARG	NH2	594	A	ILE	O	3.04
144	C	ARG	NH2	594	A	ILE	O	3.04
147	C	ARG	NH2	572	A	LEU	O	3.38
147	C	ARG	NH2	572	A	LEU	O	3.38
After Simulation								
DONOR				**ACCEPTOR**				
POS	**CHAIN**	**RES**	**ATOM**	**POS**	**CHAIN**	**RES**	**ATOM**	**Dd-a**
457	A	ARG	NH2	58	C	CYS	O	2.89
457	A	ARG	NH2	58	C	CYS	O	2.89
101	C	TYR	OH	548	A	VAL	O	3.43
168	C	GLN	OE1	594	A	ILE	O	3.42

168	C	GLN	OE1	594	A	ILE	O	3.42

Table 3.8.3: Protein-Protein Side Chain-Side Chain Hydrogen Bonds of complex 2b

Before Simulation								
DONOR				**ACCEPTOR**				
POS	**CHAIN**	**RES**	**ATOM**	**POS**	**CHAIN**	**RES**	**ATOM**	**Dd-a**
526	A	ASN	ND2	75	C	ASP	OD2	3.49
526	A	ASN	ND2	75	C	ASP	OD2	3.49
550	A	ASN	OD1	101	C	TYR	OH	2.7
550	A	ASN	OD1	101	C	TYR	OH	2.7
550	A	ASN	ND2	101	C	TYR	OH	3.38
550	A	ASN	ND2	101	C	TYR	OH	3.38
551	A	TYR	OH	75	C	ASP	OD1	2.73
573	A	ASN	ND2	99	C	GLU	OE2	2.85
573	A	ASN	ND2	99	C	GLU	OE2	2.85
573	A	ASN	OD1	121	C	SER	OG	2.72
573	A	ASN	OD1	121	C	SER	OG	2.72
573	A	ASN	OD1	123	C	ASP	OD2	3.45
573	A	ASN	OD1	123	C	ASP	OD2	3.45
73	C	ARG	NH1	526	A	ASN	ND2	3.34
73	C	ARG	NH1	526	A	ASN	ND2	3.34
73	C	ARG	NH2	527	A	GLU	OE1	2.56
73	C	ARG	NH2	527	A	GLU	OE1	2.56
75	C	ASP	OD2	526	A	ASN	ND2	3.49
75	C	ASP	OD2	526	A	ASN	ND2	3.49
99	C	GLU	OE2	573	A	ASN	ND2	2.85
99	C	GLU	OE2	573	A	ASN	ND2	2.85
101	C	TYR	OH	550	A	ASN	OD1	2.7
101	C	TYR	OH	550	A	ASN	ND2	3.38
121	C	SER	OG	573	A	ASN	OD1	2.72
123	C	ASP	OD2	573	A	ASN	OD1	3.45
123	C	ASP	OD2	573	A	ASN	OD1	3.45
147	C	ARG	NH2	573	A	ASN	OD1	3.07
147	C	ARG	NH2	573	A	ASN	OD1	3.07
After Simulation								
DONOR				**ACCEPTOR**				
POS	**CHAIN**	**RES**	**ATOM**	**POS**	**CHAIN**	**RES**	**ATOM**	**Dd-a**
550	A	ASN	ND2	99	C	GLU	OE1	2.85
550	A	ASN	ND2	99	C	GLU	OE1	2.85
550	A	ASN	ND2	101	C	TYR	OH	3.26

550	A	ASN	ND2	101	C	TYR	OH	3.26
551	A	TYR	OH	75	C	ASP	OD1	2.82
573	A	ASN	ND2	99	C	GLU	OE1	3.13
573	A	ASN	ND2	99	C	GLU	OE1	3.13
573	A	ASN	ND2	99	C	GLU	OE2	3.24
573	A	ASN	ND2	99	C	GLU	OE2	3.24
573	A	ASN	OD1	121	C	SER	OG	2.58
573	A	ASN	OD1	121	C	SER	OG	2.58
73	C	ARG	NH1	527	A	GLU	OE2	3.43
73	C	ARG	NH1	527	A	GLU	OE2	3.43
73	C	ARG	NH2	527	A	GLU	OE2	3.06
73	C	ARG	NH2	527	A	GLU	OE2	3.06
99	C	GLU	OE1	550	A	ASN	ND2	2.85
99	C	GLU	OE1	550	A	ASN	ND2	2.85
99	C	GLU	OE1	573	A	ASN	ND2	3.13
99	C	GLU	OE1	573	A	ASN	ND2	3.13
99	C	GLU	OE2	573	A	ASN	ND2	3.24
99	C	GLU	OE2	573	A	ASN	ND2	3.24
101	C	TYR	OH	550	A	ASN	ND2	3.26
121	C	SER	OG	573	A	ASN	OD1	2.58
147	C	ARG	NH2	573	A	ASN	OD1	2.77
147	C	ARG	NH2	573	A	ASN	OD1	2.77

Table 3.8.4: Protein-Protein Ionic Interactions of complex 2b

Before Simulation					
Position	**Residue**	**Chain**	**Position**	**Residue**	**Chain**
503	ARG	A	75	ASP	C
527	GLU	A	73	ARG	C
571	LYS	A	171	ASP	C
598	ASP	A	144	ARG	C
After Simulation					
Position	**Residue**	**Chain**	**Position**	**Residue**	**Chain**
407	ARG	A	51	ASP	C
527	GLU	A	73	ARG	C
571	LYS	A	123	ASP	C
598	ASP	A	144	ARG	C

Table 3.8.5: Protein-Protein Aromatic-Aromatic Interactions of complex 2b

Before Simulation						
Position	**Residue**	**Chain**	**Position**	**Residue**	**Chain**	**D(centroid-centroid)**
551	TYR	A	97	TYR	C	5.48
After Simulation						
Position	**Residue**	**Chain**	**Position**	**Residue**	**Chain**	**D(centroid-centroid)**
51	TYR	A	97	TYR	C	6.17
595	TYR	A	145	PHE	C	6.9

Table 3.8.6: Protein-Protein Cation-Pi Interactions of complex 2b

Before Simulation						
Position	**Residue**	**Chain**	**Position**	**Residue**	**Chain**	**D(cation-Pi)**
551	TYR	A	73	ARG	C	4.2
After Simulation						
Position	**Residue**	**Chain**	**Position**	**Residue**	**Chain**	**D(cation-Pi)**
125	TYR	C	571	LYS	A	3.94
551	TYR	A	73	ARG	C	4.12

Table 3.9.1: Protein-Protein Hydrophobic Interactions of complex 2c

Before Simulation					
Position	**Residue**	**Chain**	**Position**	**Residue**	**Chain**
97	TYR	A	56	TYR	B
171	ALA	A	59	ILE	B
196	TYR	A	59	ILE	B
196	TYR	A	60	PRO	B
218	TRP	A	59	ILE	B
After Simulation					
Position	**Residue**	**Chain**	**Position**	**Residue**	**Chain**
196	TYR	A	59	ILE	B
196	TYR	A	60	PRO	B
218	TRP	A	59	ILE	B

Table 3.9.2: Protein-Protein Main Chain-Side Chain Hydrogen Bonds of complex 2c

Before Simulation								
DONOR				**ACCEPTOR**				
POS	**CHAIN**	**RES**	**ATOM**	**POS**	**CHAIN**	**RES**	**ATOM**	**Dd-a**
123	A	GLU	OE1	57	B	VAL	O	3.45

123	A	GLU	OE1	57	B	VAL	O	3.45
123	A	GLU	OE2	57	B	VAL	O	2.65
123	A	GLU	OE2	57	B	VAL	O	2.65
264	A	GLN	NE2	62	B	SER	O	3.15
264	A	GLN	NE2	62	B	SER	O	3.15
266	A	GLU	OE1	63	B	ALA	O	3.34
266	A	GLU	OE1	63	B	ALA	O	3.34
313	A	ASN	ND2	65	B	SER	O	3.31
313	A	ASN	ND2	65	B	SER	O	3.31
337	A	LYS	NZ	65	B	SER	O	2.88
337	A	LYS	NZ	67	B	ARG	O	2.66
361	A	ASP	OD2	69	B	ASN	OXT	2.98
361	A	ASP	OD2	69	B	ASN	OXT	2.98
57	B	VAL	N	123	A	GLU	OE1	2.7
65	B	SER	N	290	A	ASP	OD2	2.97
69	B	ASN	N	361	A	ASP	OD2	2.48
After Simulation								
DONOR				**ACCEPTOR**				
POS	**CHAIN**	**RES**	**ATOM**	**POS**	**CHAIN**	**RES**	**ATOM**	**Dd-a**
264	A	GLN	NE2	62	B	SER	O	3.1
264	A	GLN	NE2	62	B	SER	O	3.1
337	A	LYS	NZ	65	B	SER	O	3.22
57	B	VAL	N	123	A	GLU	OE1	3.06
63	B	ALA	N	266	A	GLU	OE1	3.5
65	B	SER	N	266	A	GLU	OE1	2.89
65	B	SER	N	266	A	GLU	OE2	3.33
69	B	ASN	N	361	A	ASP	OD2	3.27

Table 3.9.3: Protein-Protein Side Chain-Side Chain Hydrogen Bonds of complex 2c

Before Simulation								
DONOR				**ACCEPTOR**				
POS	**CHAIN**	**RES**	**ATOM**	**POS**	**CHAIN**	**RES**	**ATOM**	**Dd-a**
240	A	ASN	ND2	62	B	SER	OG	2.98
240	A	ASN	ND2	62	B	SER	OG	2.98
264	A	GLN	NE2	62	B	SER	OG	3.17
264	A	GLN	NE2	62	B	SER	OG	3.17
407	A	ARG	NE	69	B	ASN	OD1	3.19
407	A	ARG	NE	69	B	ASN	ND2	3.14
407	A	ARG	NH2	69	B	ASN	OD1	2.52
407	A	ARG	NH2	69	B	ASN	OD1	2.52

409	A	ARG	NH1	69	B	ASN	OD1	2.58
409	A	ARG	NH1	69	B	ASN	OD1	2.58
62	B	SER	OG	240	A	ASN	ND2	2.98
62	B	SER	OG	242	A	ASP	OD2	2.72
62	B	SER	OG	264	A	GLN	NE2	3.17
67	B	ARG	NH1	293	A	MET	SD	3.99
67	B	ARG	NH1	293	A	MET	SD	3.99
67	B	ARG	NH1	316	A	GLU	OE1	2.68
67	B	ARG	NH1	316	A	GLU	OE1	2.68
67	B	ARG	NH1	316	A	GLU	OE2	3.24
67	B	ARG	NH1	316	A	GLU	OE2	3.24
After Simulation								
DONOR				**ACCEPTOR**				
POS	**CHAIN**	**RES**	**ATOM**	**POS**	**CHAIN**	**RES**	**ATOM**	**Dd-a**
240	A	ASN	ND2	62	B	SER	OG	2.82
240	A	ASN	ND2	62	B	SER	OG	2.82
361	A	ASP	OD1	69	B	ASN	ND2	2.95
361	A	ASP	OD1	69	B	ASN	ND2	2.95
361	A	ASP	OD2	69	B	ASN	ND2	2.93
361	A	ASP	OD2	69	B	ASN	ND2	2.93
407	A	ARG	NE	68	B	HIS	NE2	2.87
407	A	ARG	NH2	69	B	ASN	OD1	3.24
407	A	ARG	NH2	69	B	ASN	OD1	3.24
409	A	ARG	NH1	69	B	ASN	OD1	2.87
409	A	ARG	NH1	69	B	ASN	OD1	2.87
62	B	SER	OG	240	A	ASN	ND2	2.82
62	B	SER	OG	242	A	ASP	OD2	2.76
67	B	ARG	NH1	293	A	MET	SD	3.12
67	B	ARG	NH1	293	A	MET	SD	3.12
69	B	ASN	ND2	361	A	ASP	OD1	2.95
69	B	ASN	ND2	361	A	ASP	OD1	2.95
69	B	ASN	ND2	361	A	ASP	OD2	2.93
69	B	ASN	ND2	361	A	ASP	OD2	2.93

Table 3.9.4: Protein-Protein Ionic Interactions of complex 2c

Before Simulation					
Position	**Residue**	**Chain**	**Position**	**Residue**	**Chain**
316	GLU	A	67	ARG	B
After Simulation					
Position	**Residue**	**Chain**	**Position**	**Residue**	**Chain**

316	GLU	A	67	ARG	B

Table 3.10: Summary of interactions among HAESA, IDA and SERK1 before and after simulation

Complex	Inter. Bet.	H-Bond		Hydrophobic Interaction		Ionic Interaction		Cation - Pi Interaction		Aromatic - Aromatic Interaction		Aromatic - Sulphur Interaction	
		B. MD	*A. MD*	*B. MD*	*A. MD*	*B. MD*	*A. MD*	*B. MD*	*A. MD*	*B. MD*	*A. MD*	*B. MD*	*A. MD*
HAESA+ IDA+ SERK1	*HAESA + IDA*	36	24	5	5	1	1	0	0	0	0	0	0
	HAESA + SERK1	35	38	9	6	4	3	1	1	1	1	0	0
	IDA+ SERK1	4	4	0	0	1	0	0	0	0	0	0	0
HAESA+ SERK1	*HAESA + SERK1*	35	30	9	7	4	4	1	2	1	2	0	0
HAESA+ IDA	*HAESA + IDA*	36	27	5	3	1	1	0	0	0	0	0	0

Table 3.11.1: Binding free energy contribution of the key binding-site residues calculated from the binding energy decomposition for PSKR (kJmol-1) 3ai and complex 3c.

1avs3	MM Energy	Polar Energy	APolar Energy	Total Energy
ARG-109	-0.6663 ± 0.0161	-0.0024 ± 0.0003	0.0000 ± 0.0000	-0.6682 ± 0.0162
ARG-109	-0.2930 ± 0.0264	-0.0047 ± 0.0035	-0.0003 ± 0.0003	-0.2988 ± 0.0264
LYS-158	-0.8442 ± 0.0141	0.0020 ± 0.0002	0.0000 ± 0.0000	-0.8422 ± 0.0141
LYS-158	-0.2754 ± 0.0192	-0.0046 ± 0.0055	0.0003 ± 0.0002	-0.2800 ± 0.0201
ARG-175	-0.6956 ± 0.0104	0.0109 ± 0.0006	0.0000 ± 0.0000	-0.6846 ± 0.0102
ARG-175	-0.6416 ± 0.0104	0.0107 ± 0.0026	-0.0002 ± 0.0003	-0.6305 ± 0.0112
LYS-178	-1.1741 ± 0.0193	0.0350 ± 0.0017	0.0000 ± 0.0000	-1.1380 ± 0.0186
LYS-178	-0.9938 ± 0.0210	0.0271 ± 0.0079	-0.0003 ± 0.0005	-0.9675 ± 0.0231
LYS-194	-0.8610 ± 0.0096	0.0159 ± 0.0008	0.0000 ± 0.0000	-0.8450 ± 0.0088
LYS-194	-0.7996 ± 0.0091	0.0151 ± 0.0054	-0.0007 ± 0.0006	-0.7853 ± 0.0111
LYS-220	-1.0604 ± 0.0119	0.0386 ± 0.0018	0.0000 ± 0.0000	-1.0219 ± 0.0102
LYS-220	-1.0636 ± 0.0108	0.0249 ± 0.0071	0.0008 ± 0.0007	-1.0383 ± 0.0139

ARG-221	-0.8424 ± 0.0102	0.0214 ± 0.0009	0.0000 ± 0.0000	-0.8205 ± 0.0094
ARG-221	-0.8556 ± 0.0106	0.0102 ± 0.0019	-0.0008 ± 0.0004	-0.8459 ± 0.0099
ARG-231	-2.6642 ± 0.0305	0.1020 ± 0.0057	0.0000 ± 0.0000	-2.5624 ± 0.0285
ARG-231	-2.4029 ± 0.0356	0.0302 ± 0.0038	-0.0004 ± 0.0007	-2.3736 ± 0.0330
ARG-238	-1.7772 ± 0.0174	0.0686 ± 0.0031	0.0000 ± 0.0000	-1.7083 ± 0.0146
ARG-238	-1.8504 ± 0.0154	0.0414 ± 0.0047	-0.0006 ± 0.0010	-1.8087 ± 0.0149
ARG-241	-1.4797 ± 0.0144	0.0900 ± 0.0037	0.0000 ± 0.0000	-1.3896 ± 0.0110
ARG-241	-1.5528 ± 0.0141	0.0584 ± 0.0033	-0.0007 ± 0.0005	-1.4954 ± 0.0127
ARG-248	-2.2573 ± 0.0394	0.3003 ± 0.0132	0.0000 ± 0.0000	-1.9558 ± 0.0294
ARG-248	-2.2530 ± 0.0362	0.2235 ± 0.0088	0.0009 ± 0.0004	-2.0292 ± 0.0322
LYS-271	-1.2141 ± 0.0178	0.1041 ± 0.0041	0.0000 ± 0.0000	-1.1092 ± 0.0145
LYS-271	-1.3773 ± 0.0212	0.0859 ± 0.0093	0.0002 ± 0.0004	-1.2921 ± 0.0220
LYS-286	-1.8824 ± 0.0162	0.1090 ± 0.0050	0.0000 ± 0.0000	-1.7731 ± 0.0131
LYS-286	-2.0994 ± 0.0186	0.0796 ± 0.0085	-0.0001 ± 0.0003	-2.0202 ± 0.0203
ARG-300	-13.9191 ± 0.4817	7.0695 ± 0.4613	-0.0500 ± 0.0053	-6.9089 ± 0.1261
ARG-300	-11.6455 ± 0.3475	4.5093 ± 0.3236	-0.0362 ± 0.0058	-7.1805 ± 0.1176
ARG-307	-2.1454 ± 0.0226	0.2354 ± 0.0081	0.0000 ± 0.0000	-1.9105 ± 0.0188
ARG-307	-2.8485 ± 0.0261	0.2495 ± 0.0103	0.0000 ± 0.0005	-2.6004 ± 0.0237
GLY-324	-0.7305 ± 0.0503	0.2733 ± 0.0289	-0.0034 ± 0.0007	-0.4616 ± 0.0298
GLY-324	-0.5295 ± 0.0177	0.2561 ± 0.0105	0.0000 ± 0.0000	-0.2731 ± 0.0102
THR-325	-2.2794 ± 0.1747	1.5829 ± 0.1305	-0.0731 ± 0.0054	-0.7721 ± 0.0772
THR-325	-0.3325 ± 0.0546	0.2812 ± 0.0481	-0.0095 ± 0.0025	-0.0598 ± 0.0214
ARG-327	-6.2649 ± 0.0641	1.0168 ± 0.0387	0.0000 ± 0.0000	-5.2520 ± 0.0487
ARG-327	-6.3859 ± 0.0761	0.5745 ± 0.0217	-0.0002 ± 0.0007	-5.8110 ± 0.0645
ARG-331	-1.2923 ± 0.0370	0.1341 ± 0.0132	0.0000 ± 0.0000	-1.1582 ± 0.0270
ARG-331	-2.5789 ± 0.0269	0.3607 ± 0.0110	0.0000 ± 0.0008	-2.2180 ± 0.0222
ARG-341	-0.8814 ± 0.0205	0.0978 ± 0.0046	0.0000 ± 0.0000	-0.7844 ± 0.0171
ARG-341	-1.3626 ± 0.0220	0.1403 ± 0.0051	-0.0001 ± 0.0006	-1.2239 ± 0.0194
ALA-348	-0.9634 ± 0.0342	0.0481 ± 0.0489	-0.0761 ± 0.0055	-0.9905 ± 0.0557
ALA-348	-0.9042 ± 0.0219	0.5728 ± 0.0173	-0.0087 ± 0.0020	-0.3401 ± 0.0190
SER-372	-2.8567 ± 0.1329	2.7350 ± 0.1177	-0.1910 ± 0.0069	-0.3158 ± 0.0569
SER-372	-3.3884 ± 0.1292	3.1838 ± 0.1306	-0.0878 ± 0.0072	-0.2870 ± 0.0453
VAL-396	-1.3378 ± 0.0506	-0.2802 ± 0.0200	-0.1661 ± 0.0075	-1.7857 ± 0.0537
VAL-396	-0.3567 ± 0.0223	-0.2109 ± 0.0111	-0.0222 ± 0.0028	-0.5877 ± 0.0272
GLU-404	-0.7940 ± 0.0540	0.7547 ± 0.0210	0.0000 ± 0.0000	-0.0392 ± 0.0391
GLU-404	1.7114 ± 0.0429	-0.2867 ± 0.0252	0.0006 ± 0.0004	1.4233 ± 0.0268
ASP-408	-2.4125 ± 0.0159	0.6324 ± 0.0130	0.0000 ± 0.0000	-1.7801 ± 0.0105
ASP-408	-1.0663 ± 0.0243	0.5374 ± 0.0152	-0.0003 ± 0.0005	-0.5287 ± 0.0165
ASP-409	-1.9935 ± 0.0149	0.7389 ± 0.0103	0.0000 ± 0.0000	-1.2551 ± 0.0137
ASP-409	-0.6398 ± 0.0202	0.2520 ± 0.0086	-0.0005 ± 0.0005	-0.3890 ± 0.0156
GLU-415	-1.6326 ± 0.0186	0.4630 ± 0.0071	0.0000 ± 0.0000	-1.1702 ± 0.0139
GLU-415	-0.6724 ± 0.0251	0.2688 ± 0.0105	0.0002 ± 0.0005	-0.4043 ± 0.0202
VAL-421	-2.1187 ± 0.0338	-1.1632 ± 0.0456	-0.4322 ± 0.0075	-3.7148 ± 0.0551
VAL-421	-0.7075 ± 0.0412	-1.1137 ± 0.0177	-0.2059 ± 0.0048	-2.0272 ± 0.0413
ASP-461	-2.9613 ± 0.0217	0.9073 ± 0.0140	0.0000 ± 0.0000	-2.0541 ± 0.0111

ASP-461	-2.7741 ± 0.0237	0.8810 ± 0.0149	0.0001 ± 0.0002	-1.8933 ± 0.0163
GLU-478	-2.7414 ± 0.0218	0.6458 ± 0.0131	0.0000 ± 0.0000	-2.0961 ± 0.0110
GLU-478	-2.7715 ± 0.0219	0.5109 ± 0.0123	-0.0006 ± 0.0006	-2.2620 ± 0.0172
GLU-487	-2.4262 ± 0.0187	0.5090 ± 0.0087	0.0000 ± 0.0000	-1.9173 ± 0.0132
GLU-487	-2.8067 ± 0.0240	0.7948 ± 0.0116	0.0011 ± 0.0010	-2.0095 ± 0.0201
PHE-503	-1.4611 ± 0.0670	0.5453 ± 0.0355	-0.0554 ± 0.0046	-0.9686 ± 0.0385
PHE-503	-0.7214 ± 0.0293	0.1804 ± 0.0136	-0.0071 ± 0.0019	-0.5478 ± 0.0203
PHE-505	-4.7353 ± 0.0914	2.2688 ± 0.0471	-0.3987 ± 0.0078	-2.8663 ± 0.0649
PHE-505	-3.1874 ± 0.0743	1.8739 ± 0.0472	-0.1780 ± 0.0078	-1.4896 ± 0.0433
PHE-506	-13.0952 ± 0.2260	11.4676 ± 0.1911	-1.2826 ± 0.0150	-2.9056 ± 0.1045
PHE-506	-12.3159 ± 0.2594	10.6705 ± 0.2102	-1.1938 ± 0.0154	-2.8403 ± 0.1068
MET-507	-5.8067 ± 0.1205	3.0278 ± 0.0968	-0.2986 ± 0.0067	-3.0772 ± 0.0884
MET-507	-12.7059 ± 0.3406	6.7738 ± 0.2032	-0.2457 ± 0.0084	-6.1670 ± 0.1543
ARG-514	-3.3507 ± 0.0818	0.2455 ± 0.0286	-0.0001 ± 0.0001	-3.1061 ± 0.0634
ARG-514	-6.0804 ± 0.1976	1.1055 ± 0.0920	-0.0147 ± 0.0029	-4.9871 ± 0.1490
ALA-515	-1.7877 ± 0.0575	0.3092 ± 0.0323	-0.2525 ± 0.0076	-1.7322 ± 0.0403
ALA-515	-2.2322 ± 0.0790	1.0372 ± 0.0716	-0.2387 ± 0.0093	-1.4302 ± 0.0411
PHE-524	-2.8222 ± 0.0677	1.4815 ± 0.0520	-0.3558 ± 0.0081	-1.6968 ± 0.0394
PHE-524	-0.8139 ± 0.0423	-0.0325 ± 0.0319	-0.1621 ± 0.0053	-1.0069 ± 0.0293
GLU-529	-16.4005 ± 0.2463	11.8038 ± 0.2809	-0.0001 ± 0.0001	-4.5911 ± 0.0862
GLU-529	-33.8019 ± 0.4043	24.5546 ± 0.5128	-0.1349 ± 0.0067	-9.3820 ± 0.3026
GLU-541	-2.1149 ± 0.0186	0.3782 ± 0.0088	0.0000 ± 0.0000	-1.7381 ± 0.0116
GLU-541	-3.1108 ± 0.0219	0.6258 ± 0.0091	0.0004 ± 0.0003	-2.4847 ± 0.0172
GLU-542	-2.3768 ± 0.0187	0.4888 ± 0.0086	0.0000 ± 0.0000	-1.8890 ± 0.0114
GLU-542	-3.5441 ± 0.0279	1.1399 ± 0.0183	-0.0007 ± 0.0007	-2.4041 ± 0.0161
ASP-553	-8.2444 ± 0.0960	4.8020 ± 0.1046	0.0000 ± 0.0000	-3.4406 ± 0.0478
ASP-553	-14.1079 ± 0.1417	5.9032 ± 0.0957	0.0005 ± 0.0005	-8.2109 ± 0.0943
GLU-574	-3.4951 ± 0.0330	0.8443 ± 0.0150	0.0000 ± 0.0000	-2.6495 ± 0.0259
GLU-574	-8.6749 ± 0.0906	2.3157 ± 0.0459	-0.0004 ± 0.0004	-6.3607 ± 0.0777
ASP-577	-4.8760 ± 0.0473	1.7341 ± 0.0371	0.0000 ± 0.0000	-3.1413 ± 0.0295
ASP-577	-8.1725 ± 0.0796	2.3376 ± 0.0374	-0.0004 ± 0.0003	-5.8325 ± 0.0628
GLU-626	-1.5497 ± 0.0177	0.1311 ± 0.0030	0.0000 ± 0.0000	-1.4191 ± 0.0174
GLU-626	-2.6414 ± 0.0291	0.1853 ± 0.0057	0.0015 ± 0.0009	-2.4554 ± 0.0277
GLU-633	-0.7329 ± 0.0065	0.0151 ± 0.0004	0.0000 ± 0.0000	-0.7176 ± 0.0061
GLU-633	-1.8283 ± 0.0177	0.1101 ± 0.0103	0.0008 ± 0.0008	-1.7175 ± 0.0211

Table 3.11.2: Binding free energy contribution of the key binding-site residues calculated from the binding energy decomposition for PSKR (kJmol-1) 3aii and complex 3b.

1bvs2	MM Energy	Polar Energy	APolar Energy	Total Energy
ARG-30	-83.6018 ± 0.2166	0.1233 ± 0.0668	0.0071 ± 0.0043	-83.4710 ± 0.2238
ARG-30	-88.2926 ± 0.3250	-0.0798 ± 0.070	0.0012 ± 0.0039	-88.3784 ± 0.3421
ARG-40	-49.4973 ± 0.1352	0.0167 ± 0.0276	0.0006 ± 0.0069	-49.4787 ± 0.1397
ARG-40	-49.0353 ± 0.2028	-0.0048 ± 0.027	-0.0051 ± 0.0061	-49.0428 ± 0.200
LYS-49	-65.6478 ± 0.2448	-0.0514 ± 0.062	0.0091 ± 0.0064	-65.6923 ± 0.2411

LYS-49	-65.6941 ± 0.3339	0.2772 ± 0.0653	-0.0074 ± 0.0056	-65.4055 ± 0.3152
ARG-77	-40.1804 ± 0.1160	0.0628 ± 0.0325	0.0054 ± 0.0067	-40.1060 ± 0.1164
ARG-77	-42.4775 ± 0.1466	0.0194 ± 0.0278	0.0031 ± 0.0052	-42.4512 ± 0.1460
ARG-80	-47.6792 ± 0.1725	0.0232 ± 0.0300	-0.0043 ± 0.0059	-47.6614 ± 0.1656
ARG-80	-50.7469 ± 0.1798	0.0266 ± 0.0244	-0.0018 ± 0.0041	-50.7206 ± 0.1865
LYS-86	-63.1318 ± 0.2679	0.0405 ± 0.0652	-0.0053 ± 0.0068	-63.0885 ± 0.2747
LYS-86	-69.0060 ± 0.3841	0.2663 ± 0.0635	-0.0024 ± 0.0036	-68.7733 ± 0.3773
LYS-87	-86.2544 ± 0.5341	0.3126 ± 0.1805	-0.0136 ± 0.0064	-85.9527 ± 0.4944
LYS-87	-105.4179 ± 1.110	13.3308 ± 1.14	-0.2428 ± 0.0211	-92.2834 ± 0.51
LYS-91	-71.2261 ± 0.4216	-0.0025 ± 0.079	0.0003 ± 0.0076	-71.2130 ± 0.4215
LYS-91	-64.6023 ± 0.3642	0.1126 ± 0.0636	0.0017 ± 0.0049	-64.4896 ± 0.3612
LYS-98	-48.2101 ± 0.1467	0.0392 ± 0.0722	-0.0058 ± 0.0059	-48.1832 ± 0.1664
LYS-98	-46.5746 ± 0.1773	0.0817 ± 0.0573	-0.0012 ± 0.0039	-46.4935 ± 0.1935
ARG-103	-41.9316 ± 0.1129	0.0470 ± 0.0285	-0.0032 ± 0.0058	-41.8929 ± 0.1218
ARG-103	-43.6130 ± 0.1420	0.0070 ± 0.0247	-0.0022 ± 0.0038	-43.6027 ± 0.1465
ARG-109	-73.4827 ± 0.4552	-0.1043 ± 0.043	-0.0005 ± 0.0050	-73.6124 ± 0.459
ARG-109	-83.6302 ± 0.5141	-0.1239 ± 0.086	-0.0300 ± 0.0065	-83.7876 ± 0.479
LYS-113	-94.5144 ± 0.7078	0.8395 ± 0.2731	-0.0093 ± 0.0052	-93.6761 ± 0.6071
LYS-113	-96.4352 ± 1.0603	8.1238 ± 0.7876	-0.0693 ± 0.0080	-88.2790 ± 0.5884
LYS-124	-40.1631 ± 0.1140	0.0997 ± 0.0730	-0.0113 ± 0.0064	-40.0726 ± 0.1320
LYS-124	-40.4573 ± 0.1382	-0.0734 ± 0.061	0.0070 ± 0.0037	-40.5270 ± 0.1470
LYS-158	-87.6139 ± 0.7266	1.1010 ± 0.2637	-0.0049 ± 0.0055	-86.5232 ± 0.6262
LYS-158	-87.0473 ± 0.9329	5.3241 ± 0.5955	-0.0510 ± 0.0074	-81.7883 ± 0.6353
ARG-175	-44.6824 ± 0.1487	-0.0499 ± 0.032	0.0044 ± 0.0059	-44.7246 ± 0.1511
ARG-175	-45.4151 ± 0.1259	-0.0405 ± 0.025	-0.0078 ± 0.0035	-45.4644 ± 0.131
LYS-178	-58.8704 ± 0.2356	-0.0996 ± 0.062	-0.0050 ± 0.0073	-58.9764 ± 0.242
LYS-178	-62.5064 ± 0.2136	-0.2141 ± 0.059	0.0023 ± 0.0065	-62.7228 ± 0.2243
LYS-194	-38.4294 ± 0.0971	0.0344 ± 0.0644	0.0076 ± 0.0049	-38.3889 ± 0.1192
LYS-194	-38.3110 ± 0.0893	0.0396 ± 0.0545	-0.0044 ± 0.0035	-38.2743 ± 0.1070
LYS-220	-36.9844 ± 0.0648	0.1041 ± 0.0593	0.0006 ± 0.0036	-36.8775 ± 0.0864
LYS-220	-37.8717 ± 0.0634	-0.0392 ± 0.056	0.0044 ± 0.0038	-37.9054 ± 0.0851
ARG-221	-39.9966 ± 0.0890	0.0362 ± 0.0339	-0.0135 ± 0.0054	-39.9743 ± 0.0963
ARG-221	-40.6905 ± 0.1114	-0.0166 ± 0.027	-0.0021 ± 0.0034	-40.7170 ± 0.117
ARG-231	-54.7334 ± 0.2037	0.0865 ± 0.0311	-0.0049 ± 0.0046	-54.6626 ± 0.2236
ARG-231	-53.4100 ± 0.2265	-0.7158 ± 0.117	-0.0085 ± 0.0040	-54.1423 ± 0.238
ARG-238	-37.0352 ± 0.0622	0.0328 ± 0.0329	0.0045 ± 0.0065	-36.9979 ± 0.0699
ARG-238	-38.6014 ± 0.0667	0.0257 ± 0.0321	0.0024 ± 0.0055	-38.5769 ± 0.0727
ARG-241	-36.6114 ± 0.0546	0.0154 ± 0.0327	-0.0052 ± 0.0070	-36.6006 ± 0.0635
ARG-241	-38.0068 ± 0.0583	0.0035 ± 0.0265	-0.0062 ± 0.0060	-38.0093 ± 0.0639
LYS-271	-46.1451 ± 0.0988	0.0758 ± 0.0666	0.0047 ± 0.0042	-46.0721 ± 0.1163
LYS-271	-48.1065 ± 0.1098	-0.0028 ± 0.056	-0.0029 ± 0.0031	-48.1062 ± 0.122
LYS-286	-36.2973 ± 0.0484	0.0874 ± 0.0658	0.0024 ± 0.0043	-36.2044 ± 0.0765
LYS-286	-37.2624 ± 0.0485	-0.0374 ± 0.060	-0.0010 ± 0.0031	-37.2965 ± 0.075
ARG-300	-63.5847 ± 0.1191	0.5667 ± 0.0304	0.0069 ± 0.0053	-63.0142 ± 0.1143
ARG-300	-70.4054 ± 0.1993	3.8880 ± 0.0674	-0.0030 ± 0.0044	-66.5208 ± 0.1563

ARG-307	-37.7952 ± 0.0503	0.0756 ± 0.0367	0.0129 ± 0.0063	-37.7068 ± 0.0628
ARG-307	-38.9705 ± 0.0738	0.0647 ± 0.0312	0.0003 ± 0.0045	-38.9064 ± 0.0770
ARG-327	-46.4175 ± 0.0993	0.0909 ± 0.0325	0.0052 ± 0.0046	-46.3231 ± 0.1043
ARG-327	-49.8394 ± 0.1553	0.1248 ± 0.0292	0.0018 ± 0.0037	-49.7115 ± 0.1603
ARG-331	-38.3687 ± 0.0502	0.1444 ± 0.0378	0.0052 ± 0.0069	-38.2214 ± 0.0650
ARG-331	-40.0768 ± 0.0501	0.1975 ± 0.0320	-0.0085 ± 0.0056	-39.8866 ± 0.0565
LYS-340	-39.9020 ± 0.0463	0.0720 ± 0.0662	0.0041 ± 0.0055	-39.8280 ± 0.0779
LYS-340	-40.9482 ± 0.0472	0.0925 ± 0.0593	-0.0008 ± 0.0044	-40.8548 ± 0.0712
ARG-341	-44.1830 ± 0.0832	0.0336 ± 0.0348	0.0037 ± 0.0056	-44.1471 ± 0.0831
ARG-341	-45.0072 ± 0.0855	0.1261 ± 0.0280	0.0008 ± 0.0035	-44.8814 ± 0.0926
LYS-343	-54.3521 ± 0.1289	0.1412 ± 0.0614	-0.0068 ± 0.0053	-54.2192 ± 0.1472
LYS-343	-55.3147 ± 0.1279	0.3906 ± 0.0589	-0.0012 ± 0.0048	-54.9121 ± 0.1359
ARG-349	-60.6347 ± 0.1619	0.3498 ± 0.0349	-0.0002 ± 0.0033	-60.2887 ± 0.1576
ARG-349	-65.5745 ± 0.2700	2.2603 ± 0.0730	-0.0056 ± 0.0032	-63.3189 ± 0.2075
LYS-361	-38.6189 ± 0.0451	0.0924 ± 0.0734	-0.0044 ± 0.0072	-38.5262 ± 0.0827
LYS-361	-39.7034 ± 0.0364	0.1466 ± 0.0654	-0.0065 ± 0.0062	-39.5602 ± 0.0737
LYS-390	-42.9838 ± 0.0515	0.2087 ± 0.0661	-0.0066 ± 0.0062	-42.7779 ± 0.0801
LYS-390	-44.8081 ± 0.0616	0.3896 ± 0.0577	-0.0004 ± 0.0044	-44.4195 ± 0.0807
LYS-416	-49.6144 ± 0.0912	0.2310 ± 0.0686	0.0000 ± 0.0067	-49.3843 ± 0.1053
LYS-416	-52.3038 ± 0.1133	0.4387 ± 0.0572	-0.0063 ± 0.0040	-51.8680 ± 0.1213
LYS-418	-62.4265 ± 0.1500	0.9152 ± 0.0600	0.0079 ± 0.0066	-61.5096 ± 0.1438
LYS-418	-67.9956 ± 0.2109	3.7504 ± 0.0714	0.0020 ± 0.0035	-64.2379 ± 0.1761
ARG-426	-51.7754 ± 0.1676	0.2563 ± 0.0331	0.0061 ± 0.0061	-51.5120 ± 0.1608
ARG-426	-58.5863 ± 0.1247	0.7312 ± 0.0255	0.0062 ± 0.0041	-57.8518 ± 0.1218
ARG-433	-46.0392 ± 0.0842	0.1676 ± 0.0321	-0.0014 ± 0.0052	-45.8742 ± 0.0882
ARG-433	-45.2495 ± 0.0753	0.2179 ± 0.0294	-0.0060 ± 0.0054	-45.0370 ± 0.0790
ARG-450	-55.7534 ± 0.1706	0.5000 ± 0.0317	-0.0023 ± 0.0056	-55.2583 ± 0.1695
ARG-450	-55.2139 ± 0.1208	0.8257 ± 0.0277	0.0030 ± 0.0040	-54.3920 ± 0.1183
LYS-463	-58.1443 ± 0.1288	0.4013 ± 0.0683	-0.0123 ± 0.0072	-57.7528 ± 0.1435
LYS-463	-60.9076 ± 0.1344	0.7287 ± 0.0585	-0.0001 ± 0.0046	-60.1728 ± 0.1406
LYS-481	-53.8739 ± 0.0888	0.5667 ± 0.0612	0.0036 ± 0.0048	-53.3056 ± 0.1036
LYS-481	-56.7547 ± 0.1592	0.7213 ± 0.0577	0.0059 ± 0.0049	-56.0294 ± 0.1550
LYS-485	-56.0942 ± 0.1209	0.4190 ± 0.0703	-0.0032 ± 0.0059	-55.6789 ± 0.1337
LYS-485	-58.6814 ± 0.1015	0.8320 ± 0.0576	-0.0056 ± 0.0057	-57.8582 ± 0.1121
ARG-492	-106.7721 ± 0.628	2.7035 ± 0.240	-0.0688 ± 0.0097	-104.1249 ± 0.49
ARG-492	-152.2550 ± 0.880	49.3453 ± 0.85	-1.5760 ± 0.0219	-104.4975 ± 0.3
LYS-508	-77.6407 ± 0.3394	5.6747 ± 0.1957	-0.0002 ± 0.0067	-71.9700 ± 0.2133
LYS-508	-75.9197 ± 0.2426	4.2128 ± 0.1056	-0.0022 ± 0.0042	-71.6992 ± 0.1818
ARG-509	-96.6419 ± 0.4316	5.0071 ± 0.1656	-0.0630 ± 0.0088	-91.7212 ± 0.3630
ARG-509	-134.8584 ± 1.471	52.9770 ± 1.43	-0.9558 ± 0.0337	-82.8731 ± 0.2501
ARG-514	-127.5172 ± 1.067	52.4303 ± 1.1692	-1.7018 ± 0.0264	-76.7606 ± 0.4150
ARG-514	-83.9748 ± 0.8528	10.1506 ± 0.773	-0.3283 ± 0.0220	-74.1496 ± 0.3168
LYS-547	-83.4504 ± 0.2302	1.1594 ± 0.0633	0.0009 ± 0.0057	-82.2943 ± 0.2321
LYS-547	-97.2830 ± 0.3672	3.3928 ± 0.1074	-0.0015 ± 0.0061	-93.8923 ± 0.3332
LYS-548	-108.2394 ± 0.369	6.6631 ± 0.312	-0.0704 ± 0.0099	-101.6404 ± 0.3141

LYS-548	-111.0137 ± 0.655	21.6623 ± 0.91	-0.2259 ± 0.0125	-89.5402 ± 0.5148
LYS-555	-77.9235 ± 0.2641	1.3776 ± 0.0664	-0.0028 ± 0.0048	-76.5563 ± 0.2740
LYS-555	-77.4596 ± 0.1385	3.3579 ± 0.0532	0.0014 ± 0.0030	-74.1018 ± 0.1321
ARG-582	-54.2076 ± 0.1741	0.4763 ± 0.0342	0.0033 ± 0.0062	-53.7343 ± 0.1652
ARG-582	-54.2032 ± 0.0876	0.5130 ± 0.0315	-0.0020 ± 0.0067	-53.6918 ± 0.0867
LYS-599	-151.8072 ± 1.084	79.9082 ± 1.5700	-0.9213 ± 0.016	-72.8004 ± 0.6562
LYS-599	-108.4803 ± 0.554	17.0134 ± 0.38	-0.0735 ± 0.0073	-91.5300 ± 0.3941
ARG-635	-72.0394 ± 0.6142	3.2165 ± 0.4392	-0.6014 ± 0.0208	-69.4197 ± 0.3022
ARG-635	-91.6653 ± 0.5998	16.3478 ± 0.612	-0.8338 ± 0.0253	-76.1374 ± 0.3218

Table 3.11.3: Binding free energy contribution of the key binding-site residues calculated from the binding energy decomposition for Phytosulphokine (kJmol-1) 3ai and complex 3c.

	MM Energy	**Polar Energy**	**APolar Energy**	**Total Energy**
THR-31	-21.2975 ± 0.3434	20.0159 ± 0.2818	-2.5223 ± 0.0167	-3.8066 ± 0.1797
THR-31	-40.5678 ± 0.4988	28.1400 ± 0.3588	-2.4759 ± 0.0195	-14.8964 ± 0.2438
GLN-32	-117.8896 ± 0.8207	119.2362 ± 1.3447	-3.5545 ± 0.0240	-2.1566 ± 0.7372
GLN-32	-115.1895 ± 1.1424	100.9623 ± 1.6353	-3.2948 ± 0.0311	-17.4842 ± 0.8586

Table 3.11.4: Binding free energy contribution of the key binding-site residues calculated from the binding energy decomposition for SERK1 (kJmol-1) 3aii and complex 3b.

	MM Energy	**Polar Energy**	**APolar Energy**	**Total Energy**
GLU-29	-48.9972 ± 0.6057	14.1781 ± 0.674	-0.0297 ± 0.0092	-34.8427 ± 0.329
GLU-29	-29.2876 ± 0.2462	2.1146 ± 0.1277	0.0105 ± 0.0084	-27.1578 ± 0.2174
ASP-31	-28.7104 ± 0.3649	1.8001 ± 0.2024	-0.0242 ± 0.0074	-26.9203 ± 0.3336
ASP-31	-26.2942 ± 0.4374	3.4931 ± 0.4339	-0.0327 ± 0.0090	-22.8350 ± 0.4040
ASP-42	-37.5365 ± 0.2966	-1.1552 ± 0.121	-0.0117 ± 0.0069	-38.6937 ± 0.249
ASP-42	-50.0711 ± 0.3829	6.0372 ± 0.2458	0.0123 ± 0.0072	-44.0446 ± 0.2704
ASP-51	-36.0653 ± 0.4282	-2.2587 ± 0.231	-0.0219 ± 0.0057	-38.3449 ± 0.388
ASP-51	-63.8608 ± 0.9271	49.0028 ± 1.488	-1.1379 ± 0.0202	-16.0425 ± 0.718
GLU-68	-69.1150 ± 0.7803	32.0690 ± 0.784	-0.8951 ± 0.0221	-37.9615 ± 0.402
GLU-68	-34.6577 ± 0.5100	3.7676 ± 0.3441	-0.0578 ± 0.0084	-30.9545 ± 0.3275
GLU-80	-29.4906 ± 0.2729	-0.2506 ± 0.104	-0.0027 ± 0.0090	-29.7336 ± 0.263
GLU-80	-36.0719 ± 0.3547	1.8676 ± 0.1372	-0.0141 ± 0.0093	-34.2148 ± 0.3180
GLU-88	-22.7662 ± 0.3112	1.2729 ± 0.1890	-0.0067 ± 0.0073	-21.5094 ± 0.2777
GLU-88	-28.0097 ± 0.4432	4.7467 ± 0.4621	-0.0590 ± 0.0111	-23.3370 ± 0.3227
ASP-115	-16.2286 ± 0.1529	0.8170 ± 0.0846	-0.0003 ± 0.0076	-15.4055 ± 0.1694
ASP-115	-15.6878 ± 0.1529	0.4611 ± 0.0911	0.0078 ± 0.0064	-15.2100 ± 0.1795
PHE-145	-12.3189 ± 0.0907	4.3128 ± 0.0401	-1.3533 ± 0.0152	-9.3633 ± 0.0867
PHE-145	-9.0429 ± 0.2119	3.0810 ± 0.0852	-1.1382 ± 0.0300	-7.0987 ± 0.1683

Table 3.12.1: Protein-Protein Hydrophobic Interactions of complex 3a.

Before Simulation					
Position	**Residue**	**Chain**	**Position**	**Residue**	**Chain**
111	PHE	A	38	VAL	C
421	VAL	A	29	ILE	P
443	LEU	A	29	ILE	P
467	TYR	A	29	ILE	P
505	PHE	A	29	ILE	P
507	MET	A	29	ILE	P
524	PHE	A	29	ILE	P
525	PRO	A	61	PHE	C
526	PRO	A	61	PHE	C
596	PHE	A	46	VAL	C
596	PHE	A	79	ALA	C
After Simulation					
Position	**Residue**	**Chain**	**Position**	**Residue**	**Chain**
111	PHE	A	38	VAL	C
396	VAL	A	29	ILE	P
421	VAL	A	29	ILE	P
505	PHE	A	29	ILE	P
507	MET	A	29	ILE	P
524	PHE	A	29	ILE	P
525	PRO	A	61	PHE	C
596	PHE	A	76	LEU	C
596	PHE	A	79	ALA	C
621	PRO	A	97	TYR	C

Table 3.12.2: Protein-Protein Main Chain-Main Chain Hydrogen Bonds of complex 3a.

Before Simulation								
DONOR				**ACCEPTOR**				
POS	**CHAIN**	**RES**	**ATOM**	**POS**	**CHAIN**	**RES**	**ATOM**	**Dd-a**
325	A	THR	N	32	P	GLN	O	3.46
After Simulation								
DONOR				**ACCEPTOR**				
POS	**CHAIN**	**RES**	**ATOM**	**POS**	**CHAIN**	**RES**	**ATOM**	**Dd-a**
506	A	PHE	N	29	P	ILE	O	2.76

Table 3.12.3: Protein-Protein Main Chain-Side Chain Hydrogen Bonds of complex 3a.

Before Simulation								
DONOR				ACCEPTOR				
POS	CHAIN	RES	ATOM	POS	CHAIN	RES	ATOM	Dd-a
87	A	LYS	NZ	38	C	VAL	O	3.28
325	A	THR	OG1	32	P	GLN	O	2.61
346	A	ASN	ND2	32	P	GLN	OXT	2.9
346	A	ASN	ND2	32	P	GLN	OXT	2.9
398	A	THR	OG1	29	P	ILE	O	2.73
595	A	SER	OG	77	C	GLY	O	2.97
62	C	HIS	N	574	A	GLU	OE2	2.83
73	C	ARG	NH1	619	A	THR	O	3.01
73	C	ARG	NH1	619	A	THR	O	3.01
29	P	ILE	N	445	A	ASP	OD2	2.95
31	P	THR	N	372	A	SER	OG	3.2
After Simulation								
DONOR				ACCEPTOR				
POS	CHAIN	RES	ATOM	POS	CHAIN	RES	ATOM	Dd-a
514	A	ARG	NE	67	C	ASN	O	3.43
595	A	SER	OG	77	C	GLY	O	2.64
59	C	THR	OG1	517	A	GLN	O	2.75
62	C	HIS	N	574	A	GLU	OE1	2.93
73	C	ARG	NH2	597	A	LEU	O	3.11
73	C	ARG	NH2	597	A	LEU	O	3.11
73	C	ARG	NE	598	A	SER	O	3.41
73	C	ARG	NH1	598	A	SER	O	3.42
73	C	ARG	NH1	598	A	SER	O	3.42
75	C	ASP	OD1	597	A	LEU	O	3.26
75	C	ASP	OD1	597	A	LEU	O	3.26

Table 3.12.4: Protein-Protein Side Chain-Side Chain Hydrogen Bonds of complex 3a.

Before Simulation								
DONOR				ACCEPTOR				
POS	CHAIN	RES	ATOM	POS	CHAIN	RES	ATOM	Dd-a
349	A	ARG	NH1	32	P	GLN	OE1	3.16
349	A	ARG	NH1	32	P	GLN	OE1	3.16
616	A	GLN	NE2	75	C	ASP	OD1	3.07
616	A	GLN	NE2	75	C	ASP	OD1	3.07
616	A	GLN	OE1	101	C	TYR	OH	2.43

616	A	GLN	OE1	101	C	TYR	OH	2.43
75	C	ASP	OD1	616	A	GLN	NE2	3.07
75	C	ASP	OD1	616	A	GLN	NE2	3.07
101	C	TYR	OH	616	A	GLN	OE1	2.43
147	C	ARG	NH1	618	A	GLN	OE1	3.11
147	C	ARG	NH1	618	A	GLN	OE1	3.11
After Simulation								
DONOR				**ACCEPTOR**				
POS	**CHAIN**	**RES**	**ATOM**	**POS**	**CHAIN**	**RES**	**ATOM**	**Dd-a**
616	A	GLN	NE2	75	C	ASP	OD1	2.99
616	A	GLN	NE2	75	C	ASP	OD1	2.99
616	A	GLN	OE1	101	C	TYR	OH	2.5
616	A	GLN	OE1	101	C	TYR	OH	2.5
619	A	THR	OG1	99	C	GLU	OE2	2.85
634	A	HIS	ND1	168	C	GLN	NE2	2.78
75	C	ASP	OD1	616	A	GLN	NE2	2.99
75	C	ASP	OD1	616	A	GLN	NE2	2.99
101	C	TYR	OH	616	A	GLN	OE1	2.5
147	C	ARG	NH1	618	A	GLN	OE1	3
147	C	ARG	NH1	618	A	GLN	OE1	3
168	C	GLN	NE2	634	A	HIS	ND1	2.78
168	C	GLN	NE2	634	A	HIS	ND1	2.78
31	P	THR	OG1	370	A	SER	OG	2.91

Table 3.12.5: Protein-Protein Ionic Interactions of complex 3a.

Before Simulation					
Position	**Residue**	**Chain**	**Position**	**Residue**	**Chain**
514	ARG	A	68	GLU	C
574	GLU	A	62	HIS	C
After Simulation					
Position	**Residue**	**Chain**	**Position**	**Residue**	**Chain**
158	LYS	A	31	ASP	C
574	GLU	A	62	HIS	C

Table 3.12.6: Protein-Protein Aromatic-Aromatic Interactions of complex 3a.

Before Simulation						
NO PROTEIN-PROTEIN AROMATIC-AROMATIC INTERACTIONS FOUND						
After Simulation						
Position	**Residue**	**Chain**	**Position**	**Residue**	**Chain**	**D(centroid-centroid)**
620	PHE	A	97	TYR	C	6.55

Table 3.12.7: Protein-Protein Cation-Pi Interactions of complex 3a.

Before Simulation						
NO PROTEIN-PROTEIN CATION-PI INTERACTIONS FOUND						
After Simulation						
Position	**Residue**	**Chain**	**Position**	**Residue**	**Chain**	**D(cation-Pi)**
620	PHE	A	73	ARG	C	4.03

Table 3.13.1: Protein-Protein Hydrophobic Interactions of complex 3b.

Before Simulation					
Position	**Residue**	**Chain**	**Position**	**Residue**	**Chain**
111	PHE	A	38	VAL	C
525	PRO	A	61	PHE	C
526	PRO	A	61	PHE	C
596	PHE	A	46	VAL	C
596	PHE	A	79	ALA	C
After Simulation					
Position	**Residue**	**Chain**	**Position**	**Residue**	**Chain**
111	PHE	A	38	VAL	C
525	PRO	A	61	PHE	C
526	PRO	A	61	PHE	C
596	PHE	A	46	VAL	C
596	PHE	A	76	LEU	C
596	PHE	A	79	ALA	C
621	PRO	A	97	TYR	C

Table 3.13.2: Protein-Protein Main Chain-Side Chain Hydrogen Bonds of complex 3b.

Before Simulation								
DONOR				ACCEPTOR				
POS	CHAIN	RES	ATOM	POS	CHAIN	RES	ATOM	Dd-a
87	A	LYS	NZ	38	C	VAL	O	3.28
595	A	SER	OG	77	C	GLY	O	2.97
62	C	HIS	N	574	A	GLU	OE2	2.83
73	C	ARG	NH1	619	A	THR	O	3.01
73	C	ARG	NH1	619	A	THR	O	3.01
After Simulation								
DONOR				ACCEPTOR				
POS	CHAIN	RES	ATOM	POS	CHAIN	RES	ATOM	Dd-a
87	A	LYS	NZ	38	C	VAL	O	2.94
514	A	ARG	NE	67	C	ASN	O	3.46
514	A	ARG	NH1	67	C	ASN	O	3.42
514	A	ARG	NH1	67	C	ASN	O	3.42
514	A	ARG	NH2	67	C	ASN	O	3.19
514	A	ARG	NH2	67	C	ASN	O	3.19
615	A	GLY	N	123	C	ASP	OD1	3.41
62	C	HIS	N	574	A	GLU	OE1	3.17
62	C	HIS	N	574	A	GLU	OE2	3.43
97	C	TYR	OH	619	A	THR	O	2.63

Table 3.13.3: Protein-Protein Side Chain-Side Chain Hydrogen Bonds of complex 3b.

Before Simulation								
DONOR				ACCEPTOR				
POS	CHAIN	RES	ATOM	POS	CHAIN	RES	ATOM	Dd-a
616	A	GLN	NE2	75	C	ASP	OD1	3.07
616	A	GLN	NE2	75	C	ASP	OD1	3.07
616	A	GLN	OE1	101	C	TYR	OH	2.43
616	A	GLN	OE1	101	C	TYR	OH	2.43
75	C	ASP	OD1	616	A	GLN	NE2	3.07
75	C	ASP	OD1	616	A	GLN	NE2	3.07
101	C	TYR	OH	616	A	GLN	OE1	2.43
147	C	ARG	NH1	618	A	GLN	OE1	3.11
147	C	ARG	NH1	618	A	GLN	OE1	3.11
After Simulation								
DONOR				ACCEPTOR				
POS	CHAIN	RES	ATOM	POS	CHAIN	RES	ATOM	Dd-a
616	A	GLN	NE2	75	C	ASP	OD1	2.69

616	A	GLN	NE2	75	C	ASP	OD1	2.69
616	A	GLN	OE1	101	C	TYR	OH	2.94
616	A	GLN	OE1	101	C	TYR	OH	2.94
619	A	THR	OG1	99	C	GLU	OE2	2.8
75	C	ASP	OD1	616	A	GLN	NE2	2.69
75	C	ASP	OD1	616	A	GLN	NE2	2.69
101	C	TYR	OH	616	A	GLN	OE1	2.94
147	C	ARG	NH1	618	A	GLN	OE1	3.13
147	C	ARG	NH1	618	A	GLN	OE1	3.13
147	C	ARG	NH2	618	A	GLN	OE1	2.93
147	C	ARG	NH2	618	A	GLN	OE1	2.93

Table 3.13.4: Protein-Protein Ionic Interactions of complex 3b.

Before Simulation					
Position	**Residue**	**Chain**	**Position**	**Residue**	**Chain**
514	ARG	A	68	GLU	C
574	GLU	A	62	HIS	C
After Simulation					
Position	**Residue**	**Chain**	**Position**	**Residue**	**Chain**
158	LYS	A	31	ASP	C
574	GLU	A	62	HIS	C

Table 3.13.5: Protein-Protein Cation-Pi Interactions of complex 3b.

Before Simulation						
NO PROTEIN-PROTEIN CATION-PI INTERACTIONS FOUND						
After Simulation						
Position	**Residue**	**Chain**	**Position**	**Residue**	**Chain**	**D(cation-Pi)**
620	PHE	A	73	ARG	B	3.88

Table 3.14.1: Protein-Protein Hydrophobic Interactions of complex 3c

Before Simulation					
Position	**Residue**	**Chain**	**Position**	**Residue**	**Chain**
421	VAL	A	29	ILE	P
443	LEU	A	29	ILE	P
467	TYR	A	29	ILE	P
505	PHE	A	29	ILE	P
507	MET	A	29	ILE	P
524	PHE	A	29	ILE	P

After Simulation					
Position	**Residue**	**Chain**	**Position**	**Residue**	**Chain**
507	MET	A	29	ILE	P

Table 3.14.2: Protein-Protein Main Chain-Main Chain Hydrogen Bonds of complex 3c

Before Simulation								
DONOR				**ACCEPTOR**				
POS	**CHAIN**	**RES**	**ATOM**	**POS**	**CHAIN**	**RES**	**ATOM**	**Dd-a**
325	A	THR	N	32	P	GLN	O	3.46
After Simulation								
DONOR				**ACCEPTOR**				
POS	**CHAIN**	**RES**	**ATOM**	**POS**	**CHAIN**	**RES**	**ATOM**	**Dd-a**
31	P	THR	N	506	A	PHE	O	3.43

Table 3.14.3: Protein-Protein Main Chain-Side Chain Hydrogen Bonds of complex 3c

Before Simulation								
DONOR				**ACCEPTOR**				
POS	**CHAIN**	**RES**	**ATOM**	**POS**	**CHAIN**	**RES**	**ATOM**	**Dd-a**
325	A	THR	OG1	32	P	GLN	O	2.61
346	A	ASN	ND2	32	P	GLN	OXT	2.9
346	A	ASN	ND2	32	P	GLN	OXT	2.9
398	A	THR	OG1	29	P	ILE	O	2.73
29	P	ILE	N	445	A	ASP	OD2	2.95
31	P	THR	N	372	A	SER	OG	3.2
After Simulation								
DONOR				**ACCEPTOR**				
POS	**CHAIN**	**RES**	**ATOM**	**POS**	**CHAIN**	**RES**	**ATOM**	**Dd-a**
372	A	SER	OG	29	P	ILE	O	2.65
372	A	SER	OG	31	P	THR	O	3.15
506	A	PHE	N	31	P	THR	OG1	2.96

Table 3.14.4: Protein-Protein Side Chain-Side Chain Hydrogen Bonds of complex 3c

Before Simulation								
DONOR				**ACCEPTOR**				
POS	**CHAIN**	**RES**	**ATOM**	**POS**	**CHAIN**	**RES**	**ATOM**	**Dd-a**
349	A	ARG	NH1	32	P	GLN	OE1	3.16
349	A	ARG	NH1	32	P	GLN	OE1	3.16
After Simulation								

NO PROTEIN-PROTEIN SIDE CHAIN-SIDE CHAIN HYDROGEN BONDS FOUND

Table 3.15: Summary of interactions among PSKR, Phytosulphokine and SERK1 before and after simulation

Complex	**Inter. Bet.**	**H-Bond**		**Hydrophobic Interaction**		**Ionic Interaction**		**Cation - Pi Interaction**		**Aromatic - Aromatic Interaction**		**Aromatic - Sulphur Interaction**	
		B. MD	*A. MD*	*B. MD*	*A. MD*	*B. MD*	*A. MD*	*B. MD*	*A. MD*	*B. MD*	*A. MD*	*B. MD*	*A. MD*
PSKR+ Phytosulphokine+ SERK1	*PSKR+ Phytosuphokine*	9	2	6	5	0	0	0	0	0	0	0	0
	PSKR+ SERK1	14	24	5	5	2	2	0	1	0	1	0	0
	Phytosuphokine + SERK1	0	0	0	0	0	0	0	0	0	0	0	0
PSKR+ SERK1	*PSKR+ SERK1*	14	22	5	7	2	2	0	1	0	0	0	0
PSKR+ Phytosulphokine	*PSKR+ Phytosuphokine*	9	4	6	1	0	0	0	0	0	0	0	0

3.4 Contribution of PAMP and co-receptor in PRR mediated PTI

3.4.1 Complex 1

On the basis of MM/PBSA, the binding energies of complex 1ai and complex 1aiii are -805.273 $kJmol^{-1}$ and -8.659 $kJmol^{-1}$, respectively. Alongside, binding energy of complex 1c is -723.444 $kJmol^{-1}$, which is another notable value. But an interaction looks unimaginable for complex 1b as its binding energy is 1063.383 $kJmol^{-1}$. Furthermore, in complex 1b, polar solvation energy and electrostatic energy is maximum which causes BAK1 non-interactive with FLS2. From this synopsis, it can be finalized that, co-receptor BAK1 does not perform a considerable role for interactions to occur between FLS2 and flg22. Moreover, when it is about complex 1c, the maximum intermolecular electrostatic energy and MM/PBSA values compared to complex 1ai indicates that FLS2 can communicate with flg22 both in the presence or absence of BAK1. (Table 3.16) (Fig 3.3.1 a)

3.4.2 Complex 2

The binding energies of complex 2ai and complex 2aiii are -633.586 $kJmol^{-1}$ and -328.179 $kJmol^{-1}$, respectively. Alongside, binding energy of complex 2c is -641.859 $kJmol^{-1}$, which is more than the value of complex 2ai. But an interaction looks unimaginable for complex 2b as its binding energy is 932.704 $kJmol^{-1}$. Furthermore, in complex 2b, polar solvation energy is maximum which causes SERK1 non-interactive with HAESA. From this synopsis, it can be finalized that, co-receptor SERK1 does not perform a considerable role for interactions to occur between HAESA and IDA. Moreover, when it is about complex 2c, the maximum intermolecular electrostatic energy and MM/PBSA values compared to complex 2ai indicates that HAESA can communicate with IDA both in the presence or absence of SERK1. (Table 3.16) (Fig 3.3.1 b)

3.4.3 Complex 3

From another point of view, binding energies of complex 3aii and complex 3aiii are -347.837 $kJmol^{-1}$ and -5.593 $kJmol^{-1}$, respectively. Alongside, binding energy of complex 3b is -440.530 $kJmol^{-1}$, which is more than the value of complex 3aii. But an interaction looks unimaginable for complex 3c as its binding energy is 6.087 $kJmol^{-1}$. Furthermore, in complex 3c, polar solvation energy is maximum which causes Phytosulphokine non-interactive with PSKR. From this synopsis, it can be finalized that, co-receptor SERK1 performs a considerable role for interactions to occur between PSKR and Phytosulphokine. Moreover, when it is about complex 3b, the

maximum intermolecular electrostatic energy and MM/PBSA values compared to complex 3aii indicates that PSKR can communicate with SERK1 both in the presence or absence of Phytosulphokine. (Table 3.16) (Fig 3.3.1 c)

In the instance of pattern triggered immunity, most PAMPs employ one or many co-receptors and operate as a molecular glue to make a heterodimeric complex of PRR, co-receptor and PAMP. For BRI1, co-receptor BAK1 is being employed by ligand brassinolide, which begins the heterodimerization process. Each complexes of this work demonstrate similar binding mechanism as BRI1 mediated complex. Additionally, in the presence of co-receptor BAK1 and SERK1, the PAMP flg22 and IDA ties with FLS2 and HAESA other hand in the absence of flg22 and IDA the ectodomains of FLS2 and HAESA cannot interact with BAK1 and SERK1. However, in the presence or absence of PAMP phytosulphoine, the co-receptor SERK1 interacts with PSKR.

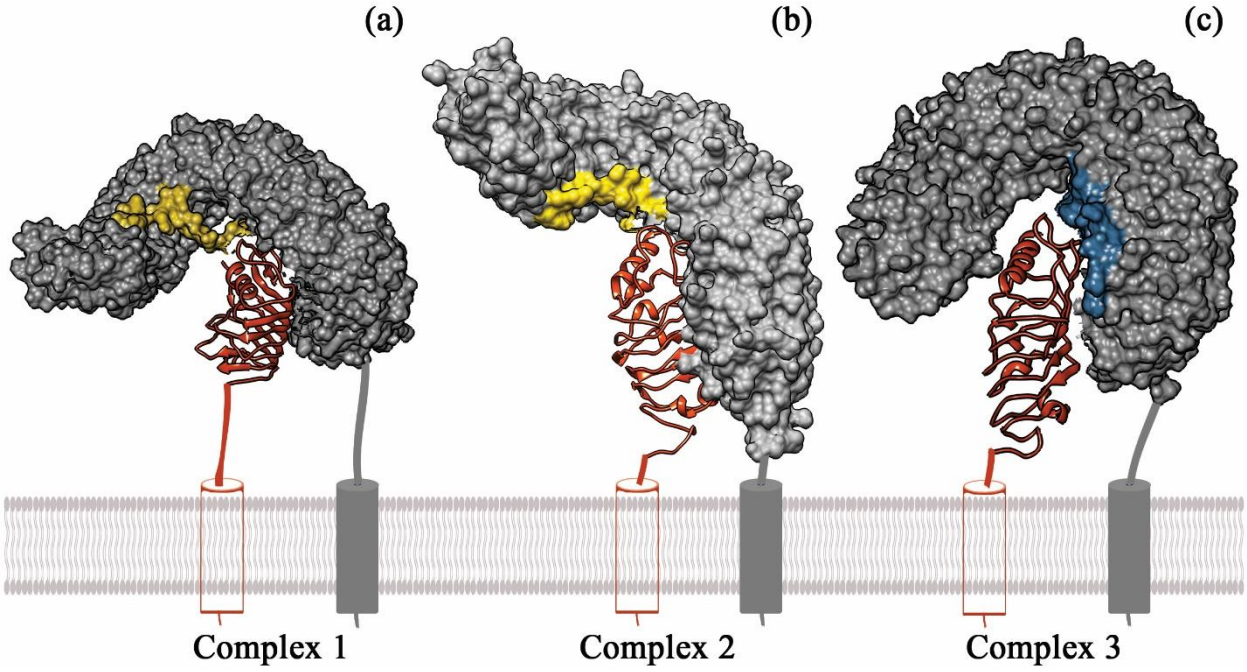

Fig 3.4.1: Surface structure of PRRs and PAMPs and binding pattern visualization of co-receptors. (a) Surface structure of FLS2 and flg22 and binding pattern visualization of BAK1; (b) Surface structure of HAESA and IDA and binding pattern visualization of SERK1; (c) Surface structure of PSKR and Phytosulphokine and binding pattern visualization of SERK1.

Table 3.16: Binding free energy values and the individual energy components for the complexes (kJ/mol)

Complex	ΔE_{vdw}[a]	ΔE_{elec}[b]	ΔE_{polar}[c]	ΔE_{sasa}[d]	ΔE_{bind}[e]
Complex 1ai	-348.922 ± 35.575	-1376.808 ± 109.702	972.027 ± 141.640	-51.569 ± 3.853	-805.273 ± 65.295
Complex 1aii	-277.355 ± 32.529	1050.341 ± 91.268	325.891 ± 130.402	-31.808 ± 6.188	1067.069 ± 82.809
Complex 1aiii	-69.609 ± 13.682	-82.447 ± 51.476	153.442 ± 80.271	-10.044 ± 3.839	-8.659 ± 55.113
Complex 1b	-415.517 ± 39.497	759.292 ± 91.932	769.964 ± 94.450	-50.356 ± 5.842	1063.383 ± 77.556
Complex 1c	-356.036 ± 30.555	-1482.611 ± 123.257	1167.752 ± 169.325	-52.548 ± 3.225	-723.444 ± 86.838
Complex 2ai	-245.919 ± 23.274	-926.402 ± 99.178	570.308 ± 115.737	-31.573 ± 2.901	-633.586 ± 43.115
Complex 2aii	-386.888 ± 32.122	-167.323 ± 137.350	1205.530 ± 161.156	-53.262 ± 7.288	932.704 ± 117.635
Complex 2aiii	-72.570 ± 12.180	-545.690 ± 58.203	301.286 ± 91.525	-11.205 ± 3.821	-328.179 ± 65.974
Complex 2b	-227.093 ± 36.160	-376.695 ± 205.392	684.790 ± 281.341	-28.476 ± 7.649	805.971 ± 129.383
Complex 2c	-189.582 ± 31.028	-923.203 ± 156.118	497.071 ± 217.195	-26.144 ± 5.657	-641.859 ± 60.235
Complex 3ai	-133.807 ± 16.592	-306.852 ± 78.825	505.852 ± 121.976	-18.462 ± 1.670	46.731 ± 43.134
Complex 3aii	-364.937 ± 41.888	-625.297 ± 107.510	687.465 ± 150.459	-45.069 ± 7.465	-347.837 ± 125.931
Complex 3aiii	-0.700 ± 0.222	-9.573 ± 4.453	4.899 ± 58.227	-0.219 ± 2.754	-5.593 ± 58.248

Complex 3b	-495.662 ± 37.067	-685.959 ± 97.802	797.877 ± 148.463	-56.786 ± 7.040	-440.530 ± 109.154
Complex 3c	-104.858 ± 20.188	-421.876 ± 103.287	548.977 ± 132.562	-16.156 ± 3.108	6.087 ± 38.811

[a]Van der Waals energy. [b]Electrostatic energy. [c]Polar solvation energy. [d]Solvent Accessible Surface Area (SASA) energy. [e]Binding Free energy.

3.5 Determination of the most stable, compact complex

3.5.1 Root Mean Square Deviation (RMSD)

The stability of the MD simulation was computed in terms of deviations by analyzing Root mean square deviation (RMSD). The time evolution of the RMSDs of all the complexes (backbone only) are monitored as a function of time. The RMSDs of complex 1a, 1b, 1c, 2a, 2b, 2c, 3a, 3b, 3c are shown in Fig. 3.4.1 a, b and c respectively. In complex 1a, it takes 12ns to equilibrate. Before 12ns of the period, it gives maximum deviation at 7ns and 12ns which are 0.55nm and 0.56nm. Though in between this period graph slightly goes down at 9ns after equilibration it moves forward stably with a standard deviation (SD) of 0.45nm. From 12 ns it gives a stable view and deviated in between 0.40nm to 0.50nm till the end of the simulation. In the complex 2a, it takes 5ns to equilibrate. Before 5ns of the period, it gives maximum deviation at 1.3ns and 2.1ns which are 0.50nm and 0.55nm. Though in between this period graph slightly goes down at 3ns after equilibration it moves forward stably with a standard deviation (SD) of 0.20nm. From 5 ns it gives a stable view and deviated in between 0.41nm to 0.46nm till the end of the simulation. In complex 3a, it takes 20ns to equilibrate. Before 20ns of the period, it gives maximum deviation at 17ns and 14ns which are 0.57nm and 0.49nm. Though in between this period graph slightly goes down at 11ns(0.22nm) after equilibration it moves forward stably with a standard deviation (SD) of 0.40nm. From 20 ns it gives a stable view and deviated in between 0.35nm to 0.45nm till the end of the simulation. For, complex 1a and 2a, RMSD shows almost similar characteristic in a sense of period of equilibration. Both of the complexes equilibrated at the very initial stage of their simulation. But in case of complex 3a, 20ns of simulation period needs to equilibrate, though similarity between complex 1a and 4a is found. After equilibration both of the complexes show quite similar standard deviation (SD) which is between 0.40 nm to 0.45nm. In complex 1c,

deviation is not that much stable as before. Rather, at the very beginning of the simulation process graph shows deviation. But after 14ns it tries to form stability, but from 24ns it deviates at 0.40nm which is considered as lowest in terms of that condition. This instability continues till the end of simulation. In complex 2c, deviation is not that much stable as before. Rather, at the very beginning of the simulation process graph shows stability. But after 10ns it continues maximum deviation, at 25ns it deviates at 1.125nm which is considered as second highest in terms of that condition. Again, instability is observed in this case from 20ns to 21ns because between this period it shows some high RMSD like 0.85nm to 1.15nm and some very low RMSD (0.25nm to 0.35nm) are also observed. In complex 3c, deviation is not that much stable as before. Rather, at the very beginning of the simulation process graph shows stability. But after 15ns it continues maximum deviation, at 16ns it deviates at 0.83nm which is considered as highest in terms of that condition. Again, instability is observed in this case from 16ns to 20ns because between this period it shows some high RMSD like 0.80nm to 0.83nm. For, complex 1c, 2c, 3c, all of them show similar characteristics. All of them show instability, though complex 2c tries to be stable but continuous deviations during entire simulation period make it unstable complex like others. RMSD of complex 1b is analyzed similarly. As observed before in the case of complex 1c, an unstable deviation is found here, RMSD also shows instability. As it is observed that RMSD of complex 1a shows stability from 12ns but in this case, it stables from 8ns to 17ns with a standard deviation of 0.62nm. From 8ns to 17ns RMSD of complex 1b has deviated from 0.55nm to 0.75nm. RMSD of complex 2b is analyzed similarly. As observed before in the case of complex 2c, an unstable deviation is found, similarly RMSD of complex 2b also shows instability. As it is observed that in complex 2a RMSD shows stability from 5ns but in this case, it unstable from 5ns with a standard deviation of 0.98nm till the end of the simulation period. From 5ns till the end of the period RMSD of complex 2b has deviated from 0.94nm to 1.95nm. RMSD of complex 3b is analyzed similarly. Initial stage of this complex is equilibrated and shows stability. At 11ns it deviates to 0.36nm and after 14ns it dramatically goes up to 0.56nm, though from 20ns to 23ns of the simulation, the RMSD shows slight stability with a standard deviation of 0.35nm but it discontinues till the end of the simulation. As observed before in the case of complex 3c, an unstable deviation is found similarly for RMSD of complex 3b also shows instability. Like complex 1c, 2c, 3c, complex 1b, 2b, 3b also show instability during their simulation period. Though complex 3b shows stability at the initial stage of simulation but it cannot continue stability and gives lower deviation

dramatically. In terms of all situations, it is observed that, complex 1a, 2a, 3a show more stability. To form a stable complex PRR needs co-receptor alongside PAMP to mediate PTI of *A.thaliana*.

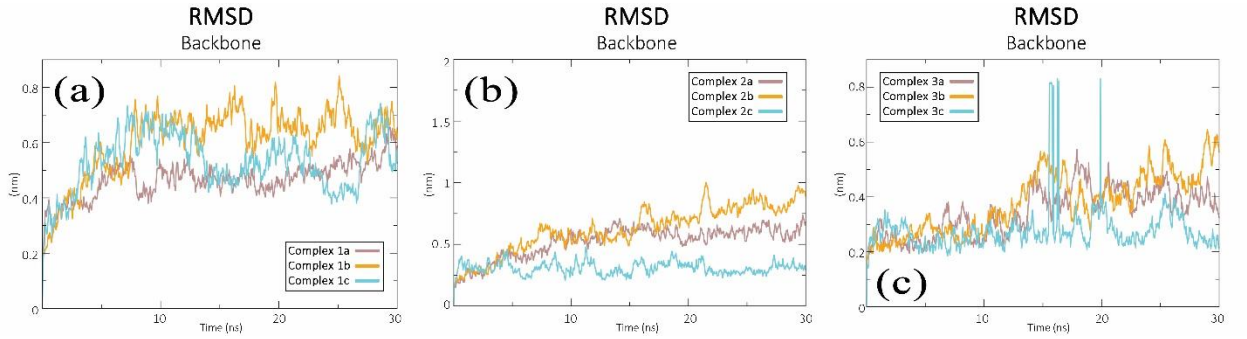

Fig 3.5.1.1: (a) RMSD value of complex 1a, 1b and 1c from 30ns MD trajectories. RMSD of FLS2 and flg22 when BAK1 is present in the complex (brown). RMSD of FLS2 and BAK1 when flg22 is absent in the complex (orange). RMSD of FLS2 and flg22 when BAK1 is absent in the complex (cyan) (b) RMSD value of complex 2a, 2b and 2c from 30ns MD trajectories. RMSD of HAESA and IDA when SERK1 is present in the complex (brown). RMSD of HAESA and SERK1 when IDA is absent in the complex (orange). RMSD of HAESA and IDA when SERK1 is absent in the complex (cyan) (c) RMSD value of complex 3a, 3b and 3c from 30ns MD trajectories. RMSD of PSKR and Phytosulphokine when SERK1 is present in the complex (brown). RMSD of PSKR and SERK1 when Phytosulphokine is absent in the complex (orange). RMSD of PSKR and Phytosulphokine when SERK1 is absent in the complex (cyan).

3.5.2 Radius of Gyration

To measure the compactness of all systems, the radius of gyration (Rg) values was measured. It could be seen that the Rg of the complex 1c fluctuated more compared to that of the complex 1a and complex 1b. This trend is most pronounced in the 27 ns of the simulation; as the complex 1c reaches the highest value of about 4.0 nm in the 20 ns and then drops and reaches the lowest value of about 3.7 nm near 25 ns mark. Whereas, the graph remains relatively steady for the complex 1a in this time frame; though it also reaches its highest (around 3.81 nm) and lowest (around 3.46 nm) points at around 7.5 ns and 2.3 ns, respectively. Though in complex 1b at the very beginning of the simulation (0.5ns) it gives the lowest value of 3.55nm after 10ns it rises to 3.81nm and continues the stability. In complex 1c, many instabilities occur. More variations in the Rg values signify a more changing structure, which is consistent with higher fluctuations in the complex 1b

and complex 1c; as the proteins are more freely able to uncoil and recoil. On the other hand, when the FLS2 is interacting with both flg22 and BAK1 in a single complex, it is bound in place and less able to uncoil resulting in a less fluctuating graph. From another point of view the complex 2b fluctuated more compared to that of the complex 2a and complex 2c. This trend is most pronounced in the 21 ns of the simulation; as the complex 2b reaches the highest value of about 3.68 nm in the first 16 ns and then drops and reaches the lowest value of about 3.40 nm near 20 ns mark. Whereas, the graph remains relatively steady for the complex 3a in this time frame; though it also reaches its highest (around 3.4 nm) and lowest (around 3.25 nm) points at around 16.6 ns and 3 ns, respectively. Though in complex 2c at the very beginning of the simulation (3ns) it gives the lowest value of 3.32nm after 16.6ns it rises to 3.6nm and continues the stability. More variations in the Rg values signify a more changing structure, which is consistent with higher fluctuations in the complex 2b and complex 2c; as the proteins are more freely able to uncoil and recoil. On the other hand, when the HAESA is interacting with both IDA and SERK1 in a single complex, it is bound in place and less able to uncoil resulting in a less fluctuating graph. Other hand, the Rg of the complex 3a fluctuated more compared to that of the complex 3b and complex 3c. This trend is most pronounced in the 20 ns of the simulation; as the complex 3a reaches the highest value of about 3.35 nm in the first 18 ns and then drops and reaches the lowest value of about 3.10 nm near 25 ns mark. Whereas, the graph remains relatively steady for the complex 4a in this time frame. Though in complex 3b, at the very beginning of the simulation (4ns) it gives the lowest value of 3.04nm after 15ns it rises to 3.3nm and continues the stability. In complex 3c, many instabilities occur. Though at 20ns it rises to 3.16nm at 22ns it drops to 2.98nm. More variations in the Rg values signify a more changing structure, which is consistent with higher fluctuations in the complex 3b and complex 3c; as the proteins are more freely able to uncoil and recoil. On the other hand, when the SERK1 is interacting with both PSKR and phytosulphokine in a single complex, it is bound in place and less able to uncoil resulting in a less fluctuating graph. Final consideration for all the complexes is, complex 1 and 2 show similar characteristics in terms of compactness, for showing less coiling complex 1a and 2a give low fluctuation than their other simulated complexes. But in case of complex 3, though complex 3c gives less fluctuation rate but stability founds in complex 3a, which indicated to remain a compact complex alongside PRR and PAMP, co-receptor has to be present inside the complex.

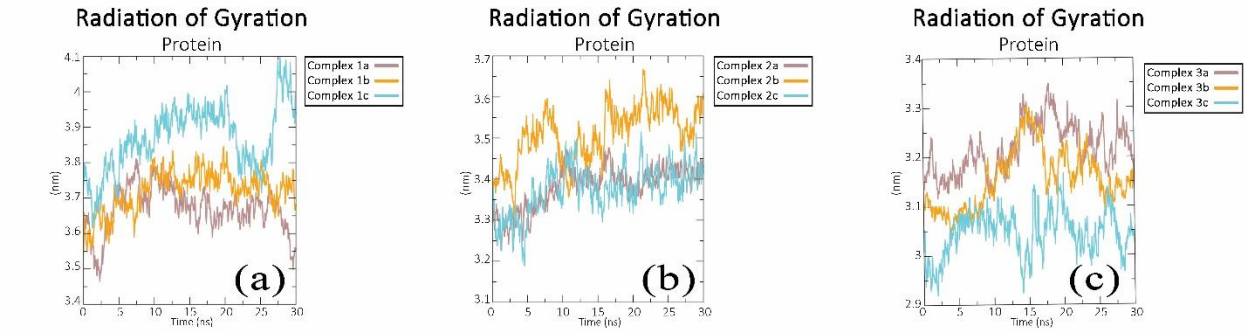

Fig 3.5.2.1: (a) Rg value of complex 1a, 1b and 1c from 30ns MD trajectories. Rg of FLS2 and flg22 when BAK1 is present in the complex (brown). Rg of FLS2 and BAK1 when flg22 is absent in the complex (orange). Rg of FLS2 and flg22 when BAK1 is absent in the complex (cyan) (b) Rg value of complex 2a, 2b and 2c from 30ns MD trajectories. Rg of HAESA and IDA when SERK1 is present in the complex (brown). Rg of HAESA and SERK1 when IDA is absent in the complex (orange). Rg of HAESA and IDA when SERK1 is absent in the complex (cyan) (c) Rg value of complex 3a, 3b and 3c from 30ns MD trajectories. Rg of PSKR and Phytosulphokine when SERK1 is present in the complex (brown). Rg of PSKR and SERK1 when Phytosulphokine is absent in the complex (orange). Rg of PSKR and Phytosulphokine when SERK1 is absent in the complex (cyan).

3.5.3 Solvent Accessible Surface Area (SASA)

The solvent assessable surface areas (SASA) were also calculated over the 30 ns time of simulation. It was seen to be considerably lower for the complex 1c than complex 1b, showing a steady mean value of about 350 nm^2. Opposed to this, the complex 1b had a much higher mean value of about 415 nm2. Again, SASA value of complex 2a is 430 nm^2. Moreover, complex 2a gives considerably lower SASA value than complex 2b, showing a steady mean value of about 381 nm^2. Opposed to this, the complex 2b had a much higher mean value of about 386 nm^2. Again, SASA value of complex 2c is 305 nm^2. Additionally, complex 3a is considerably lower than complex 3c, showing a steady mean value of about 345 nm^2. Opposed to this, the complex 3b had a much higher mean value of about 350 nm^2. Again, SASA value of complex 3c is 275 nm^2 which is very low. Overview of this analysis indicates that complex 1a, 2a and 3a greatly increased the surface area, which the solvent (water) could access. Other complexes cannot increase surface area that much.

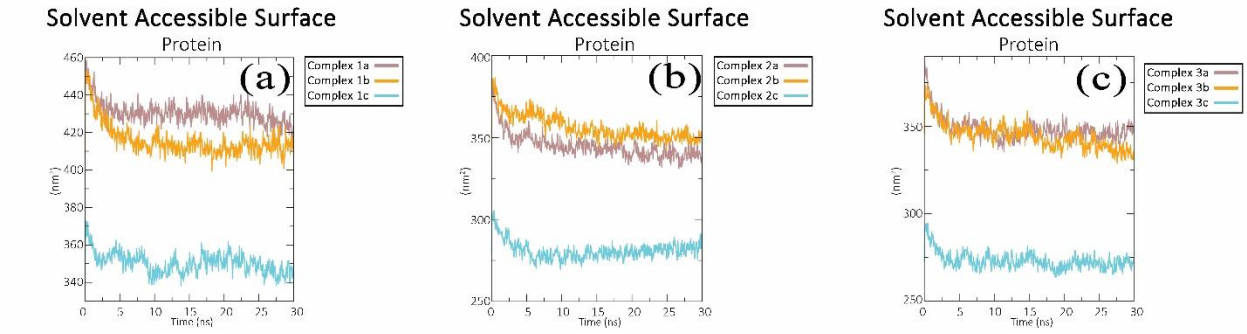

Fig 3.5.3.1: (a) SASA value of complex 1a, 1b and 1c from 30ns MD trajectories. SASA of FLS2 and flg22 when BAK1 is present in the complex (brown). SASA of FLS2 and BAK1 when flg22 is absent in the complex (orange). SASA of FLS2 and flg22 when BAK1 is absent in the complex (cyan) (b) Rg value of complex 2a, 2b and 2c from 30ns MD trajectories. SASA of HAESA and IDA when SERK1 is present in the complex (brown). SASA of HAESA and SERK1 when IDA is absent in the complex (orange). SASA of HAESA and IDA when SERK1 is absent in the complex (cyan) (c) Rg value of complex 3a, 3b and 3c from 30ns MD trajectories. SASA of PSKR and Phytosulphokine when SERK1 is present in the complex (brown). SASA of PSKR and SERK1 when Phytosulphokine is absent in the complex (orange). SASA of PSKR and Phytosulphokine when SERK1 is absent in the complex (cyan).

3.6 H-Bond

Hydrogen bond number was calculated over the 30 ns time of simulation for protein-protein criteria. The protein-protein hydrogen bonds show the overall curve lifting graph throughout the simulation. For a better understanding of forming hydrogen bond within two proteins index file was used which help to calculate overall hydrogen bond formation at a different period. It is visible that maximum 23 hydrogen bond is found between FLS2 and flg22 at 1250ps in complex 1ai and in complex 1c, maximum 22 hydrogen bonds are formed at 16650ps. Protein Interaction Calculation (PIC) data also said that there is notable sustainable hydrogen bond interaction exist between FLS2 and flg22, rather no sustainable hydrogen bond interaction exists between FLS2 and BAK1. In details, Arg72 of flg22 accepts atoms from Gln268 of FLS2 and remain same after simulation where it is a main chain-side chain hydrogen bond interaction. Again, Gln65 of flg22 also creates side chain-side chain hydrogen bond interaction with Arg152 of FLS2. flg22 makes a very negligible amount of sustainable main chain-side chain hydrogen bond with FLS2 in complex 1c. Moreover, there are very few hydrogen bonds found in complex 1aiii.

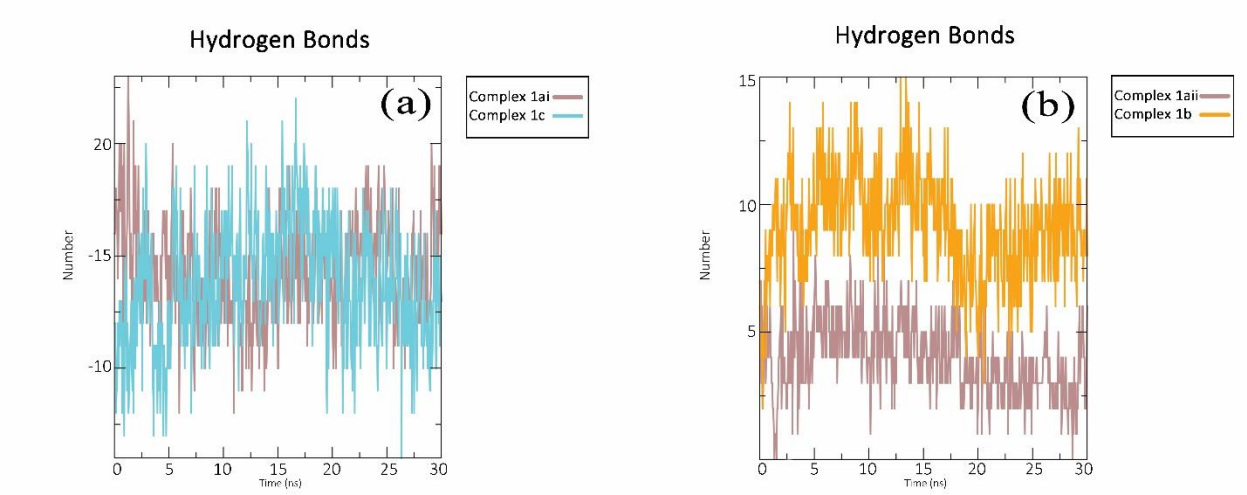

Fig 3.6.1: (a) H-bond value of complex 1ai and 1c from 30ns MD trajectories. H-bond of FLS2 and flg22 when BAK1 is present in the complex (brown). H-bond of FLS2 and flg22 when BAK1 is absent in the complex (cyan). (b) H-bond value of complex 1aii and 1b from 30ns MD trajectories. H-bond of FLS2 and BAK1 when flg22 is present in the complex (brown). H-bond of FLS2 and BAK1 when flg22 is absent in the complex (orange).

It is visible that maximum 10 hydrogen bond is found between HAESA and IDA at 850ps and 1850ps in complex 2ai and in complex 2c, maximum 10 hydrogen bond is formed at 10850ps. Protein Interaction Calculation (PIC) data also said that there are very few sustainable hydrogen bond interactions happen between HAESA and IDA, rather sustainable hydrogen bond interactions occur between HAESA and SERK1 with a very high number. In details, Arg73 of SERK1 donates atoms to Asn526 and Glu527 of HAESA and remain same after simulation where it is a side chain-side chain hydrogen bond interaction. Again, Asp123 and Arg147 of SERK1 also create side chain-side chain hydrogen bond interaction with Asn573 of HAESA. IDA makes a very negligible amount of sustainable main chain-side chain hydrogen bond with HAESA in complex 2c.

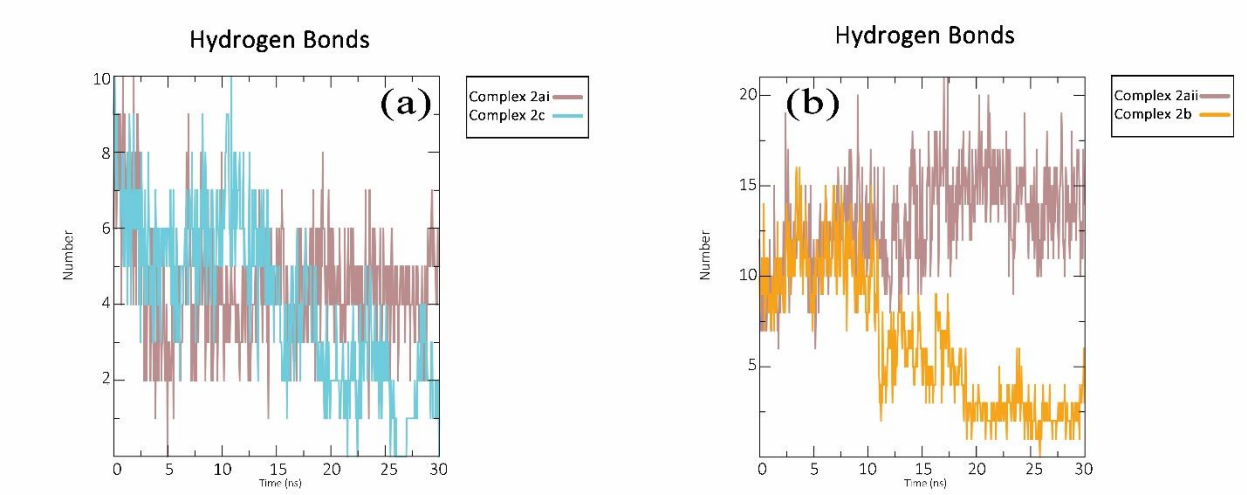

Fig 3.6.2: (a) H-bond value of complex 2ai and 2c from 30ns MD trajectories. H-bond of HAESA and IDA when SERK1 is present in the complex (brown). H-bond of HAESA and IDA when SERK1 is absent in the complex (cyan). (b) H-bond value of complex 2aii and 2b from 30ns MD trajectories. H-bond of HAESA and SERK1 when IDA is present in the complex (brown). H-bond of HAESA and SERK1 when IDA is absent in the complex (orange).

It is visible that maximum 9 hydrogen bonds are found between PSKR and phytosulphokine at 19600ps in complex 3ai and in complex 3c, maximum 11 hydrogen bonds are formed at 25300ps and 25850ps. Protein Interaction Calculation (PIC) data also said that there are very few sustainable hydrogen bond interactions happen between PSKR and phytosulphokine, rather sustainable hydrogen bond interactions occur between PSKR and SERK1 with a very high number. In details, Asp31 of SERK1 donates atoms to Lys158 of PSKR to form ionic interaction. Again, Thr31 of phytosulphokine also create side chain-side chain hydrogen bond interaction with Ser370 of PSKR in complex 3ai and main chain-side chain hydrogen bond interaction with Phe506 of PSKR in complex 3c.

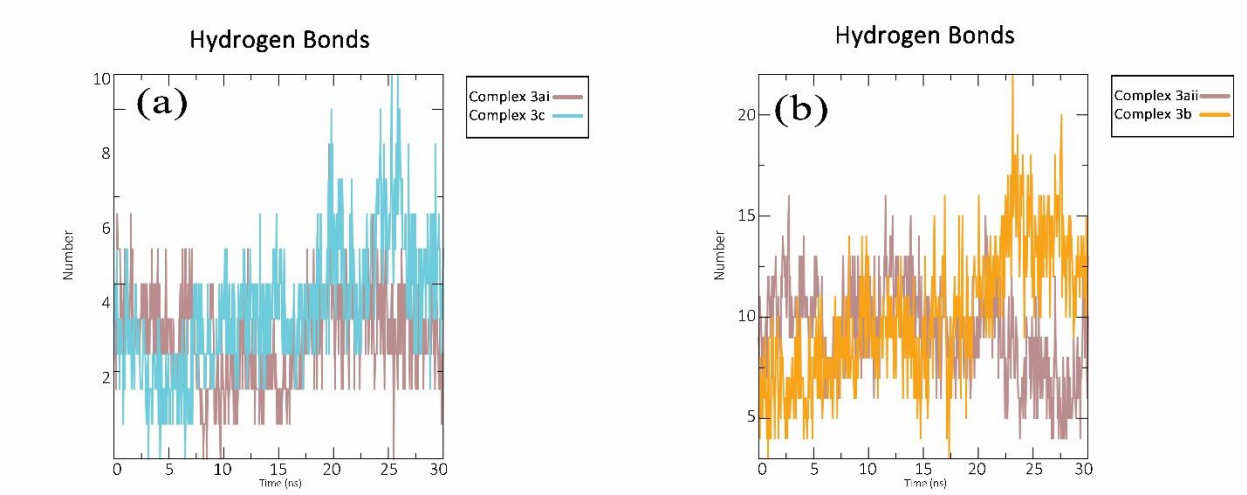

Fig 3.6.3: (a) H-bond value of complex 3ai and 3c from 30ns MD trajectories. H-bond of PSKR and Phytosulphokine when SERK1 is present in the complex (brown). H-bond of PSKR and Phytosulphokine when SERK1 is absent in the complex (cyan). (b) H-bond value of complex 3aii and 3b from 30ns MD trajectories. H-bond of PSKR and SERK1 when Phytosulphokine is present in the complex (brown). H-bond of PSKR and SERK1 when Phytosulphokine is absent in the complex (orange).

Complex 2 and complex 3 at their different simulated system show similar characteristics. Both of them show sustainable and different types of hydrogen bonds between the PRR and co-receptor where complex 1 shows sustainable hydrogen bonds between the PRR and PAMP. But in the case of complex 1, producing few hydrogen bonds between PAMP and co-receptor after the simulation period make co-receptor prominent component for mediating PTI. In case of complex 2 and 3, direct interaction between PRR and co-receptor make it clear to the necessity of existence of co-receptor in the complex. From PIC data, the number of every possible interaction are summarized. Where it is found that at the very initial stage or before simulation there are 31 hydrogen bonds, 9 hydrophobic interactions and 5 ionic interaction are happened in complex 1ai. Though the number of hydrogen bonds increase in this situation after the 30ns simulation period some hydrophobic interactions are also increased and the ionic interaction is reduced to 3. Moreover, in complex 1c, hydrogen bonds are decreased. On the other hand, the number of hydrogen bonds of FLS2 and BAK1 is 27 before the simulation. In complex 1aii hydrogen bonds are drastically decreased. But in complex 1b, numbers of hydrogen bond are increased. Hydrophobic and ionic interaction remain stable. (Table 3.5) From PIC data, the number of every possible interaction are summarized. Where

it is found that at the very initial stage or before simulation there are 36 hydrogen bonds, 5 hydrophobic interactions and 1 ionic interaction have happened in complex 2ai. Though the number of hydrogen bonds reduces in this situation remain the same after the 30ns simulation period, number of hydrophobic interactions and ionic interaction are remaining same. Moreover, in complex 1c hydrogen bonds are also reduced. On the other hand, the number of hydrogen bonds of HAESA and SERK1 is 35 before the simulation. In complex 2aii, hydrogen bonds are increased. But in complex 2b, numbers of hydrogen bond are reduced. Hydrophobic and ionic interaction reduction shows similar characteristics in both complexes. (Table 3.10) From PIC data, the number of every possible interaction are summarized. Where it is found that at the very initial stage or before simulation there are 9 hydrogen bonds, 6 hydrophobic interactions have happened in complex 3ai. Though the number of hydrogen bonds reduces in this situation after the 30ns simulation period, hydrophobic interactions are also decreased even no ionic interaction is produced. Moreover, in complex 3c hydrogen bonds are slightly increased than complex 3ai. In another case, though before simulation there were 14 hydrogen bonds found in complex 3aii, after simulation hydrogen bonds are increased to 24. But in complex 3b, number of hydrogen bonds are decreased to 22. There are no negligible other interactions found in between PSKR and phytosulphokine. (Table 3.15) From this summarized data it is clearly visible that, it is supporting the analysis of hydrogen bond interactions of all of the complexes.

3.7 Discussion

This study describes the computational analysis of a plant PRRs and reports on the interaction of PRR-RLKs to PAMPs and co-receptors. Different analytical approaches used in this study for understanding Pattern Triggered Immunity (PTI) of *Arabidopsis* thaliana towards PAMP by using LRR domain.

Despite that BRI1, ligand is required for heterodimerization, it can make homodimer in the absence of ligand brassinolide. This PAMP's binding to the simulated complexes stabilize the ectodomains of the receptors and triggers the kinase domain. The requirement of these simulated complexes is precisely defined in the case of receptor tyrosine kinases (RTKs), toll-like receptors (TLRs) and cytokine receptors. Moreover, one of the major principles of binding for PAMPs is their direction of binding towards the PRR's ectodomains. The PAMP and the LRR domain are either directed in the same way or in the entirely reverse way. In these cases, although the structure of flg22 is

slightly different from other PAMPs, it can be pronounced that, flg22 interacts directly with the FLS2 LRR. Gln65 (N-terminus residue) of flg22 interacts with Glu81, Tyr128, Arg152 and Asn153 of FLS2 whereas Ile85 (C-terminus residue) of flg22 interacts with His417, Asn441, Ser461 and Ala463of FLS2. (Fig 3.8.1 a) IDA also binds directly with the HAESA LRR. Tyr56 (N-terminus residue) of IDA binds with Asn99, Ser100, Asn124, Ser147, Gly148 and Asn149 of HAESA whereas Asn69 (C-terminus residue) of IDA binds with Asn340, Val360, Asp361, Arg407 and Arg409 of HAESA. (Fig 3.8.1 b) But, Phytosulphokine interacts inversely with the PSKR LRR. Ile29 (N-terminus residue) of Phytosulphokine interacts with Ser372 and Thr398 of PSKR and Phe506, Lys508 and Tyr518 of island domain whereas Gln32 (Cterminus residue) of Phytosulphokine binds with Asn298, Asp322, Thr325, Asn326, Asn346, Arg349 and Ser370 of PSKR and Pro504, Lys508 and Gln517 of island domain. (Fig 3.8.1 c)

From RMSF and RMSD studies, during the presence of co-receptor, the interaction between PAMP and PRR goes to a stable form after a certain period of simulation and also prominent residues are found very low fluctuated during this time. From H-bond analysis and protein interaction calculation (PIC) data, it is observed, previously described favourable residues give a various type of interactions alongside hydrogen bond.

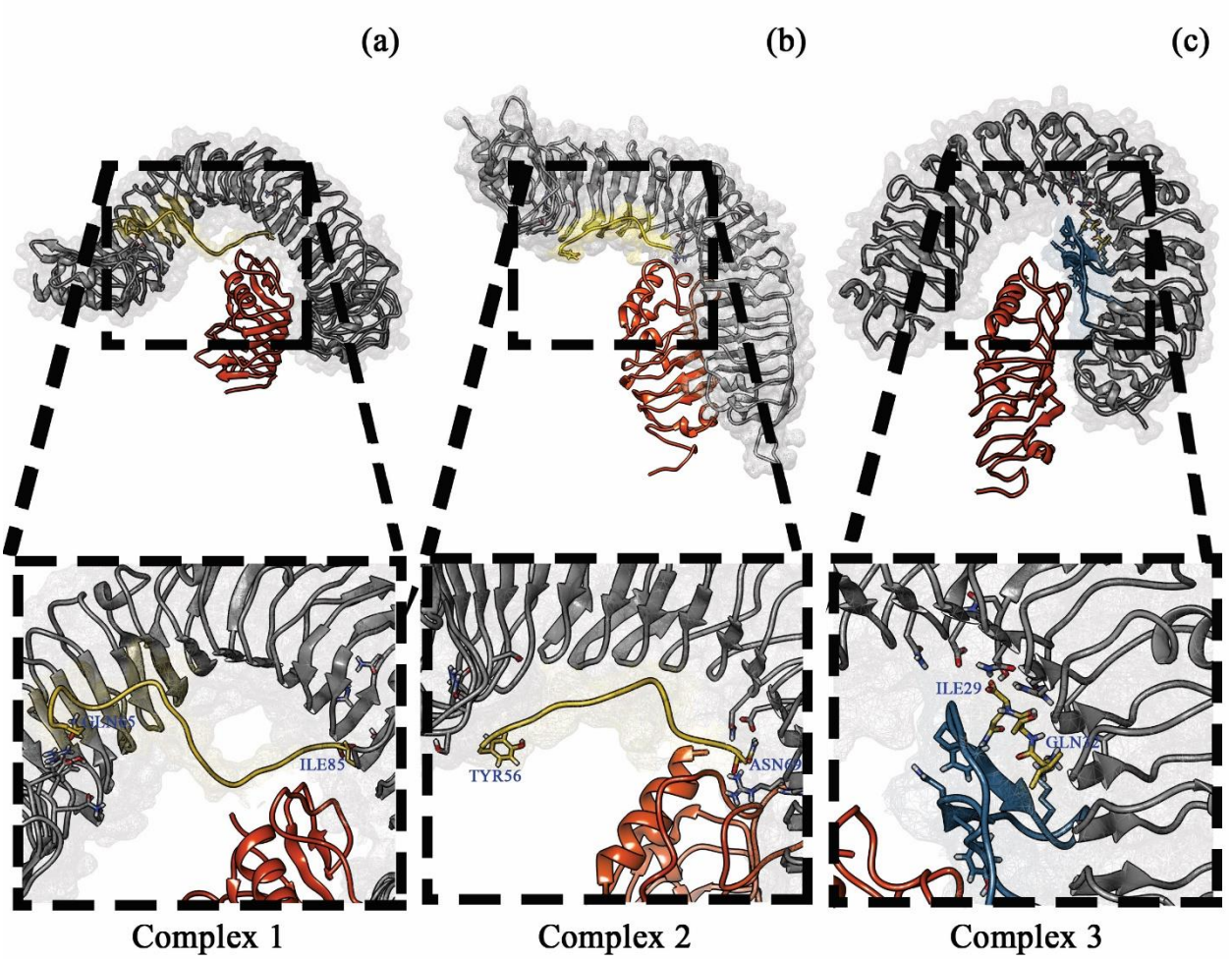

Fig 3.7.1: Binding pattern of PAMPs inside the mesh structure with PRRs. (a) Binding pattern of flg22 inside the mesh structure with FLS2; (b) Binding pattern of IDA inside the mesh structure with HAESA; (c) Binding pattern of Phytosulphokine inside the mesh structure with PSKR.

In the case of LRR-RK and co-receptor interaction, a large number of residues from the internal portion of the ectodomains of SERKs bind with numerous types of receptors. Without interacting with small molecules or peptidyl hormones SERKs highly overlap on LRR-RK ectodomains.[4] When FLS2/HAESA and BAK1/SERK1 are interacting within themselves, binding energy is getting negatively higher in the presence of PAMP but the binding affinity is positively higher without PAMP in the complexes. Though different situation is found in case of PSKR and SERK1 interaction in this study.

Past studies show that various peptidyl hormones or ligands can tightly bind with LRR-RKs with their favourable co-receptors. The interacting heterodimeric complex takes co-receptor near to the

transmembrane helices which assist to do interaction between co-receptor and the cytoplasmic kinase domains.[4] In this thesis, it is also determined that in the presence of co-receptors, PAMPs can bind considerably with PRRs and the position of co-receptor is closely one end of PRR.

As a result, it can be said that any mutations of the residues found from this study can considerably influence the plant's capability to trigger pattern triggered immunity. Again, co-receptors help to recognize PAMPs, so mutation of the prominent residues of co-receptors also cause conformational changes in binding with LRR-RK which also affect the recognition of PAMPs.

Chapter 4

Conclusions and Recommendations

4.1 Conclusion:

From the analysis of 30ns trajectories by using RMSD, RMSF, H-bond, PIC and MM/PBSA it can be said that for immune response against PAMP, there should be a favourable co-receptor present inside the complex. Though from 30ns trajectories RMSD it is found that after 30ns the whole complex tends to be stable but more stability can be found if the simulation period will be extended 100ns or more. Moreover, the prominent residues found through MM/PBSA calculation is calculated from 30ns trajectories. If the simulation period will be extended in future differences of binding energies of prominent residues can be obtained.

From H-bond and PIC result after 30ns simulation there are notable differences found in different types of interaction alongside H-bond than before the simulation. Extended simulation period will provide that what types of interactions are more responsible and which interaction is going less important.

But from 30ns trajectories, as it is found for immune response from PRRs co-receptors play a notable role, so it can be assumed that after the extension of the simulation period it will remain the same.

4.2 Recommendations for Future Works:

This research can be more developed by taking some measure such as:

1. This thesis can be enhanced by running the molecular dynamic simulation for extended period of time (100 ns or more), this would allow more selective and conclusive results from the study. More understanding of protein nature can be built.

2. This study might be useful to study on the importance of prominent residues of PRRs, PAMPs and co-receptors. By mutating on the prominent residues found from this study may be enlightened on the importance of the specific residues for triggering innate immunity system of *Arabidopsis thaliana.*

REFERENCES

1. Boller, T. and G.J.A.r.o.p.b. Felix, *A renaissance of elicitors: perception of microbe-associated molecular patterns and danger signals by pattern-recognition receptors.* 2009. **60**: p. 379-406.
2. Boller, T. and S.Y.J.S. He, *Innate immunity in plants: an arms race between pattern recognition receptors in plants and effectors in microbial pathogens.* 2009. **324**(5928): p. 742-744.
3. Chisholm, S.T., et al., *Host-microbe interactions: shaping the evolution of the plant immune response.* 2006. **124**(4): p. 803-814.
4. Hohmann, U., K. Lau, and M.J.A.r.o.p.b. Hothorn, *The structural basis of ligand perception and signal activation by receptor kinases.* 2017. **68**: p. 109-137.
5. Jones, J.D. and J.L.J.n. Dangl, *The plant immune system.* 2006. **444**(7117): p. 323.
6. Zipfel, C.J.T.i.i., *Plant pattern-recognition receptors.* 2014. **35**(7): p. 345-351.
7. Ting, J.P. and B.K.J.A.R.I. Davis, *CATERPILLER: a novel gene family important in immunity, cell death, and diseases.* 2005. **23**: p. 387-414.
8. nature, A.G.I.J., *Analysis of the genome sequence of the flowering plant Arabidopsis thaliana.* 2000. **408**(6814): p. 796.
9. Meyerowitz, E.M. and C.R. Somerville, *Arabidopsis*. 1994: Cold Spring Harbor Laboratory Press.
10. Meinke, D.W., et al., *Arabidopsis thaliana: a model plant for genome analysis.* 1998. **282**(5389): p. 662-682.
11. Feldmann, K.A. and S.A. Goff, *The first plant genome sequence—Arabidopsis thaliana*, in *Advances in Botanical Research*. 2014, Elsevier. p. 91-117.
12. Sparrow, A., H. Price, and A. Underbrink. *A survey of DNA content per cell and per chromosome of prokaryotic and eukaryotic organisms: some evolutionary considerations*. in *Brookhaven symposia in biology*. 1972.
13. Sparrow, A.H. and J.P.J.S. Miksche, *Correlation of nuclear volume and DNA content with higher plant tolerance to chronic radiation.* 1961. **134**(3474): p. 282-283.
14. Lin, X., et al., *Sequence and analysis of chromosome 2 of the plant Arabidopsis thaliana.* 1999. **402**(6763): p. 761.

15. Mayer, K., et al., *Sequence and analysis of chromosome 4 of the plant Arabidopsis thaliana.* 1999. **402**(6763): p. 769.
16. Theologis, A., et al., *Sequence and analysis of chromosome 1 of the plant Arabidopsis thaliana.* 2000. **408**(6814): p. 816.
17. Meyerowitz, E.M.J.P.p., *Prehistory and history of Arabidopsis research.* 2001. **125**(1): p. 15-19.
18. Yanofsky, M.F., et al., *The protein encoded by the Arabidopsis homeotic gene agamous resembles transcription factors.* 1990. **346**(6279): p. 35.
19. Laibach, F., *Zur Frage nach der Individualität der Chromosomen im Pflanzenreich*. 1907.
20. Ezhova, T.J.G., *Arabidopsis thaliana (L.) Heynh. as a model object for studying genetic control of morphogenesis.* 1999. **35**(11): p. 1522-1537.
21. Titova, N.J.S.B., *Poiski rastitePnoy drozophily.* 1935. **2**: p. 61-67.
22. Laibach, F.J.B.A., *Arabidopsis thaliana (L.) Heynh. als Objekt für genetische und entwicklungsphysiologische Untersuchungen.* 1943. **44**: p. 439-455.
23. Rédei, G.P.J.A.r.o.g., *Arabidopsis as a genetic tool.* 1975. **9**(1): p. 111-127.
24. Tsuda, K. and F.J.C.o.i.p.b. Katagiri, *Comparing signaling mechanisms engaged in pattern-triggered and effector-triggered immunity.* 2010. **13**(4): p. 459-465.
25. Tsuda, K., et al., *Network properties of robust immunity in plants.* 2009. **5**(12): p. e1000772.
26. Block, A., et al., *Phytopathogen type III effector weaponry and their plant targets.* 2008. **11**(4): p. 396-403.
27. Cunnac, S., M. Lindeberg, and A.J.C.o.i.m. Collmer, *Pseudomonas syringae type III secretion system effectors: repertoires in search of functions.* 2009. **12**(1): p. 53-60.
28. Göhre, V. and S.J.A.R.P. Robatzek, *Breaking the barriers: microbial effector molecules subvert plant immunity.* 2008. **46**: p. 189-215.
29. Böhm, H., et al., *Immune receptor complexes at the plant cell surface.* 2014. **20**: p. 47-54.
30. Ranf, S.J.C.o.i.p.b., *Sensing of molecular patterns through cell surface immune receptors.* 2017. **38**: p. 68-77.
31. Xin, X.-F., et al., *Bacteria establish an aqueous living space in plants crucial for virulence.* 2016. **539**(7630): p. 524.

32. Rosebrock, T.R., et al., *A bacterial E3 ubiquitin ligase targets a host protein kinase to disrupt plant immunity.* 2007. **448**(7151): p. 370.
33. Collier, S.M. and P.J.T.i.p.s. Moffett, *NB-LRRs work a "bait and switch" on pathogens.* 2009. **14**(10): p. 521-529.
34. Kumpf, R.P., et al., *Floral organ abscission peptide IDA and its HAE/HSL2 receptors control cell separation during lateral root emergence.* 2013. **110**(13): p. 5235-5240.
35. Lease, K.A. and J.C.J.P.p. Walker, *The Arabidopsis unannotated secreted peptide database, a resource for plant peptidomics.* 2006. **142**(3): p. 831-838.
36. Shiu, S.-H. and A.B.J.P.o.t.N.A.o.S. Bleecker, *Receptor-like kinases from Arabidopsis form a monophyletic gene family related to animal receptor kinases.* 2001. **98**(19): p. 10763-10768.
37. Dunning, F.M., et al., *Identification and mutational analysis of Arabidopsis FLS2 leucine-rich repeat domain residues that contribute to flagellin perception.* 2007. **19**(10): p. 3297-3313.
38. Sun, Y., et al., *Structural basis for flg22-induced activation of the Arabidopsis FLS2-BAK1 immune complex.* Science, 2013. **342**(6158): p. 624-628.
39. Santiago, J., et al., *Mechanistic insight into a peptide hormone signaling complex mediating floral organ abscission.* 2016. **5**: p. e15075.
40. Jinn, T.-L., et al., *HAESA, an Arabidopsis leucine-rich repeat receptor kinase, controls floral organ abscission.* 2000. **14**(1): p. 108-117.
41. Stenvik, G.-E., et al., *The EPIP peptide of INFLORESCENCE DEFICIENT IN ABSCISSION is sufficient to induce abscission in Arabidopsis through the receptor-like kinases HAESA and HAESA-LIKE2.* 2008. **20**(7): p. 1805-1817.
42. Morillo, S.A. and F.E. Tax, *Functional analysis of receptor-like kinases in monocots and dicots.* Current opinion in plant biology, 2006. **9**(5): p. 460-469.
43. Wang, J., et al., *Allosteric receptor activation by the plant peptide hormone phytosulfokine.* Nature, 2015. **525**(7568): p. 265-268.
44. Matsubayashi, Y., et al., *An LRR receptor kinase involved in perception of a peptide plant hormone, phytosulfokine.* Science, 2002. **296**(5572): p. 1470-1472.

45. Amano, Y., et al., *Tyrosine-sulfated glycopeptide involved in cellular proliferation and expansion in Arabidopsis.* Proceedings of the National Academy of Sciences, 2007. **104**(46): p. 18333-18338.
46. Matsubayashi, Y., *Posttranslationally modified small-peptide signals in plants.* Annual review of plant biology, 2014. **65**: p. 385-413.
47. Murphy, E., S. Smith, and I. De Smet, *Small signaling peptides in Arabidopsis development: how cells communicate over a short distance.* The Plant Cell, 2012. **24**(8): p. 3198-3217.
48. Matsubayashi, Y., et al., *Disruption and overexpression of Arabidopsis phytosulfokine receptor gene affects cellular longevity and potential for growth.* Plant Physiology, 2006. **142**(1): p. 45-53.
49. Hanks, S.K. and T.J.T.F.j. Hunter, *Protein kinases 6. The eukaryotic protein kinase superfamily: kinase (catalytic) domain structure and classification.* 1995. **9**(8): p. 576-596.
50. Hanks, S.K., A.M. Quinn, and T.J.S. Hunter, *The protein kinase family: conserved features and deduced phylogeny of the catalytic domains.* 1988. **241**(4861): p. 42-52.
51. Akira, S. and K.J.N.r.i. Takeda, *Toll-like receptor signalling.* 2004. **4**(7): p. 499.
52. Medzhitov, R. and C.A.J.S. Janeway, *Decoding the patterns of self and nonself by the innate immune system.* 2002. **296**(5566): p. 298-300.
53. Zipfel, C., et al., *Perception of the bacterial PAMP EF-Tu by the receptor EFR restricts Agrobacterium-mediated transformation.* 2006. **125**(4): p. 749-760.
54. Nürnberger, T., et al., *Innate immunity in plants and animals: striking similarities and obvious differences.* 2004. **198**(1): p. 249-266.
55. Ausubel, F.M.J.N.i., *Are innate immune signaling pathways in plants and animals conserved?* 2005. **6**(10): p. 973.
56. Zipfel, C. and G.J.C.o.i.p.b. Felix, *Plants and animals: a different taste for microbes?* 2005. **8**(4): p. 353-360.
57. Espinosa, A. and J.R.J.C.m. Alfano, *Disabling surveillance: bacterial type III secretion system effectors that suppress innate immunity.* 2004. **6**(11): p. 1027-1040.
58. Kim, M.G., et al., *Two Pseudomonas syringae type III effectors inhibit RIN4-regulated basal defense in Arabidopsis.* 2005. **121**(5): p. 749-759.

59. Nomura, K., M. Melotto, and S.-Y.J.C.o.i.p.b. He, *Suppression of host defense in compatible plant–Pseudomonas syringae interactions.* 2005. **8**(4): p. 361-368.
60. Jones, D.A. and D.J.C.o.i.i. Takemoto, *Plant innate immunity–direct and indirect recognition of general and specific pathogen-associated molecules.* 2004. **16**(1): p. 48-62.
61. Nimchuk, Z., et al., *Recognition and response in the plant immune system.* 2003. **37**(1): p. 579-609.
62. Karlova, R., et al., *The Arabidopsis somatic embryogenesis receptor-like kinase1 protein complex includes brassinosteroid-insensitive1*. 2006. **18**(3): p. 626-638.
63. Albrecht, C., et al., *The Arabidopsis thaliana SOMATIC EMBRYOGENESIS RECEPTOR-LIKE KINASES1 and 2 control male sporogenesis.* 2005. **17**(12): p. 3337-3349.
64. Hecht, V., et al., *The Arabidopsis SOMATIC EMBRYOGENESIS RECEPTOR KINASE 1 gene is expressed in developing ovules and embryos and enhances embryogenic competence in culture.* 2001. **127**(3): p. 803-816.
65. Kwaaitaal, M.A.C.J., S. De Vries, and E.J.P. Russinova, *Arabidopsis thaliana Somatic Embryogenesis Receptor Kinase 1 protein is present in sporophytic and gametophytic cells and undergoes endocytosis.* 2005. **226**(1-2): p. 55-65.
66. Shah, K., et al., *The Arabidopsis kinase-associated protein phosphatase controls internalization of the somatic embryogenesis receptor kinase 1*. 2002. **16**(13): p. 1707-1720.
67. Colcombet, J., et al., *Arabidopsis SOMATIC EMBRYOGENESIS RECEPTOR KINASES1 and 2 are essential for tapetum development and microspore maturation.* 2005. **17**(12): p. 3350-3361.
68. Hecht, V., et al., *The Arabidopsis SOMATIC EMBRYOGENESIS RECEPTOR KINASE 1 gene is expressed in developing ovules and embryos and enhances embryogenic competence in culture.* Plant Physiology, 2001. **127**(3): p. 803-816.
69. Heese, A., et al., *The receptor-like kinase SERK3/BAK1 is a central regulator of innate immunity in plants.* Proceedings of the National Academy of Sciences, 2007. **104**(29): p. 12217-12222.
70. Roux, M., et al., *The Arabidopsis leucine-rich repeat receptor–like kinases BAK1/SERK3 and BKK1/SERK4 are required for innate immunity to hemibiotrophic and biotrophic pathogens.* The Plant Cell, 2011. **23**(6): p. 2440-2455.

71. Chinchilla, D., et al., *A flagellin-induced complex of the receptor FLS2 and BAK1 initiates plant defence.* Nature, 2007. **448**(7152): p. 497-500.
72. Schulze, B., et al., *Rapid heteromerization and phosphorylation of ligand-activated plant transmembrane receptors and their associated kinase BAK1*. Journal of Biological Chemistry, 2010. **285**(13): p. 9444-9451.
73. Schwessinger, B., et al., *Phosphorylation-dependent differential regulation of plant growth, cell death, and innate immunity by the regulatory receptor-like kinase BAK1*. PLoS Genet, 2011. **7**(4): p. e1002046.
74. Barnes, J.E.J.N., *Evolution of compact groups and the formation of elliptical galaxies.* 1989. **338**(6211): p. 123.
75. Karplus, M. and G.A.J.N. Petsko, *Molecular dynamics simulations in biology.* 1990. **347**(6294): p. 631.
76. Karplus, M., J.A.J.N.S. McCammon, and M. Biology, *Molecular dynamics simulations of biomolecules.* 2002. **9**(9): p. 646.
77. Becker, O.M., et al., *Computational biochemistry and biophysics*. 2001: Marcel Dekker New York.
78. Tuckerman, M.E. and G.J. Martyna, *Understanding modern molecular dynamics: techniques and applications*. 2000, ACS Publications.
79. van Gunsteren, W.F., P.K. Weiner, and A.J. Wilkinson, *Computer simulation of biomolecular systems: theoretical and experimental applications*. Vol. 3. 2013: Springer Science & Business Media.
80. Allen, M.P.J.C.s.m.f.s.p.t.p., *Introduction to molecular dynamics simulation.* 2004. **23**: p. 1-28.
81. Bhaduri, A., et al., *Conserved spatially interacting motifs of protein superfamilies: application to fold recognition and function annotation of genome data.* 2004. **54**(4): p. 657-670.
82. Gromiha, M.M., S.J.P.i.b. Selvaraj, and m. biology, *Inter-residue interactions in protein folding and stability.* 2004. **86**(2): p. 235-277.
83. Reva, B.A., et al., *Recognition of protein structure on coarse lattices with residue-residue energy functions.* 1997. **10**(10): p. 1123-1130.

84. Russell, R.B. and G.J.J.J.o.m.b. Barton, *Structural features can be unconserved in proteins with similar folds: An analysis of side-chain to side-chain contacts secondary structure and accessibility.* 1994. **244**(3): p. 332-350.
85. Šali, A. and T.L.J.J.o.m.b. Blundell, *Comparative protein modelling by satisfaction of spatial restraints.* 1993. **234**(3): p. 779-815.
86. Shao, X. and N.V.J.N.A.R. Grishin, *Common fold in helix–hairpin–helix proteins.* 2000. **28**(14): p. 2643-2650.
87. Tina, K., R. Bhadra, and N.J.N.a.r. Srinivasan, *PIC: protein interactions calculator.* 2007. **35**(suppl_2): p. W473-W476.
88. Krupa, A., G. Preethi, and N.J.J.o.m.b. Srinivasan, *Structural modes of stabilization of permissive phosphorylation sites in protein kinases: distinct strategies in Ser/Thr and Tyr kinases.* 2004. **339**(5): p. 1025-1039.
89. Van Roey, P., et al., *Crystallographic and mutational studies of Mycobacterium tuberculosis recA mini-inteins suggest a pivotal role for a highly conserved aspartate residue.* 2007. **367**(1): p. 162-173.
90. Jones, S., J.M.J.P.i.b. Thornton, and m. biology, *Protein-protein interactions: a review of protein dimer structures.* 1995. **63**(1): p. 31-65.
91. Nooren, I.M. and J.M.J.T.E.j. Thornton, *Diversity of protein–protein interactions.* 2003. **22**(14): p. 3486-3492.
92. Ofran, Y. and B.J.J.o.m.b. Rost, *Analysing six types of protein–protein interfaces.* 2003. **325**(2): p. 377-387.
93. Rekha, N., et al., *Interaction interfaces of protein domains are not topologically equivalent across families within superfamilies: Implications for metabolic and signaling pathways.* 2005. **58**(2): p. 339-353.
94. Saha, R.P., et al., *Interaction geometry involving planar groups in protein–protein interfaces.* 2007. **67**(1): p. 84-97.
95. Bahadur, R.P., et al., *A dissection of specific and non-specific protein–protein interfaces.* 2004. **336**(4): p. 943-955.
96. De, S., et al., *Interaction preferences across protein-protein interfaces of obligatory and non-obligatory components are different.* 2005. **5**(1): p. 15.

97. Valdar, W.S. and J.M.J.J.o.m.b. Thornton, *Conservation helps to identify biologically relevant crystal contacts.* 2001. **313**(2): p. 399-416.
98. Genheden, S. and U.J.E.o.o.d.d. Ryde, *The MM/PBSA and MM/GBSA methods to estimate ligand-binding affinities.* 2015. **10**(5): p. 449-461.
99. de Ruiter, A. and C.J.C.o.i.c.b. Oostenbrink, *Free energy calculations of protein–ligand interactions.* 2011. **15**(4): p. 547-552.
100. Miller III, B.R., et al., *MMPBSA. py: an efficient program for end-state free energy calculations.* 2012. **8**(9): p. 3314-3321.
101. Foloppe, N. and R.J.C.m.c. Hubbard, *Towards predictive ligand design with free-energy based computational methods?* 2006. **13**(29): p. 3583-3608.
102. Homeyer, N. and H.J.M.I. Gohlke, *Free energy calculations by the molecular mechanics Poisson− Boltzmann surface area method.* 2012. **31**(2): p. 114-122.
103. Wang, J., T. Hou, and X.J.C.C.-A.D.D. Xu, *Recent advances in free energy calculations with a combination of molecular mechanics and continuum models.* 2006. **2**(3): p. 287-306.
104. Gohlke, H. and D.A.J.J.o.c.c. Case, *Converging free energy estimates: MM-PB (GB) SA studies on the protein–protein complex Ras–Raf.* 2004. **25**(2): p. 238-250.
105. Hou, T., et al., *Assessing the performance of the molecular mechanics/Poisson Boltzmann surface area and molecular mechanics/generalized Born surface area methods. II. The accuracy of ranking poses generated from docking.* 2011. **32**(5): p. 866-877.
106. Moreira, I.S., P.A. Fernandes, and M.J.J.T.C.A. Ramos, *Unravelling Hot Spots: a comprehensive computational mutagenesis study.* 2007. **117**(1): p. 99-113.
107. Réblová, K., et al., *An RNA molecular switch: Intrinsic flexibility of 23S rRNA helices 40 and 68 5′-UAA/5′-GAN internal loops studied by molecular dynamics methods.* 2010. **6**(3): p. 910-929.
108. Sirin, S., et al., *A computational approach to enzyme design: predicting ω-aminotransferase catalytic activity using docking and MM-GBSA scoring.* 2014. **54**(8): p. 2334-2346.
109. Sun, H., et al., *Assessing the performance of MM/PBSA and MM/GBSA methods. 5. Improved docking performance using high solute dielectric constant MM/GBSA and MM/PBSA rescoring.* 2014. **16**(40): p. 22035-22045.

110. Kumari, R., et al., *g_mmpbsa A GROMACS tool for high-throughput MM-PBSA calculations.* 2014. **54**(7): p. 1951-1962.
111. Connolly, M.L.J.S., *Solvent-accessible surfaces of proteins and nucleic acids.* 1983. **221**(4612): p. 709-713.
112. Lee, B. and F.M.J.J.o.m.b. Richards, *The interpretation of protein structures: estimation of static accessibility.* 1971. **55**(3): p. 379-IN4.
113. Richards, F., *Annu. Rev. Biophys. Bioeng.* 1977.
114. Greer, J. and B.L.J.P.o.t.N.a.o.S. Bush, *Macromolecular shape and surface maps by solvent exclusion.* 1978. **75**(1): p. 303-307.
115. Jiang, F. and S.-H.J.J.o.m.b. Kim, *"Soft docking": matching of molecular surface cubes.* 1991. **219**(1): p. 79-102.
116. Shrake, A. and J.J.J.o.m.b. Rupley, *Environment and exposure to solvent of protein atoms. Lysozyme and insulin.* 1973. **79**(2): p. 351-371.
117. Huggins, M.L.J.A.C.I.E.i.E., *50 years of hydrogen bond theory.* 1971. **10**(3): p. 147-152.
118. McDonald, I.K. and J.M.J.J.o.m.b. Thornton, *Satisfying hydrogen bonding potential in proteins.* 1994. **238**(5): p. 777-793.
119. Creighton, T.E.J.C.o.i.s.b., *Stability of folded conformations: Current opinion in structural biology 1991, 1: 5–16.* 1991. **1**(1): p. 5-16.
120. Dill, K.A.J.B., *Dominant forces in protein folding.* 1990. **29**(31): p. 7133-7155.
121. Van Der Spoel, D., et al., *GROMACS: fast, flexible, and free.* 2005. **26**(16): p. 1701-1718.
122. van der Spoel, D., P.J. van Maaren, and H.J.J.T.J.o.c.p. Berendsen, *A systematic study of water models for molecular simulation: derivation of water models optimized for use with a reaction field.* 1998. **108**(24): p. 10220-10230.
123. Sun, Y., et al., *Structural basis for flg22-induced activation of the Arabidopsis FLS2-BAK1 immune complex.* 2013. **342**(6158): p. 624-628.
124. Morita, J., et al., *Crystal structure of the plant receptor-like kinase TDR in complex with the TDIF peptide.* 2016. **7**: p. 12383.

APPENDIXES

Different bioinformatics tools used in this study

Serial No.	Tool	Used for
1	Gromacs	MD simulation
2	Protein interaction calculator: PIC (online)	Residual bond identification
3	Chimera	Molecular visualization
4	g_mmpbsa	Binding free energy calculation
5	xmgrace	Graph generation and analysis